TRANSCRIPTION INITIATION CONTROL MEDIATED BY THE GLOBAL REGULATOR, SPX, IN *BACILLUS SUBTILIS*

By

Ann An-Ting Lin

A DISSERTATION

presented to the Division of Environmental and Biomolecular Systems

at Oregon Health & Science University

School of Medicine

in partial fulfillment of the

requirements for the degree of

Doctor of Philosophy

In Biochemistry and Molecular Biology

School of Medicine

Oregon Health & Science University

Certificate of Approval

This is to certify that the PhD Dissertation of

Ann An-Ting Lin

has been approved

_____

Dr. Peter Zuber, Dissertation Advisor, Professor

_____

Dr. Michiko M. Nakano, Research Professor

_____

Dr. James Whittaker, Associate Professor

_____

Dr. Michael Bartlett, Associate Professor,

Portland State University

TABLE OF CONTENETS

LIST OF TABLES

LIST OF FIGURES

ACKNOWLEDGEMENTS

First, I would like to express my appreciation to my advisor, Dr. Peter Zuber, for giving me the opportunity to pursue my Ph.D. degree and guiding me through the difficulties in experiments and thesis with patience and encouragement.

I would like to acknowledge my dissertation committee members: Dr. Michiko Nakano for her encouragement and assistance in both work and life; Dr. James Whittaker for his knowledge and suggestions; and Dr. Michael Bartlett for his kindness of being my thesis committee.

I would also like to thank the EBS faculty and staffs for all the valuable classes and helps throughout my study in these years. I would like to thank the lovely members in Zuber and Nakano lab, from past to present, for their support, technical assistance, and friendship, let me work happily in the lab. Special thanks to Nancy Christie, for her kindiness and generosity to take care of all kinds of problems from my first day here till now. Also thanks all the EBS friends and Oregon friends for their wonderful smiles and cares. Thank to Chiung, for always being there and staying up with me.

I am greatly indebted to my family, especially my mom, my sister, and my Latte. Without their love, encouragement and companion, I could never get through these days here by myself.

ABSTRACT

Transcription Initiation Control Mediated by the Global Regulator, Spx, in *Bacillus subtilis*

Ann An-Ting Lin

Doctor of Philosophy

Division of Environmental and Biomolecular Systems within

the Institute of Environmental Health

Oregon Health and Science University

School of Medicine

June, 2013

Thesis Advisor: Peter Zuber

Bacillus subtilis Spx is a global transcriptional regulator that belongs to the ArsC (arsenate reductase) protein family. It bears an N-terminal C10TSC13 redox disulfide center that is oxidized in active Spx, allowing *B. subtilis* to survive under oxidative stress by stimulating transcription of genes that function in detoxification and restoration of thiol homeostasis. Instead of initially binding to target promoter DNA, Spx interacts with C-terminal domain of RNA polymerase (RNAP) α subunit (αCTD) to form a complex prior to target gene recognition. Previous research showed that an αCTD/Spx complex interacts with a sequence upstream of the *trxB* (thioredoxin reductase) promoter region (-56 to -21), specifically two putative Spx responsive cis-acting elements at positions -44 and -33 resided within target promoter *trxA* (thioredoxin) and *trxB* DNA.

To investigate whether two Spx proteins interact with RNAP to activate transcription, the composition of Spx/RNAP complex was examined in vitro and in vivo by using two Spx variants with different epitopic tags in a series of affinity chromatography analyses. The result showed that only one Spx monomer interacts with RNAP to form an active complex in vitro and in vivo. In vitro affinity interaction assay and in vitro transcription also confirmed that only one Spx monomer engages in the transcriptionally active Spx/RNAP/DNA ternary complex.

The G52 residue in Spx and Y263 residue in αCTD are known to constitute part of the interface of Spx and αCTD contact. Mutational analysis of Spx found that Spx(R91A) mutation affects both Spx-dependent transcriptional activation and repession, suggestive of a function of R91 in RNAP interaction. The anti-HA chromatography analysis showed that R91 residue in Spx is required for α binding to Spx. The G52R, R91A double mutant abolished transcriptional activity of Spx in vivo as well as in vitro RNAP binding ability. The results suggests that Spx has multiple contacts with the α dimer. The affinity interaction assay and far-western blotting showed that only intact α but not αCTD interacted stably with Spx. The result suggests that the intact α subunit is required for optimal α/Spx interaction, which may involve more than one contact interface.

Spx redox control involves residue R92, which is conserved in ArsC where it stabilizes the active site cysteine thiolate. Intramolecular epistasis tests showed that substitution of R92 with alanine reduced Spx activity only in Spx protein that is able to form a disulfide between C10 and C13, implicating R92 in redox control of Spx activity.

The Spx response cis-acting element AGCA at position -44 is conserved and was also found in another Spx-activated gene, *nfrA*. In vivo and in vitro transcriptional analysis

showed this AGCA motif in *nfrA* promoter is required for Spx-dependent transcriptional activation as that in *trxB* promoter. The -44 AGCA element was proposed to be the site of contact for the αCTD/oxidized Spx complex. The DNA/RNAP crosslinking analysis showed that Spx, in complex with RNAP, contacted with the *trxB* promoter at position -44, and repositioned σ^A. Hence, a mechanism for Spx-dependent transcriptional activation is proposed here: By interacting with RNAP and the -44 element, Spx, in its oxidized form, remodels RNAP and repositions σ^A to engage the -35 and -10 core promoter elements. Proper σ^A interaction with the core promoter, mediated by Spx that is in contact with the -44 cis-acting element is required for initiating transcription from Spx-controlled promoters.

CHAPTER 1

INTRODUCTION

1.1 BACTERIAL GENE EXPRESSION/TRANSCRIPTION

1.1.1 Bacterial Transcription machinery

Transcription is the first step of gene expression. Bacterial gene transcription is catalyzed by the multi-subunit DNA-dependent RNA polymerase (RNAP), which initiates RNA synthesis from gene promoters. The complete RNAP holoenzyme contains a conserved catalytic core enzyme and a sigma (σ) factor. The core enzyme consists of two alpha subunits, a beta subunit, a beta-prime subunit and an omega subunit ($\alpha_2\beta\beta'\omega$), which constitutes an enzyme capable of catalyzing RNA synthesis, but does not efficiently initiate gene-specific transcription. The σ factor interacts with core enzyme to form the holoenyme ($\alpha_2\beta\beta'\omega\sigma$) and is required for specific promoter recognition to direct gene transcription (Burgess, 1971). In general, a bacterial genome encodes a primary σ factor responsible for the transcription of essential housekeeping genes, and multiple alternative σ factors to transcriptionally control the response to different environmental or metabolic stimuli. Different σ factors recognize different consensus promoter DNA sequences (Campbell *et al.*, 2002). The number of σ factors varies between bacterial species. Since the σ factor in the RNAP holoenzyme determines the specificity of RNAP to the promoter and the association of σ factor with core RNAP is transient, σ

substitution during the transcription cycle provides the opportunity to reprogram RNAP and to regulate expression of different sets of genes through promoter selection. Under different environmental conditions that bacteria encounter, alternative σ factors will be activated to recognize different promoters and transcribe corresponding genes in response to specific environmental changes.

1.1.2 RNAP and promoter DNA interaction

Most σ factors belong to σ^{70}-related family and share up to four highly conserved domains with *Escherichia coli* primary σ factor, σ^{70} (Lonetto *et al.*, 1992). The σ^{70}-related factor contains four distinct domains, region 1-4, which are connected by a flexible linker (Helmann & Chamberlin, 1988). The σ region 2 and 4 recognize the consensus -10 (TATAAT) and -35 (TTGACA) hexamers located 10 and 35 bp upstream from the transcription start site in promoter DNA, respectively (Dombroski *et al.*, 1992, McClure, 1985). Also, the σ region 3 functions in the recognition of -10 extended element that is located immediately upstream of the -10 hexamer (Barne *et al.*, 1997, Sanderson *et al.*, 2003). Moreover, the σ region 1.2 can recognize the discriminator, which is a GC-rich sequence located downstream the -10 element (-4 to -6) usually in genes specifying ribosomal RNAs (Haugen *et al.*, 2006, Zhang *et al.*, 2012). Besides the σ factor, the α subunit of the RNAP can participate in promoter recognition by interaction with the UP (upstream) element, which is a ~20 bp AT-rich sequence upstream of the -35 hexamer in the promoter region (Ross *et al.*, 1993, Barker *et al.*, 2001). Since there are many transcription determinants in the promoter region, and the

contribution of each element varies in different promoters, these features contribute to the overall complexity of transcription regulation and a broad range of promoter strengths.

1.1.3 Structures of RNA Polymerase

The structures of *Thermus aquaticus* RNAP (Taq RNAP) (Fig. 1) (Murakami *et al.*, 2002, Vassylyev *et al.*, 2002, Zhang *et al.*, 1999) and those of many σ factors (Paget & Helmann, 2003) have been solved and biochemically analyzed. The molecular weight of multi-subunit core RNAP is around 400 kDa. The crystal structure of *Taq* core RNAP revealed a crab-claw like structure with a 27 Å wide internal channel which can accommodate double-stranded DNA, and the catalytic site is located inside the channel with a chelated Mg^{2+} ion (Zhang et al., 1999). The β and β' subunits form the pincers of the claw and contain the active center responsible for RNA synthesis. The α dimer contacts the β-β' interface through its amino-terminal domains (αNTD), and the carboxyl-terminal domain of α subunit (αCTD) is attached through a flexible linker to αNTD. The αCTD is capable of interacting with upstream promoter DNA or DNA-bound transcriptional regulators. Because of the flexible linker, the structure of αCTD is dynamic in the context of an intact RNAP. Recent X-ray crystal structure of *E. coli* RNAP σ^{70} holoenzyme reveals that an αCTD is positioned next to σ domain 4 with a fully stretched linker (Murakami, 2013). The ω subunit interacts with β' subunit and facilitates the assembly of functional RNAP (Ghosh *et al.*, 2001, Minakhin *et al.*, 2001). The σ factor which is responsible for the RNAP promoter specificity interacts with several domains surrounding the active site channel of *Taq* core enzyme: the β'-clamp, β'-

jaw, β-flap and β upstream and downstream lobes (Murakami et al., 2002, Vassylyev et al., 2002). The structure of *E. coli* RNAP σ^{70} holoenzyme also reveals that $\sigma_{1.1}$ is positioned at the RNAP DNA-binding channel and contains a basic patch on its surface, which may play an important role in open promoter complex formation (Murakami, 2013).

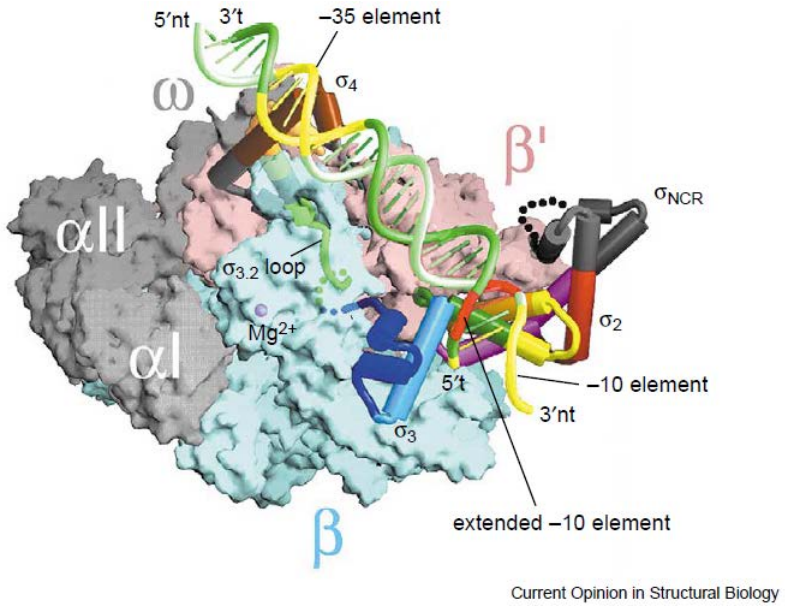

Figure 1.1. Structure of the complex of RNAP holoenzyme and DNA (Murakami & Darst, 2003). The X-ray structure of the *Taq* RNAP holoenzyme-DNA complex was solved by Murakami et al. (Murakami *et al.*, 2002). The αCTDs are not shown in this figure. The αNTDs, and ω subunits are shown in gray, the β and β' subunits are in cyan and pink respectively. The σ subunit is shown as colored cylinders. The DNA template strand and non-template strand are shown in dark and light green, respectively. The -35 and -10 consensus elements are in yellow, and the extended -10- element is in red.

1.1.4 Stages of Transcription

Transcription proceeds through three stages, initiation, elongation, and termination. Transcription initiation in bacteria begins with the recognition and binding of RNAP holoenzyme to target promoter sequence. This involves establishment of the closed complex, which precedes DNA duplex melting, and requires interaction of σ region 4 with the -35 element. The closed complex undergoes isomerization to form an open complex in which the DNA around position -10 region is unwound and transcription bubble forms from position -11 to approximately +2 relative to transcription start site. Hence, the template strand of DNA is accessible and used by the RNAP at the active site (Murakami & Darst, 2003). In the presence of appropriate ribonucleotides, short abortive transcripts, around 2 to 12 nucleotides in length, are synthesized. Once the length of RNA is about 12 nucleotides and long enough to to displace the $\sigma_{3.2}$ loop in the exit channel of RNAP, abortive transcription ends, and the σ factor will usually dissociate from RNAP, a process called promoter clearance. Then, an effective elongation complex is formed, and the RNAP moves downstream along the DNA template, and nucleotides are added to the growing RNA chain in a process called transcription elongation. Transcription proceeds until the RNAP reaches a termination signal on the DNA, the elongation complex dissociates and newly synthesized RNA is released (Murakami & Darst, 2003).

Gene expression can be regulated at either the initiation, elongation or termination stages of transcription; however, control most frequently occurs during initiation. Promoter recognition and RNAP binding is the first step of transcription initiation. On the promoter region, there are many elements serving for interaction with RNAP holoenzyme including the UP element, the -35 hexamer, the extended -10 element, the -

10 hexamer, and the discriminator element from position -4 to -6. In the σ factor, there are determinants in the conserved four domains responsible for recognition of most promoter elements. The αCTD is also capable of recognizing UP DNA element and interacting with many transcription regulators. Besides the utilization of alternative σ factors, and the interaction between RNAP and promoter, there are a large number of other transcriptional regulators that function in productive interaction of RNAP with promoter DNA.

1.2 TRANSCRIPTION ACTIVATION

1.2.1 Activation of Transcription initiation

The process of transcription initiation consists of a series of steps including promoter recognition and RNAP binding to form closed complex, isomerization to form open complex, promoter clearance to form an effective elongation complex (Murakami & Darst, 2003). From the view of kinetics, to activate transcription, increasing the rate of polymerase passage through the initiation pathway is required (Roy *et al.*, 1998). Transcription factors that can either stabilize the initial RNAP-promoter complex, or accelerate the transition to the open complex can serve as activators.

In early 1990s, the terms of Class I and Class II activation were introduced for the transcriptional activation mechanism operated by cyclic AMP receptor protein (CRP) (Savery *et al.*, 1996). In Class I activation, the activator binds to the target sequence located upstream of the -35 element and recruits RNAP to the promoter by direct contact

with RNAP αCTD. In Class II activation, the activator binds to the target sequence overlapping the promoter -35 hexamer and/or the promoter proximal αCTD, and interacts with the σ domain 4 (σ_4) of RNAP. This classification has been used for years, however, more and more studies on transcription activation uncovered the complexity of regulatory mechanisms, and this simple classification is not sufficient to apply to all types of activation.

Based on a recent review by Busby and collaborators (Lee *et al.*, 2012), the mechanisms for simple bacterial transcription activation, in which only one regulator functions, could be divided into two classes; activation focused on the promoter (promoter-centric) or on the RNA polymerase holoenzyme (RNAP-centric). If regulatory factors interact with the promoter to improve the recognition or productive binding of RNAP to the promoter, these are called promoter-centric mechanisms. In this mechanism, factors could either provide additional determinants for promoter interaction or reverse the action of a negative regulator, such as a repressor. However, in RNAP-centric mechanism, factors alter promoter preference of RNAP by interacting with RNA polymerase. Here the mechanisms are explained with examples in detail.

1.2.2 Promoter-centric activation mechanism

1.2.2.1 Activation by altering promoter conformation: MerR and BmtR

The transcription regulators of the MerR family are dimeric proteins sharing similar structure comprised of an N-terminal helix-turn-helix (HTH) DNA binding domains followed by coiled coils and C-terminal ligand-specific binding domains (Brown *et al.*,

2003). MerR, the regulator of mercury resistance operons of Gram-negative bacteria, found on transposons Tn*21* and Tn*501*, regulates the expression of a mercury resistance determinant in response to mercury (Helmann *et al.*, 1989). BmtR is also a MerR family member found in *Bacillus subtilis* that controls expression of efflux pumps in the presence of xenometabolites (Brown et al., 2003, Heldwein & Brennan, 2001). Both MerR and BmtR activate gene expression by distorting the DNA sequence and promote RNAP transcription initiation at a suboptimal promoter (Brown et al., 2003). The target promoters for these activators have nonoptimal spacing between the -35 and -10 elements, so that when RNAP interacts with the promoter UP element and -35 element, the -10 element is misplaced. After receiving the signal, MerR or BmtR binds to the region between the -35 and -10 elements at the promoter, and twists the promoter DNA, resulting in RNAP being able to interact with the -10 element and initiate transcription (Newberry & Brennan, 2004, Heldwein & Brennan, 2001). This is one example for the promoter-centric activation by inducing a conformational change in promoter DNA.

1.2.2.2 Activation by direct contact with RNAP

Compared to activators solely interacting with promoter DNA, more activators interact both with promoter and with RNAP to recruit RNAP. For the majority of promoters that are dependent on a single activator, the activator binds to DNA target either upstream of or overlapping the -35 element, so that activator can make a direct contact with RNAP, thereby recruiting RNAP to the promoter elements (Lee et al., 2012).

1.2.2.2.1 Contact with σ domain 4

Many transcription activators in the AraC family use σ factor region 4 (σ_4) as a target for transcription activation. The AraC family is a large group of related transcriptional regulators with a helix-turn-helix (HTH) DNA-binding domain, and can operate as either monomer or dimer to regulate genes involved in carbon metabolism, stress response, and pathogenesis. There are two distinct groups in the AraC family. In one group, which includes AraC and MelR, there is a signal receiving/binding domain near the N-terminus of the regulator and adjoining the HTH domain. The signal-receiving domain directly senses a specific signal and effects dimerization. Proteins in the second group, including SoxS and MarA, contain only the HTH DNA binding domain, and their activity is regulated by another factor (Martin & Rosner, 2001). AraC and MelR, the arabinose and melibiose operon regulatory proteins respectively, activate transcription of target genes in response to inducer, L-arabinose and melibiose, respectively (Schleif, 2010, Grainger *et al.*, 2004). When arabinose or melibiose binds to AraC or MelR, it triggers the activator interaction with σ_4, which binds the target promoter -35 element through its C-terminal HTH domain to promote the initial binding of RNAP to the promoter. (Grainger et al., 2004, Zhang *et al.*, 1996). In the case of MelR, a conserved aspartate residue (D261) was identified to contact residue R588 in the region 4 of σ^{70}. Because the positioning of σ4 with respect to the rest of RNAP at the promoter is critical and less flexible (Murakami & Darst, 2003), these activators have to bind precisely to the same face of promoter that σ_4 interacts in order to contact their target (Lee et al., 2012).

1.2.2.2.2 Contact with αCTD

For transcription regulation, αCTD can interact not only with promoter UP elements, but also with transcription regulators. Compared to other components of RNAP, αCTD is flexible to move because it is connected to αNTD and the rest of RNAP by a nonstructured linker. Hence, the mechanisms of activator-dependent transcription regulation through the αCTD interaction are variable for different activators and promoters. CRP, which activates target promoters by interacting with αCTD, regulates Class I and Class II promoters in different ways. To activate the *lac* operon promoter, a Class I promoter, the homodimeric cAMP-CRP binds to a 22-bp DNA target centered between position -61 and -62 at *lac* promoter, where it is not in a position to contact σ_4 (Ebright & Busby, 1995). The structure of the ternary CRP/holo-RNAP/promoter complex shows one αCTD bound between CRP dimer and σ_4 on *lac* operon promoter (Hudson *et al.*, 2009), and CRP making direct contact with αCTD (Benoff *et al.*, 2002). The αCTD in this ternary complex interacts with activating region 1 (AR1) of CRP via the 287 determinant (residue position 287 of α), with UP element at *lac* promoter via the 265 determinant, and with σ_4 via the 261 determinant (Chen *et al.*, 2003, Savery *et al.*, 2002, Hudson et al., 2009).

To activate the Class II promoter, CRP binds to a position overlapping the -35 element on the target promoter, which prevents αCTD from contacting σ4 and induces αCTD to bind just upstream of the upstream-positioned monomer of the DNA-bound CRP dimer. (Zhou *et al.*, 1994, Belyaeva *et al.*, 1996). For the upstream subunit of the CRP dimer, the interaction with αCTD involves AR1 and the 287 determinant of αCTD,

which promotes RNAP recruitment (Rhodius *et al.*, 1997, Niu *et al.*, 1996). However, the downstream subunit of CRP dimer interacts with αNTD via another surface on CRP, activating region 2 (AR2), and promotes the transition of promoter-bound RNAP to the open complex (Niu et al., 1996).

1.2.3 RNAP-centric activation mechanism: RNAP appropriation and pre-recruitment

For RNAP-centric activation mechanisms, instead of improving the recruitment of RNAP to promoter DNA, some transcription factors reprogram the promoter preferences of the RNAP. There are several ways to alter the promoter preferences of RNAP, including the utilization of alternative σ factors, and through RNAP pre-recruitment and appropriation by transcription factors that activate or repress transcription.

1.2.3.1 Alternative σ factors

Many bacterial species possess alternative σ factors, which can be active under specific environments or metabolic conditions. Based on the structure, bacterial σ factors consist of two distinct families, σ^{70} and σ^{54} (Helmann & Chamberlin, 1988). The proteins in σ^{70}-related family were divided into 5 groups by Helmann *et al* (Helmann & Moran Jr, 2002). Group 1 contains the primary σ factors, such as *Escherichia coli* σ^{70} and *B. subtilis* σ^{A}, which direct transcription of essential and housekeeping genes. Group 2 includes the paralogues that are closely related to Group 1 but non-essential, such as the

stress-activated *E. coli* σ^S, which has similar promoter recognition sequence with σ^{70} but exhibits a tolerance of non-canonical nucleotide positions so that σ^S can direct transcription from promoters lacking consensus -35 elements (Wise *et al.*, 1996). Group 3 is composed of divergent alternative σ factors that are of lower molecular weight, with conserved domain 2, 3 and 4 but without domain 1. These alternative σ factors are further grouped into clusters with evolutionarily conserved functions, such as heat-shock, sporulation, and flagellar synthesis (Lonetto et al., 1992). Group 4 σ factors are those factors involved in extracytoplasmic functions (ECF σ factors). The proteins in group 4 are more divergent than those in group 3, and only have regions 2 and 4 to recognize an "AAC" motif in -35 region. In many cases they are encoded by genes that are co-transcribed with a gene specifying an anti-σ factor. Several ECF σ subunits function in the transcription of genes induced by cell envelope stress, caused in some cases by antibiotics. In *B. subtilis*, there are three such ECF σ subunits, σ^M, σ^W, and σ^X, all of which are controlled by a membrane-associated anti-σ factor that undergoes proteolytic inactivation when cell wall structure/function is compromised.

Th group 5 σ subunit is composed of proteins that are homologs of TxeR, which shows less sequence similarity with σ^{70} but biochemically functions as a σ factor controlling toxin gene expression in *Clostridium diffficile* (Helmann & Moran Jr, 2002).

The interaction of σ subunit with core RNAP is transient. At the end of transcription initiation, the σ subunit is dissociated from core RNAP, and an elongation complex is formed. The ability of σ factors to interact with core RNAP is determined by their concentration and affinity for core RNAP. Different σ factors can compete for core

RNAP binding to activate transcription of specific gene sets (Ishihama, 2000). Hence, when bacteria are undergoing complex programs of development, or are under environmental stresses, modulating the activity or expression level of different σ factors allows core RNAP to engage alternative σ factors, which confer upon RNAP unique promoter preferences (Gruber & Gross, 2003). For example, *B. subtilis* σ^D controls genes encoding products that function in the assembly of the flagellar apparatus. σ^E, σ^F, σ^G, and σ^K govern spatial and temporal control of gene transcription during early and late stages of sporulation. σ^B, the first alternative σ factor identified in *B. subtilis*, is activated under energy stress and diverse environmental stresses to directly or indirectly regulate expression of over 200 genes. (Haldenwang & Losick, 1979, Rollenhagen *et al.*, 2003, Price *et al.*, 2001). Under normal conditions, σ^B is inhibited by interaction with its anti-σ factor RsbW when the positive regulator RsbV, an antagonist of RsbW, is phosphorylated. When energy is depleted or bacteria encounter stresses, such as heat, acid, ethanol, osmotic, and oxidative stresses, σ^B is activated through a PP2C (protein phosphatase 2C) phosphatase-mediated cascade. Serine phosphatases, RsbP for energy stress and RsbU for environmental stress, dephosphorylate RsbV resulting in RsbV interaction with RsbW, causing the release of σ^B (Hecker & Volker, 2001, Price et al., 2001). Then σ^B is able to interact with core RNAP and directs RNAP holoenzyme to transcribe target genes, which confers upon *B. subtilis* prevention or repair of stress-induced damage (Hecker *et al.*, 2007).

The σ^{54} differs both in amino acid sequence and in transcription mechanism from the σ^{70} class. One of its members, σ^N, regulates genes involved in nitrogen metabolism (Merrick, 1993). RNAP σ^{70} holoenzyme interacts with the -35 and -10 elements in its

target promoters to form a closed complex and spontaneously undergoes isomerization to form an open complex. However, the RNAP σ^{54} holoenyme recognizes a distinct class of promoters with conserved sequence elements around position -24 (5'-GG-3') and -12 (5'-TGC-3') upstream of the transcription start site at +1, and form a stable closed complex which is unable to melt DNA at the transcription start site to initiate transcription (Barrios *et al.*, 1999). Members of this class require specific transcription activators with ATPase activity, the bacterial enhancer-binding proteins (bEBPs), to hydrolyze ATP in order to facilitate the open complex formation and transcription initiation (Popham *et al.*, 1989).

1.2.3.2 Pre-Recruitment: SoxS

Unlike AraC and MelR, which contain a ligand-binding domain, some proteins in the AraC family have two HTH DNA binding domains and their activity is controlled by their concentration, which is often regulated at the level of transcription. Such is the case of the SoxS protein (superoxide response) of *E. coli*, MarA (multiple antibiotic resistance), and Rob (right *oriC* binding) (Martin *et al.*, 2008). All three utilize a pre-recruitment mechanism, in which the protein interacts with RNAP, followed by scanning on the part of the RNAP/activator complex for the activator binding site in target promoters (Griffith *et al.*, 2002, Griffith & Wolf, 2004, Martin *et al.*, 2002). SoxS, of the SoxRS system in *E. coli*, regulates the response to elevated superoxide endogenously generated from superoxide anion, nitric oxide, and redox-cycling compounds (Nunoshiba *et al.*, 1992). SoxR is a homodimeric protein that senses the change of cellular redox potential. When the 2Fe-2S center in SoxR dimer is oxidized, SoxR undergoes a

conformational change and activates *soxS* transcription. The newly synthesized SoxS accumulates and the monomeric SoxS interacts with RNAP, which directs the complex to recognize a 20-bp consensus sequence (Sox box) in target promoters leading to transcriptional activation. The SoxS-dependent promoters are divided into two types: Class I promoters, such as *zwf* and *fpr*, bear a Sox box located upstream of the -35 element, and Class II (such as *fumC* and *micF*) contain the Sox box at a position that overlaps with the -35 hexamer, (Griffith et al., 2002, Griffith & Wolf, 2004). There are two surfaces on SoxS that function in transcription activation, ClassI/II domain and Class II domain. Transcription activation of both types of promoters requires the interaction between the ClassI/II surface of SoxS and the 265 determinant of αCTD (Martin et al., 2002). The 265 determinant of αCTD is the surface responsible for interacting with the promoter UP element. Hence, the SoxS binding prevents the recognition by αCTD of the UP element but promotes SoxS/RNAP complex to interact with target promoters containing the Sox box in the upstream DNA sequence (Shah & Wolf, 2004). For the activation of Class II promoters, another contact between SoxS and RNAP is necessary. The residues in Class II surface of SoxS interact with RNAP σ^{70} region 4, so that the binding of SoxS/RNAP complex to a Sox box that overlaps with the -35 hexamer on Class II promoters. The class II surface substitutes for -35 to correctly position σ^{70} (Zafar *et al.*, 2011).

1.2.3.3 RNAP Appropriation by T4 phage AsiA

Bacteriophage T4, which infects *E coli*, exhibits temporal transcriptional regulation of its genome. During infection, T4 genes are differentially transcribed according to when they are required for the T4 development and are divided into three groups, early, middle and late genes. The host σ^{70}-containing RNAP is necessary for the cycle of T4 infection. The early T4 promoters share the consensus -35 and -10, and/or UP element with host promoters, so that they can be activated by host σ^{70}-containing RNAP. AsiA expressed in the early stage during infection, can manipulate host *E. coli* RNAP to transcribe genes from the T4 genome and is indispensible for the transition of transcription from early genes to middle, and late genes. The transcription of T4 middle genes lacking the -35 consensus element requires another T4 encoded activator, MotA, and a specific DNA sequence centered around the -30 region in the middle promoters (MotA box) that is recognized by MotA. When infection reaches the end of early stage, one of the host RNAP αCTDs is ADP-ribosylated by T4 Alt protein to inhibit interaction with host promoter UP elements. Moreover, AsiA interacts with σ^{70} region 4 and the β-flap domain of RNAP (Colland *et al.*, 1998). Then, MotA interacts with the σ^{70} region 4 of AsiA-bound RNAP and recognizes middle promoters with the MotA box to activate transcription of middle genes. The AsiA/RNAP interaction reprograms the promoter preference by not only preventing AsiA-bound RNAP to recognize the -35 element in host genes, but by promoting MotA-dependent transcription in the middle phase of T4 infection (Hinton *et al.*, 2005, Lambert *et al.*, 2004, Campbell *et al.*, 2008). Finally, in the late stage of T4 infection, gp55, a specialized sigma factor expressed during middle stage, replaces σ^{70} in RNAP and together with other T4-encoded transcription factors, gp33 and

gp45, directs late gene transcription (Minakhin & Severinov, 2005). Interestingly, the complex is activated through direct interaction of the beta clamp of the T4 DNA replication complex, effectively coupling late gene transcription with replication of T4 genomic DNA.

1.2.3.4 Stabilizing RNAP open complex by DksA, ppGpp

In *E. coli,* the DksA protein binds in the secondary channel of RNAP, and together with alarmone ppGpp (guanosine tetraphosphate), either activates the transcription of amino-acid biosynthesis genes or inhibits the transcription of ribosomal RNA promoters under starvation stress. The stringent response initiates when uncharged tRNA enters into the ribosomal A site, and activates the ribosome-associated RelA protein to synthesize ppGpp. During starvation for amino acids, ppGpp rapidly accumulates and interacts with RNAP to downregulate rRNA synthesis and upregulate genes involved in amino acid biosynthesis. The effect of ppGpp can be enhanced in the presence of DksA (Paul *et al.*, 2004, Paul *et al.*, 2005). At rRNA operon promoters DksA and ppGpp regulate transcription initiation by shifting the occupancy of specific RNAP/promoter intermediates to an unstable open complex (Haugen *et al.*, 2008, Rutherford *et al.*, 2009). Recently, the binding site of ppGpp on RNAP was identified (Zuo *et al.* 2013, Ross, *et al.* 2013). The ppGpp binds to the interface of two RNAP mobile modules, the shelf module and the core module, located on the outside surface of the catalytic center inside the cleft (Zuo *et al.*, 2013). ppGpp-RNAP crosslinking experiment determined that ppGpp interacts with β' and ω subunits (Ross *et al.*, 2013). The binding of ppGpp to the outside

hinge of RNAP clamp affects the movement of the claw pincers, and then affects the open complex formation (Ross *et al.*, 2013). On the other hand, the coiled-coil tip of DksA interacts with the trigger loop of RNAP and further destabilizes promoter complexes (Lennon *et al.*, 2012). Depending on the intrinsic properties of target promoter, DksA and ppGpp perform opposite regulatory functions. In the promoter of *E. coli his* operon (histidine biosynthesis), an AT-rich DNA sequence between the -10 element and the +1 transcription start site is known as a discriminator, and this promoter is activated by DksA and ppGpp. In the repressed targets, such as *rrn* P1 (P1 promoter of rRNA), the discriminator sequence is GC-rich (Dalebroux *et al.*, 2010). The discriminator region is required for interaction with RNAP σ^{70} region 1.2 (Haugen *et al.*, 2006). Models explaining the mechanisms of DksA-dependent transcriptional control are speculative at this time.

1.2.3.5 Other mechanisms: N4SSB interaction with β' subunits

N4SSB, a single-stranded DNA (ssDNA) binding protein encoded by bacteriophage N4, is required for N4 replication and recombination. It activates transcription of N4 late promoters by using *E coli* σ^{70} containing RNAP (Choi *et al.*, 1995, Cho *et al.*, 1995). Since N4SSB does not interact with double-stranded DNA (dsDNA), the mechanism that it utilizes to activate transcription of N4 late genes is not promoter-centric activation mechanism, which requires the activator to bind to an activating DNA element and recruit RNAP to a promoter. The ssDNA binding activity of N4SSB is not required for N4SSB-dependent transcription but is related to recombination and replication. (Miller *et al.*, 1997). Miller *et al.* identified some N4SSB mutants either defective in ssDNA

binding or in transcriptional activation, indicating that the functions of ssDNA binding and transcriptional activation are independent. They obtained evidence that N4SSB interacts with β' of RNAP and this interaction is necessary for transcription of N4 late genes. N4SSB interacts with the extreme C-terminal region of β' subunit (amino acid 1354 to 1407) (Miller *et al.*, 1997). The level of N4SSB protein is high (10^{-5} M) in the cell during N4 infection, and N4SSB has a high affinity for RNAP. However, N4SSB does not facilitate binding of RNAP to target promoters (Miller *et al.*, 1997), and it is still unclear how N4SSB achieves specificity for target promoter to activate transcription.

1.3 *BACILLUS SUBTILIS* AND ITS DEVELOPMENT AND TRANSCRIPTION REGULATION

1.3.1 Introduction to *Bacillus subtilis*

B. subtilis is a rod-shaped, Gram-positive, and low-G+C-content bacterium commonly found in soil. A member of genus *Bacillus*, phylum Firmicutes, *B. subtilis* can form endospores to protect from the damage caused by multiple stress-inducing conditions and protect the genome from harsh environmental conditions. Unlike its notable relatives *Bacillus anthracis*, which causes anthrax, *B. subtilis* is not a human pathogen. Instead, it is used in food industry in eastern Asia and is also widely applied to the enzyme industry due to its ability to secrete large quantities of enzymes (Westers *et al.*, 2004). *B. subtilis* is also a widely used model organism for studies in molecular biology and biochemistry due to the ease of genetic manipulation, its rapid growth rate,

and its ability to sporulate. Since the genome sequence project of *B. subtilis* was finished and published (Kunst *et al.,* 1997), and the SubtiList database had been built, genome-wide analysis to understand control of gene expression became possible. The genome of *B. subtilis* has 4,214,810 base pairs and includes more than 4,100 protein-coding genes. The identification and annotation of genes helps to further understand the metabolic and developmental pathways in *B. subtilis*. Comparing gene function, organization and regulation of *B. subtilis* with those of Gram-negative *E. coli* shows that proteins involved in macromolecular synthesis, biosynthesis and degradation are well conserved. However, the mechanism of gene regulation, activities of homolog gene products, and mechanisms of cell division are different between *E. coli* and *B. subtilis*.

Since *B. subtilis* inhabits the soil, it has evolved many strategies to alter metabolism and development in order to respond appropriately to harsh environmental fluctuations and nutrient limitation. For instance, when *B. subtilis* enters the stationary growth phase, nutrients become limited for optimal growth, and cells secrete degradative enzymes to utilize nutrients from other resources, which are normally difficult to acquire. Then, *B. subtilis* cells activate systems for motility and biofilm formation (Vlamakis *et al.,* 2013), and produce surfactin and antibiotics to resist possible competitors. Prolonged nutrient depletion at elevated cell density triggers the development of competence and sporulation to cope with the environmental conditions and survive after stress (Dubnau, 1991a, Trach *et al.,* 1991). Herein, these two important processes of adaptation are introduced below.

1.3.2 Development of *B. subtilis* and sporulation

The ability to form dormant and environmentally resistant spores helps *B. subtilis* to survive harsh conditions. The formation of endospores is common to Gram-positive bacteria. The process of sporulation is complex and involves more than 200 gene products in *B. subtilis*. Sporulation is one stage to *B. subtilis* developmental cycle, which proceeds from vegetative growth, to sporulation, germination, and finally outgrowth to regenerate the vegetative cell. Spore formation is initiated by an asymmetrical cell division and differentiation resulting in generation of the mother cell and forespore cellular compartments. This prespore state is followed by spore maturation, involving engulfment of the forespore compartment by the double membrane of the sporulation septum and acquisiton of the proteinaceous spore coat. The mother cell then lyses to release the mature spore. Germination is triggered by amino acids and/or carbohydrates, which leads to outgrowth (Piggot & Hilbert, 2004). At the stationary growth phase, when nutrition is limited and energy is depleted, the alternative σ subunit σ^H factor is produced and the master regulator of sporulation, Spo0A, is activated by the Spo0 phosphorelay involving two-component signal transduction systems. The phosphorelay consists of several histidine kinases (KinA, B, and C), and two phosphorelay proteins (Spo0F and Spo0B). The σ^H factor activates transcription of *kinA* and *spo0F*. Under starvation, the sensor kinases, KinA, KinB, and KinC transfer a phosphoryl group from ATP to Spo0F. The phosphorylated Spo0F transfers the phosphoryl group to Spo0B, and the phosphoryl group is further transferred to response regulator Spo0A (Burbulys *et al.*, 1991). The phosphorylated Spo0A initiates sporulation by activating *spoIIA* and *spoIIE*, for expression and activation of forespore-specific σ^F factor, and *spoIIG* for the expression of

mother cell-specific σ^E factor. The gene product of *spoIIE* also contributes to the asymmetrical division and activation of forespore-specific σ^F; Spo0A also activates genes regulating the site for FtsZ assembly and controls the position of the division septum so that it is formed at a polar position as opposed to the middle of the cell, as is the case during vegetative growth.

At each stage of sporulation, different σ factors regulate gene transcription. Initiation of sporulation starts with aforementioned activation of σ^H and Spo0A in the predivisional cells. After the asymmetrical division, early compartment-specific gene expression is activated by σ^E in the mother cell and by σ^F in the forespore. Notably, σ^E must be proteolytically activated by a membrane bound protease that is activated through a forespore-derived signal that is dependent on the σ^F-form of RNAP (Kroos *et al.,* 1999). During the process of engulfment, proteins produced in the mother cell degrade the septum and the membrane around the prespore migrates. When the membrane fuses at the pole of the cell, the prespore is retained in the mother cell but now detached from the pole. Expression of genes involved in formation of the cortex and coat of the spore is regulated by σ^K in the mother cell and by σ^G in the prespore. Again, proteolytic activation of σ^K is required and is stimulated by forespore-derived signals. At the last stage, when the spore has undergone maturation, the mother cell lyses and spore is released (Piggot & Hilbert, 2004). When the spore encounters nutrient, it will germinate, which requires hydrolysis of the spore cortex peptidoglycan and rehydration of the spore core. This induces transcriptional activity, ribosome formation and protein synthesis. Outgrowth follows, resulting in the release of a vegetative cell from the ruptured spore coat, thus completing the developmental cycle (Setlow, 2003).

1.3.3 Competence of *B. subtilis* and its regulation

An alternative pathway of development is the process of genetic competence establishment, which generates a cell endowed with the ability to take up exogenous DNA. Natural competence is a physiological state that is determined and regulated genetically in many bacterial species, such as *B. subtilis*, *Streptococcus pneumonie*, *S. sanguis*, and *Neisseria gonorrhoeae* (Dubnau, 1991a). The advantages for bacteria to acquire DNA include exchanging genetic materials for adaptation, using those DNA as the template for DNA repair, and as a nutritional resource (Claverys *et al.*, 2006). In *B. subtilis*, competence for DNA transformation develops in 1 to 10% of the cell population in late exponential phase or early stationary phase, when nutrients are limiting (Dubnau, 1991b). This small fraction of cells expresses a high level of the master regulator of competence, ComK, whereas the majority of cells remains in a vegetative state and has a low ComK concentrations (Leisner *et al.*, 2008). ComK activates the transcription of more than 100 genes, many of which are required for DNA uptake, such as *comC*, *comE*, *comF*, *comG* and *nucA* (Berka *et al.*, 2002, Ogura *et al.*, 2002, Dubnau, 1991b).

Activity of ComK is controlled by a regulatory cascade involving many proteins. *B. subtilis* competence is induced by a post-translationally modified 10-amino-acid peptide pheromone, ComX, in cultures of high cell density (Magnuson *et al.*, 1994). The inactive ComX precursor contains 55 residues and its activity requires the proteolytic processing and isoprenylation at a tryptophan residue by the product of its upstream gene, *comQ*. The modified ComX is exported out of the cell and sensed by ComP, the membrane-bound histidine kinase of the ComPA two-component regulatory system, which leads to

autophosphorylation of ComP. The phosphorylated ComP then donates a phosphoryl group to its cognate response regulator, ComA. ComA belongs to the LuxR family containing a HTH DNA binding domain at its C-terminus. Phosphorylation of ComA stimulates its sequence-specific DNA-binding activity. ComA targets the *srfA* operon for transcriptional activation. The *srfA* operon encodes a small peptide ComS and surfactin synthetase, which catalyzes the non-ribosomal synthesis of the peptide antibiotic surfactin. ComS enables the accumulation of ComK in the cell by interacting with MecA. MecA is an adaptor or substrate-recognition factor for the ATP-dependent protease, ClpCP. In non-competent cells, ComK is delivered to the protease by interaction with MecA. In cultures of high cell density, ComS is produced after *srfA* transcriptional activation, and interacts with MecA, thereby releasing ComK from proteolytic control, preventing degradation of ComK (Claverys *et al.*, 2006, Hamoen *et al.*, 2003).

1.4 OXIDATIVE STRESS AND TRANSCRIPTIONAL CONTROL

Bacteria encounter various environmental changes and have to monitor and quickly respond in order to thrive. In the oxygen-rich environment, to gain energy, aerobic organisms use oxygen for respiration or oxidation of nutrients. Invariably, aerobic metabolism gives rise to potentially damaging reactive oxygen species (ROS). In cellular respiratory electron transport chain reaction, molecular oxygen (O_2) is used for electron receptor and is reduced to water. The process of oxygen reduction involves step-by-step single-electron transfer. Enzymes with a reduced flavin cofactor are a major source of

superoxide. Through a series single-electron transfer, the molecular oxygen is reduced to superoxide ($O_2^{-\bullet}$), hydrogen peroxide (H_2O_2), hydroxyl radical ($OH^{\bullet}$), sequentially. Hydroxyl radical in the presence of reduced Fe++ can participate in the Fenton reaction, which leads to macromolecular damage (Imlay, 2003).

Reactive oxygen intermediates are chemically active; and their accumulation can be hazardous to the intracellular environment. In the environment that *B. subtilis* inhabits, many microorganisms compete for space and energy by producing superoxide-generating redox cycling agents and hydrogen peroxide which could be the external sources of ROS (Zuber, 2009). Thus, when the concentration of these reactive oxygen species exceeds the capacity of cell defense, oxidative stress arises (Cabiscol *et al.*, 2000).

ROS can react with free intracellular iron to cause oxidative stress and cell damage. Superoxide, the by-product of O_2 reduction in the electron transport chain can attack enzymes containing iron-sulfur clusters, which causes the loss of enzyme activity and release of reduced iron ions (Fe^{2+}). The ferrous iron reacts with hydrogen peroxide and generates hydroxyl radical by Fenton reaction (Cabiscol *et al.*, 2000). Hydroxyl radicals are highly reactive and harmful to DNA, RNA, proteins and lipids in the cells. For DNA damage, free radicals attack both base and sugar moieties and cause DNA breaks in the backbone. Free radicals can also attack poly-unsaturated fatty acid in membranes and lipids undergo peroxidation and are degraded. Hydrogen peroxide can also oxidize thiols in many enzymes, and leads to enzyme inactivation and protein denuration (Storz & Imlay, 1999, Cabiscol *et al.*, 2000, Touati, 2000, Imlay, 2003, Zuber, 2009).

Cells have evolved defense mechanisms to prevent ROS damage by maintaining the concentration of ROS at acceptably low levels, or to repair damage caused by oxidation.

Nonenzymatic antioxidants, such as NADPH and NADH pools, and glutathione (GSH), are constitutively present to maintain a reducing environment in the cells. Bacillithiol is a major low-molecular-weight thiol (LMW) in *B. subtilis* and maintains the reducing environment of the cytosol as a redox buffer (Newton *et al.*, 2009). Under oxidative stress, disulfide bonds form between cysteine thiols in proteins or between protein thiols and LMW thiols, and these LMW thiols by interacting with protein thiols, protect cysteine from further oxidation which may cause irreversible oxidative damage in proteins (Gaballa *et al.*, 2010). Some specific enzymes also function in antioxidant protection. Superoxide dismutase converts superoxide into hydrogen peroxide and oxygen. Catalase, glutathione peroxidase, and peroxiredoxins detoxify peroxides into alcohols or water. Disulfide oxidoreductases, such as thioredoxin and glutaredoxin, reduce disulfide bonds in cytosolic proteins. Oxidized glutaredoxin is reduced by GSH, and oxidized thioredoxin is reduced by thioredoxin reductase. Under oxidative stress, these proteins can be upregulated to protect cells from ROS and restore reducing environment. Other enzymes, such as those in DNA-repair system, proteolytic and lipolytic enzymes, can also be induced by oxidative stress to repair oxidative damage. Moreover, since iron plays an important role in cell function, and also a potential damaging effect under oxidative stress, its solubilization and metabolism is tightly regulated in bacteria. The uptake and entrance of iron into the cell requires specific receptors, and the storage of iron in the cell is dependent on bacterioferritin and ferritin-like proteins (Storz & Imlay, 1999, Cabiscol *et al.*, 2000, Touati, 2000, Imlay, 2008).

In *B. subtilis*, the response to oxidative stress is governed by the general stress RNAP sigma factor σ^B (mentioned in 1.2.3.1), PerR (peroxide resistance regulator), OhrR

(organic hydroperoxide resistance regulator) (Helmann *et al.*, 2003), and Spx (suppressor of *clpP* and *clpX*) (Nakano *et al.*, 2003a).

1.4.1 PerR

PerR is a dimeric zinc-binding protein which contains an N-terminal winged helix DNA-binding domain, C-terminal dimerization domain containing a Cys4 Zn-binding site and a regulatory site coordinating either a Mn^{2+} or Fe^{2+} metal ion (Lee & Helmann, 2006b). It belongs to the ferric uptake repressor (Fur) family and is the major regulator of the peroxide stress response. The binding of Zn^{2+} serves as a structural role, and the binding of Fe^{2+} is for peroxide sensing (Lee & Helmann, 2006a). The Fe^{2+} is coordinated with 3His and 2Asp residues, and the Fe^{2+}-bound PerR dimer recognizes a dyad symmetric promoter sequence to repress target gene expression. When *B. subtilis* cells are exposed to hydrogen peroxide, H_2O_2 interacts with Fe^{2+} and oxidizes the coordinating His residue to the 2-oxo-His derivative, which leads to a conformational change of the oxidized PerR. Thus, PerR can no longer bind to DNA, and target genes involved in detoxifying peroxides and preventing DNA damage are derepressed (Lee & Helmann, 2006b). Genes controlled by PerR include *mrgA* which encodes a DNA-binding protein that sequesters iron to protect DNA from Fenton chemistry. Also, *katA* (catalase), *ahpCF* (alkylhydroperoxide reductase), heme biosynthsis genes are members of the PerR regulon and are induced in the presence of H_2O_2 (Duarte & Latour, 2010, Zuber, 2009, Helmann *et al.*, 2003). Even though Mn^{2+} can bind to PerR, the Mn^{2+}-bound

PerR is much less sensitive to peroxide and retains repressive activity towards target gene transcription (Herbig & Helmann, 2001).

1.4.2 OhrR

Compared to PerR, OhrR (organic hydroperoxide resistance regulator) is weakly responsive to H_2O_2, but strongly sensitive to organic hydroperoxides (OHPs). OHP can directly oxidize macromolecules and lead to the generation of reactive lipid radicals, which are toxic. *B. subtilis* has two *ohr* (organic peroxide reductase) paralogs, *ohrA* and *ohrB*. The expression of *ohrB* is regulated by the general stress response σ^B factor, while the regulation of *ohrA* is controlled by OhrR (Fuangthong *et al.*, 2001). OhrR belongs to MarR family of repressor proteins, and is a thiol-based sensor of OHP. OhrR contains a DNA-binding domain and a peroxide-sensing cysteine (Cys15). The reduced form of OhrR homodimer binds to a sequence of pseudodyad symmetry in target promoter regions, such as *ohrA* (organic hydroperoxide reductase) and represses target gene expression (Hong *et al.*, 2005). When sensing OHPs, OhrR undergoes two-step oxidation, in which the Cys15 is first oxidized to sulfenic acid, and further forms a mix disulfide in the presence of biothiols, such as bacillithiol (Lee *et al.*, 2007). After disulfide formation, the oxidized OhrR loses its DNA-binding activity, releasing the repression of *ohrA* (Lee *et al.*, 2007, Hong *et al.*, 2005).

1.4.3 Spx

Spx belongs to the ArsC (arsenate reductase) family and is a highly conserved transcriptional regulator in low-G+C-content Gram-positive bacteria (Zuber, 2004). It is essential for survival of *B. subtilis* under oxidative stress, and can both repress and activate different sets of genes through its interaction with the C-terminal domain of RNAP alpha subunit (αCTD) (Fig. 1) (Nakano *et al.*, 2003c, Nakano *et al.*, 2003a). Spx concentration in normal conditions is maintained at a low level through the transcriptional repression by PerR and YodB repressors and by YjbH-mediated ClpXP proteolysis (Garg *et al.*, 2009, Larsson *et al.*, 2007, Leelakriangsak & Zuber, 2007, Leelakriangsak *et al.*, 2007). The N-terminus of Spx contains a CXXC motif, which serves as a thiol-based redox switch for transcriptional control (Nakano *et al.*, 2005). Under oxidative stress, the amount of Spx protein increases due to the de-repression of the *spx* gene, and decreased proteolysis. Meanwhile, an intramolecular disulfide bond forms between the cysteine residues at position 10 and 13, and the oxidized form of Spx activates genes such as *trxA* (thioredoxin) and *trxB* (thioredoxin reductase) that function in detoxification and restoring thiol homeostasis. Previous studies showed that Spx directly activates the transcription of *trxA* and *trxB*, and formation of the disulfide bond is necessary for this activation (Nakano *et al.*, 2003a, Nakano *et al.*, 2005)

The mechanism of negative transcriptional control by Spx has been demonstrated (Nakano *et al.*, 2003c, Zhang *et al.*, 2006). Spx represses activator-stimulated gene transcription in the transcriptional control of genetic competence. In the mechanism of Spx-dependent transcription repression, Spx itself does not directly interact with promoter region DNA. Through directly interacting with the same surface on αCTD of

RNAP where ComA interacts, Spx prevents the ComA/RNAP interaction and the formation of initiation complex, and thus, blocks the activator-stimulated transcription. However, how Spx activates transcription of *trxA* and *trxB* genes in response to oxidative stress is still unclear.

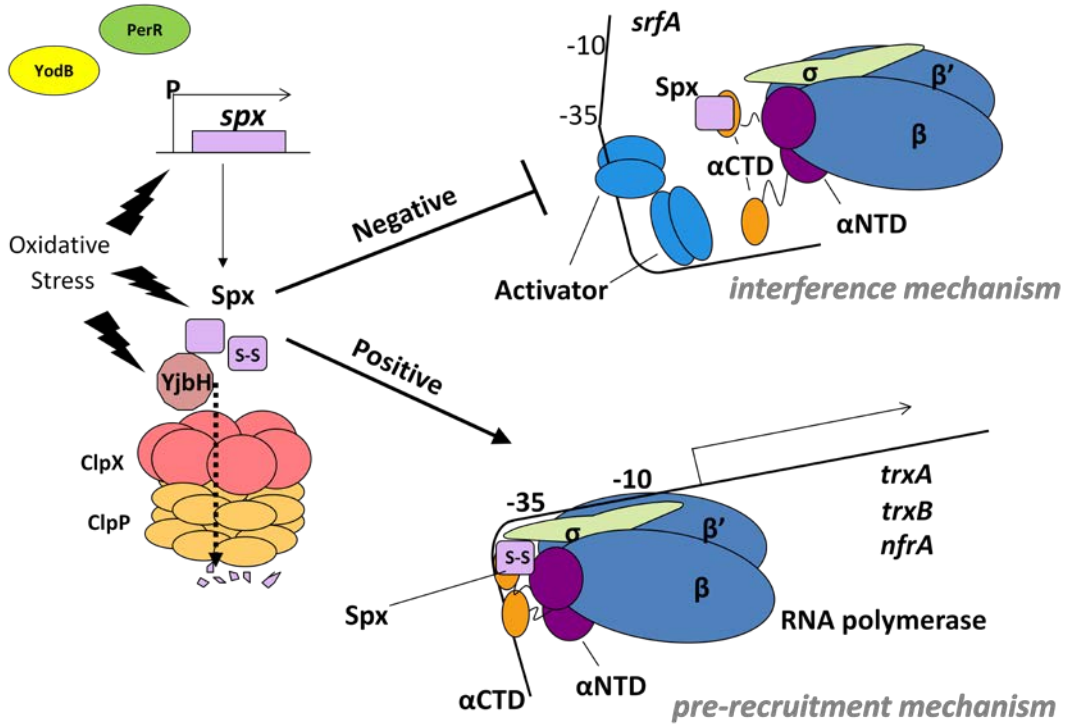

Figure 1.2. Scheme of Spx regulation in response to oxidative stress in *Bacillus subtilis*. Under oxidative stress, the level of Spx increases through inactivation of PerR and YodB repressors and decreased YjbH-mediated ClpXP proteolysis. Spx interacts with RNAP αCTD and either negatively regulates activator-mediated transcription, such as ComA-activated *srfA* transcription, or positively regulates gene involved in thiol homeostasis.

Some of the residues responsible for the interaction between Spx and αCTD of RNAP have been identified (Newberry *et al.*, 2005). The glycine residue at position 52 of Spx and the tyrosine residue at position 263 of α1 helix in the αCTD of RNAP are part of the binding interface of the two proteins. Mutation of either one of these residues abolished the Spx-dependent transcriptional repression and activation (Nakano *et al.*, 2000, Newberry *et al.*, 2005). For the repression of ComA-dependent transcription, the Cys265 and Lys267 located in the α1 helix in αCTD of RNAP are required (Zhang *et al.*, 2006), and are likely involved in Spx/RNAP interaction.

Though confirmed by DNase I footprinting and EMSA that Spx does not bind to promoter DNA by itself, the sequence downstream from -50 in the *trxB* promoter and -48 in the *trxA* promoter were shown to be required for full transcriptional activation (Nakano *et al.*, 2005), and a Spx response cis-acting element in this promoter region was identified (Reyes & Zuber, 2008). An AGCA-like motif was located around position -44 (AGCA) and -33 (AGCG) in *trxA* and *trxB* promoters (Fig.1.3). Mutations in the -44 cis-acting elements of *trxB* promoter abolished or substantially diminished Spx-dependent transcription in vivo, and EMSA results also showed that both of -44 and -33 elements in *trxB* promoter are required for interaction with αCTD/Spx complex (Nakano *et al.*, 2010b). These results suggested that the -44 element is the putative site for interacting with αCTD/Spx complex. More recently, ChIP-chip analysis using an epitope-tagged version of Spx recovered DNA that interacts with Spx/RNAP in vivo. Alignment of the sequences confirmed that an element of A/TGCA/T centered at around -44 with repect the transcription start site was commonly found the Spx/RNAP-interacting DNA (Rochat *et al.*, 2012). The *trxB* promoter region has two potential Spx response elements, the

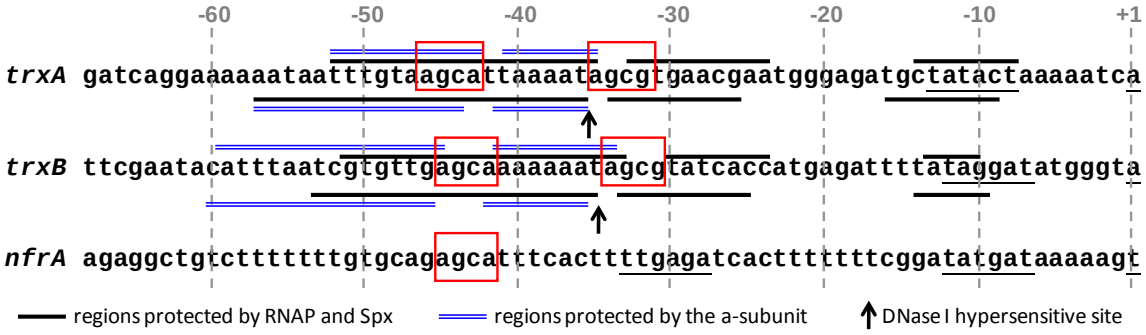

aforementioned sequence at -44, and a potential Spx response element at -33, which would overlap with the -35 region of the core promoter.

Figure 1.3. Promoter regions of *trxA*, *trxB* and *nfrA* genes. The sequences of *trxA*, *trxB* and *nfrA* promoter were aligned together. Transcription start sites (+1) and both the -10 and -35 elements are underlined. Putative Spx response cis-acting elements are shown in boxes.

Previous studies of the Spx crystal structure showed that a significant conformational difference is found between oxidized and reduced Spx, whereby the helix α4 of the reduced mutant Spx structure (residues S61 to N68 in oxidized Spx) unfolds and rotates (Nakano *et al.*, 2010a). Mutagenesis studies also showed that residues in or near helix α4 of Spx are important for *trxB* activation but not for *srfA* repression by ComA activator interference, and the αCTD/Spx(R60E) complex failed to interact with *trxB* promoter DNA in EMSA (Nakano *et al.*, 2010a). It indicates that R60 in helix α4 may be involved in DNA interaction.

Table 1.1 shows all the residues in Spx that are involved in transcription, proteolysis, and redox sensing, including formerly identified and those identified in my work presented in later chapters.

Table 1.1 Identified Spx residues and their functions

Spx residue	Function	Reference
C10, C13	Redox sensing, intramolecular disulfide formation	(Nakano *et al.*, 2005)
G52	αCTD interaction	(Newberry *et al.*, 2005)
R60	DNA binding	(Nakano *et al.*, 2010b)
R91	α interaction	This study (Lin *et al.*, 2013)
R92	Redox control	This study (Lin *et al.*, 2013)
A130, N131	ClpXP-proteolysis	(Nakano *et al.*, 2003a)

1.5 SPX FAMILY OF PROTEINS

In *B. subtilis*, an Spx paralogue, MgsR (modulator of the general stress response) expressed exclusively in a σ^B-dependent manner, was identified in response to ethanol stess (Reder *et al.*, 2008). MgsR protein is functionally and evolutionarily related to Spx as a global transcription regulator. MgsR-regulated genes are subject to both positive and negative transcriptional control under ethanol stress. The CXXC motif and the glycine residue involved in αCTD interaction are conserved in MgsR and necessary for MgsR activity (Reder *et al.*, 2008). Similar to Spx, MgsR activity is also controlled at multiple levels: a positive autoregulatory loop on *mgs*R transcription, a post-translational redox-sensitive activation by intramolecular disulfide formation in response to ethanol stress,

and proteolytic degradation of MgsR by both the ClpXP and ClpCP proteases (Reder *et al.*, 2012).

Spx is highly conserved in Gram-positive bacteria. A large number of Spx-like proteins were found and identified in *B. subtilis* (Spx) (Nakano *et al.*, 2001), *B. anthracis* (SpxA1 and SpxA2) (Barendt, Zuber *et al.* unpublished), *Lactococcus lactis* (TrmA and SpxB) (Duwat *et al.*, 1999, Frees *et al.*, 2001, Veiga *et al.*, 2007), *Listeria monocytogenes* (YjbD) (Borezee *et al.*, 2000), *Streptococcus mutans* (SpxA and SpxB) (Kajfasz *et al.*, 2009, Kajfasz *et al.*, 2010), *S. pneumoni*ae (SpxA1 and SpxA2) (Turlan *et al.*, 2009), *S. sanguinis* (SpxA1) (Chen *et al.*, 2012), and *Staphylococcus aureus* (Spx) (Pamp *et al.*, 2006). All of these Spx proteins perform important roles in response to general stress. The number of paralogous Spx-like proteins varies in different bacteria. In *L. lactis*, there are up to seven paralogs of Spx/TrmA family (Veiga *et al.*, 2007).

Turlan *et al.* performed a bioinformatic analysis on ArsC/Spx-like proteins in different species. They retrieved proteins containing the COG1393 (the arsenate reductase and related proteins in the glutaredoxin family) domain and constructed the phylogenetic tree of COG1393 domains from 781 prokaryotic genome sequences (Fig.1.4) (Turlan *et al.*, 2009). The sequences partitioned into four distinct clades, and all the Spx-like proteins investigated partitioned into the same group, ArsC-Spx (cd03032).

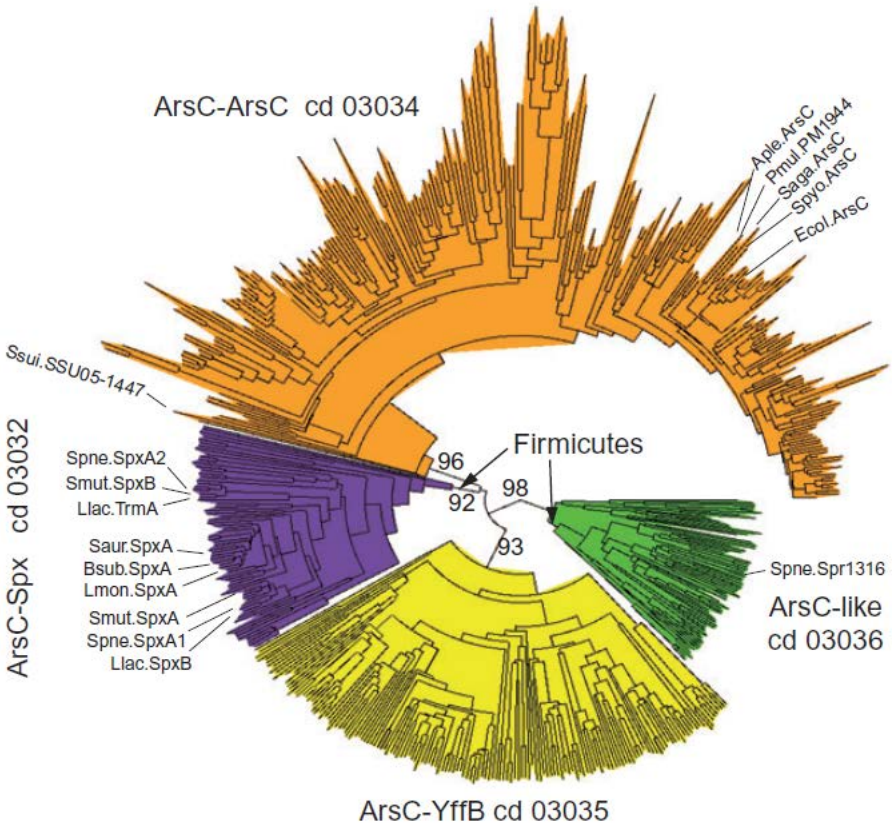

Figure 1.4. Phylogenetic tree of the COG1393 (arsenate reductase and related proteins) domains (Turlan *et al.*, 2009). The phyogenetic analysis of Spx-like proteins in different bacterial species was done by Turlan *et al*. All the Spx-like proteins investigated were partitioned into the ArsC-Spx group. Abbriviations for ArsC-Spx proteins: from *S. pneumoniae*, Spne; *B. subtilis* Spx, Bsub.SpxA; *S. aureus*, Saur.SpxA; *L. lactis* TrmA and SpxB, Llac.TrmA and Llac.SpxB, respectively; *L. monocytogenes* Spx/YjbD, Lmon.SpxA; *S. mutans* SpxA and SpxB, Smut.SpxA and Smut.SpxB respectively. Abbriviations for ArsC-ArsC proteins: *S. suis*, Ssui.SSU05-1447;*S. agalactiae*, Saga.ArsC; *S. pyogenes*, Spyo.ArsC; *Actinobacillus pleuropneumoniae*, Aple.ArsC; *Pasteurella multocida*, Pmul.PM1944; *E. coli*, Ecol.ArsC.

The objective for the research presented herein is to examine through mutational analysis, as well as analyses of Spx activity and interaction with RNAP and promoter DNA, the structural requirements for productive engagement of Spx with the transcription initiation complex. The data generated from the work has provided information that was utilized to formulate a model of how Spx activates transcription initiation from promoters of genes under its control.

CHAPTER 2

MATERIALS AND METHODS

2.1 RNA POLYMERASE PURIFICATION (SAd POLYMERASE)

In the studies presented in this thesis, three forms of purified *B. subtilis* RNA polymerase were used. They are generated from strains bearing an allele of *rpoC* that contains a sequence specifying a His_{10} tag at the C-terminal end of the β´ subunit (Qi & Hulett, 1998). The His-tagged prolymerase was purified from derivatives of strain JH642 (*trpC2 pheA*) that bear the *rpoCHis*$_{10}$ alelle. In addition to this form of the RNAP, the σ^A-depleted RNAP (SAd-RNAP) was purified from ORB5853 (Zuber *et al.*, 2011). The third form of RNAP was assembled in vitro by incubating SAd-RNAP with purified σ^A protein. ORB5853 is a JH642 derivative, bearing the *rpoCHis*$_{10}$ allele and a mutation in *rpoD*(*sigA*), L366A (kindly provided by C. P. Moran, Jr, Emory University), which weakens the interaction of the σ^A(L366A) to RNAP core enzyme. Thus the mutant σ^A was removed from RNAP after a three-column purification procedure.

To purify His-tagged RNAP, strains were grown in 2xYT liquid medium with chloramphenicol (linked to *rpoCHis*$_{10}$) and neomycin (linked to *rpoDL366A*) at 37°C until the OD_{600} of the cell culture reached 0.8-0.9 (between mid and late exponential phase). Cells were harvested by centrifugation at 2,000 xg for 25 min. The pellets were frozen at –80°C at least overnight prior to purification. Cells from 6 liters of culture were resuspend in lysis buffer (50 mM Tris-HCl pH7.8, 100 mM NaCl, 5 mM $MgCl_2$, 20%

glycerol, 5mM β-mercaptoethanol) with protease inhibitor cocktail (a tablet of Complete, Mini, EDTA-free, Roche) and were broken with three passes through a French press at 1000 psi. The lysate was centrifuged at 23,360 xg and the cleared supernatant was passed through a Millipore filter (5 μm, Millipore). The filtered cell lysate was mixed with 6 ml of Ni-NTA agarose (PerfectPro, 5prime) in a column and shaken at 4°C for an hour. After draining the resin, the beads were washed with 20 column volumes of lysis buffer containing 30 mM imidazole. RNAP was eluted with 100 ml of lysis buffer containing 200 mM imidazole. The RNAP solution from Ni-NTA column was applied onto a Heparin-Agarose column, and protein was eluted with a gradient from 100 to 800 mM NaCl in lysis buffer. Collected fractions containing RNAP were identified by SDS-polyacrylamide gel electrophoresis and staining with coomassie blue. The pooled fractions were diluted into a no salt buffer solution (50 mM Tris-HCl pH7.8, 5 mM $MgCl_2$, 20% glycerol, 5 mM β-mercaptoethanol) until the concentration of NaCl was reduced to around 100 mM NaCl. The RNAP solution was then applied to a Bio-Rad High Q cartridge column, and purified RNAP was eluted with a gradient from 100 to 800 mM NaCl in the same buffer and concentrated with an Amicon Ultra-15 Centrifugal filter (3 kDa, Millipore) until desired concentration reached. The RNAP was then dialyzed against storage buffer (10 mM Tris-HCl pH7.8, 100 mM KCl, 5 mM $MgCl_2$, 0.1 mM EDTA, and 50% glycerol) and stored at –20°C. Protein quality was examined on SDS-PAGE (Fig. 2.1).

To test purified RNAP activity, in vitro transcription of a σ^A-dependent promoter, *rpsD* (encoding ribosomal protein S4) was performed. A linear *rpsD* promoter DNA template was generated by PCR with oligonucleotides oSN03-86 and oSN03-87 (length

of PCR fragment: 186 bp, length of transcript: 71 nt). For transcription reactions, 10 nM of the template and 50 nM of holo-RNAP or SAd-RNAP were incubated without or with 50 nM σ^A in 17.8 μl of buffer containing 10 mM Tris-HCl pH 8.0, 50 mM NaCl, 5 mM $MgCl_2$, and 50 mg/ml BSA. After 10-min incubation at 37°C, 2.2 μl of nucleotide mixture (200 mM ATP, GTP and CTP, 10 mM UTP, 5 mCi α-32P-UTP) was added. After incubation at 37°C for 2, 4, 8, and 12 min, 10 μl of stop solution (1 M ammonium acetate, 0.1 mg/ml yeast RNA, and 0.03 M EDTA) was added to the reaction. The mixture was precipitated with ethanol and the pellet was dissolved with 5 μl of formamide-dye (0.3% xylene cyanol, 0.3% bromophenol blue, and 12 mM EDTA dissolved in formamide). The samples were heated at 90°C for 2 min and were applied to an 8% polyacrylamide-8M urea gel in TBE buffer (89 mM Tris base, 89 mM boric acid, 2 mM EDTA). Gels were dried on a vacuum gel dryer for 90 min. The dried gels were scanned on a Typhoon Trio+ variable imager (GE Healthcare). The purified SAd-RNAP is fully activated with supplement of σ^A, but unable to catalyze *rpsD* transcription in the absence of σ^A (Fig.2.1B).

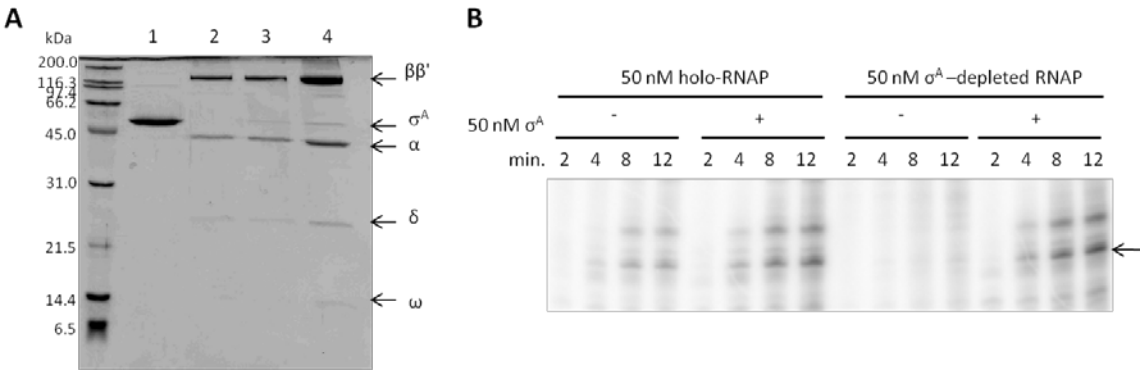

Figure 2.1. Purified *B. subtilis* RNAP and its activity. (A) Purified proteins on SDS-PAG. Purified σ^A, lane 1; SAd-RNAP, lane 2, RNAP holoenzyme purified from MH5636, lane 3; higher concentration of RNAP holoenzyme to visualize ω subunit, lane 4. (B) In vitro transcription of *rpsD*. The arrow indicates the position of *rpsD* transcript.

2.2 ECTOPIC EXPRESSION OF *SPX* ALLELES AND CONSTRUCTION OF REPORTER FUSION

Two integration vectors of *B. subtilis* were used to study the in vivo activity of *spx* mutant alleles, pDR111 for expressing ectopic *spx* alleles in vivo, pDG793 for a Lac-reporter fusion system.

pDR111 is a vector that allows the integration of expression constructs into the non-essential *amyE* (amylase) locus (Britton *et al.*, 2002). Since Spx is rapidly degraded by ClpXP protease in vivo, the ClpXP protease-resistant Spx in which the last two amino acid residues are replaced with aspartate residues were used in the study. Thus, the cloned spx^{DD} alleles are introduced at the *amyE* locus and transcribed from the isopropyl-β-d-thiogalactopyranoside (IPTG)-inducible $P_{spankhy}$ promoter. When a *B. subtilis* strain is

transformed with pDR111 derivatives, the *spx* allele will be integrated into *amyE* locus (Fig. 2.2) by double crossover recombination, and the transformants are screened for *Amy*$^-$ (amylase-negative) phenotype.

pDG793 (Guerout-Fleury *et al.*, 1996) is a *thrC* integration plasmid which contains a promoter-less reporter *lacZ* gene. By cloning promoter DNA fragments generated by PCR into pDG793, and transforming *B. subtilis*, the specific promoter-*lacZ* fusion is introduced into the *thrC* locus by double-crossover recombination, and the transformants are screened for *Thr*$^-$ (threonine auxotroph) phenotype. The activity of the fused promoter can be evaluated and quantified by β-galactosidase assay as described by J. Miller (Miller, 1972).

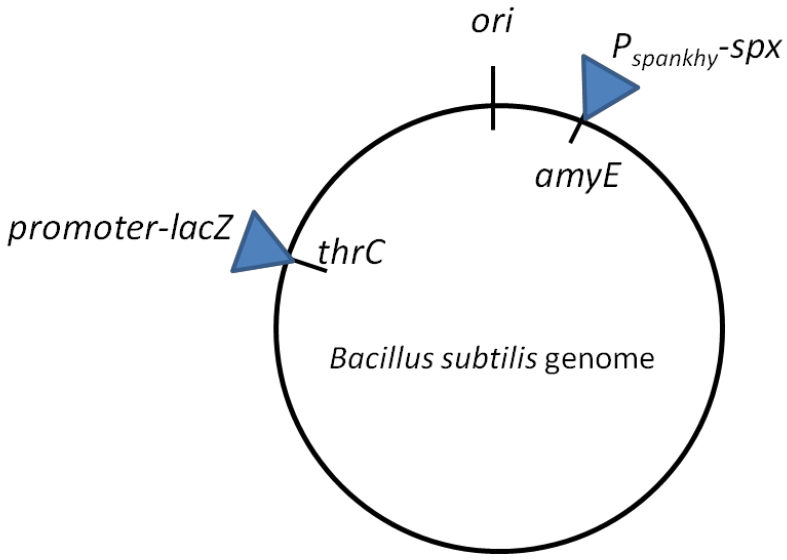

Figure 2.2. The locations of *amyE* and *thrC* loci in simplified *B. subtilis* genome map. In this study, pDR111 was used to clone *spx* and its variants, for ectopic expression under IPTG-inducible Pspankhy control at the *amyE* locus. pDG793 was used to fuse a

promoter region with *lacZ* reporter. The plasmid can undergo recombination with the chromosome at the *thrC* locus.

2.3 SUPERCOILED DNA TEMPLATE PREPARATION FOR IN VITRO TRANSCRIPTION

One of the drawbacks of using linear promoter DNA templates for in vitro transcription is increasing the possibility to obtain many unwanted, non-specific transcripts due to end-to-end transcription, template-jumping, or promoter interference. Hence, if the specific transcript is not dominant, its transcription may be difficult to detect. In addition, some transcription activators or repressors require supercoiled templates for optimal productive DNA interaction. The DNA within the nucleoid of the bacterium is thought to be supercoiled most of the time, so the use of supercoiled promoter DNA is believed to be more authentic in reflecting the DNA environment in the bacterium (Dorman, 2006).

Plasmid pRLG770 is a super-coiled DNA template designed for in vitro transcription using *E. coli* RNA polymerase (Ross *et al.*, 1990). The plasmid contains a cloning site for inserting promoter DNA of interest, two terminators downstream of the promoter insert to prevent read-through transcription, and a RNA-1 transcription unit that serves as an internal control in in vitro transcription experiments. Recently, Don Walthers successfully established a system for use of pRLG770 derivatives as supercoiled DNA templates for in vitro transcription using *B. subtilis* RNAP in our lab.

To generate a supercoiled template, a ~250-bp fragment of promoter region was amplified by PCR with oligonucleotide pair containing *EcoR*I and *Hin*dIII sites, and cloned into a TOPO vector with Zero Blunt® TOPO® PCR Cloning Kit (Invitrogen, Life technologies) for sequencing purpose. After confirming the sequence, a cut-and-paste cloning method was used to cut promoter fragment with *EcoR*I and *Hin*dIII from TOPO vector, and insert the fragment to EcoRI/*Hin*dIII digested pRLG770. Colony PCR-screens of the transformants containing promoter insert was conducted to obtain the plasmid template for transcription experiments.

To extract plasmids for in vitro transcription, modified Qiagen mini-preps (Qiagen) procedure was applied to reduce nicked, poor quality DNA, which is unsuitable for in vitro transcription as the quality of supercoiled template is important for effective in vitro transcription.

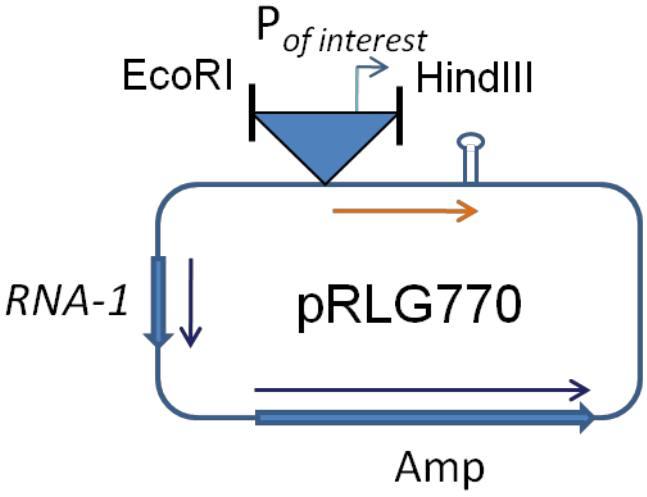

Figure 2.3. Map of pRLG770 (originally drawn by Don Walthers). The pRLG770 is a vector for in vitro transcription. In the vector, there is a selective marker for cloning, Amp for ampicillin-resistance, a gene coding for RNA-1, which is used for an internal

control of in vitro transcription reaction, and a cloning site for cloning of a promoter DNA fragment into the vector for transcription study. Terminators (blue inverted loop structure at end of orange arrow) located downstream of the promoter cloning site can prevent read-through transcription.

2.4 PROMOTER DNA-RNAP CROSSLINKING

The steps of nucleotide-specific DNA-Protein crosslinking experiment are summarized in Fig. 2.4. The protocol was described previously (Reyes & Zuber, 2008) adapted from the original method by Bartlett *et al.*(Bartlett *et al.*, 2000), and some modifications were made in the study presented herein.

2.4.1 Synthesis of ^{32}P-labeled crosslinking DNA probe

2.4.1.1 Preparation of streptavidin-bound DNA promoter

Biotinylated promoter DNA fragment bearing the sequence of a *Hae*III site near the biotin tag, was generated by PCR using forward 5'- biotinyl-oligonucleotide (oDYR06-02 for *trxB*), and oligonucleotide which is the reverse complement to the downstream portion of the promoter sequence (oDYR06-03 for *trxB*). The DNA fragment was purified by using low-melting temperature agarose gel extraction method, followed by ethanol precipitation and the pellet was dissolved in water.

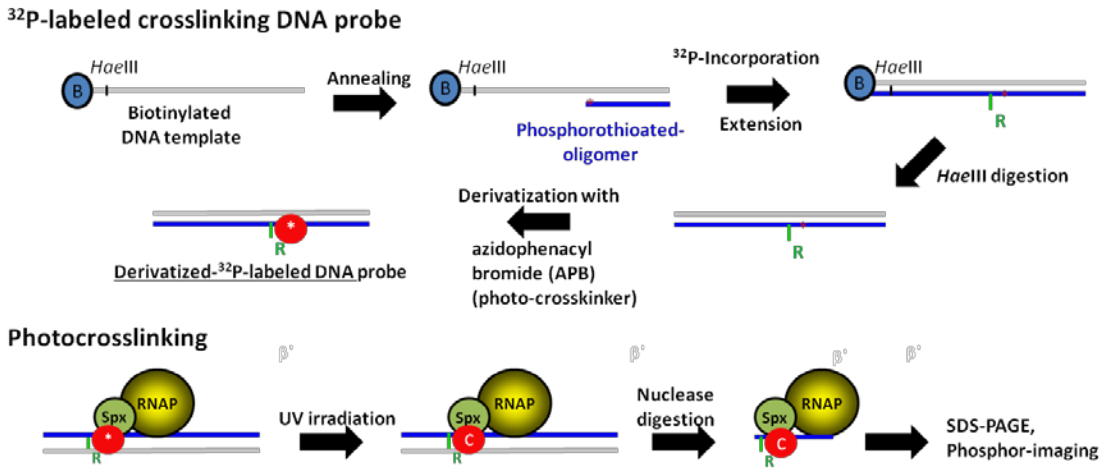

Figure 2.4. Summary of the method of promoter DNA-RNAP crosslinking experiment. To generate ^{32}P-labeled crosslinking DNA probe, biotinylated promoter DNA templates were bound to streptavidin resins and denatured to anneal the oligomers bearing a phosphorathioate modification at specific nucleotide for coupling the photo-activated crosslinker. Next to the phosphorothioated nucleotide, a α^{32}P-labeled nucleotide was incorporated and then the extension reaction was continued with unlabeled dNTP to create a dsDNA template. The streptavidin resins and biotin groups were remove by HaeIII digestion, and the dsDNA was derivatized with photo-crosslinker, APB, at the phosphorothioated site to generate a crosslinking probe. For the photo-crosslinking experiment, Spx and RNAP were incubated with the probe followed by UV irradiation to trigger the covalent linkage formation between photo-crosslinker and proteins in vicinity of crosslinking agent. The overhanging DNA in the complex was digested by DNase I. The result was resolved by SDS-PAGE and the proteins bound to radioactive labeled DNA fragment were visualized by phosphor-imaging.

For each probe, 20 μl of 1μM biotinylated DNA fragment and 10 μl of a suspension of the streptavidin-conjugated magnetic beads (Dynabeads® M280 streptavidin, Invitrogen) are required. To immobilize biotinylated DNA fragment onto the streptavidin beads, the beads were first washed twice with 200 μl of 1X Binding & Washing Buffer (B&W Buffer: 5 mM Tris-HCl, pH 7.5, 0.5 mM EDTA, 1 M NaCl) by resuspension and quick spin in a microcentrifuge. After each spin, the tube was placed on a magnetic stand to collect the beads, and the supernatent was removed. The optimal volume for interaction of biotinylated DNA and streptavidin beads is at least 200 μl, which means that at least 4 probes are prepared at one time. Hence, to prepare 4 probes, 80 μl of biotinylated DNA and 80 μl of 2X B&W buffer are mixed and incubated with 40 μl of washed beads in 1X W&B buffer at room temperature for 1 hr. The beads were briefly spun in a microcentrifuge, and the supernatant was removed. Two hundred μl of 0.1N NaOH was added to denature the DNA on beads, leaving the biotinylated single strand attached to the beads. After a 10-min incubation at 30°C, the beads were collected by brief centrifugation and the supernatant was removed, followed by a series of washing steps with 200 μl of 0.1 N NaOH, twice with 200 μl of 1X B&W buffer, 200 μl of buffer containing 5 mM Tris-HCl, pH 7.5, 0.1% BSA. Finally, the beads were resuspended in 40 μl of the same buffer, and aliquots of the bead resuspension were transferred to 4 microcentrifuge tubes. Each tube contains 10 μl of the bead-bound single-stranded DNA for one probe.

2.4.1.2 Synthesis of linear double-stranded DNA containing single phosphorothioate and adjacent radiolabeled deoxynucleotide.

To generate a double-strand DNA probe, 5 μl of 4 μM oligonucleotide containing a single 3' phosphorothioate substitution at the desired nucleotide position on the promoter, 2.5 μl of 10X NEBuffer 2 (New England BioLabs), and 7μl of water were added in each tube containing 10 μl of the bead-bound ssDNA. The reaction was incubated at 90°C for 3 min and followed by incubation at 42°C for 30 min to anneal the oligonucleotides to the strepavidin-bound ssDNA.

To radiolabel at the position adjacent to the phosphorothioate modification, 1 μl of the 20 μCi/ μl α-^{32}P-dNTP (6,000 Ci/mmol, MP Biomedicals) and 10 μl of 0.25 U/ μl Klenow Fragment (3'→ 5' exo-) enzyme (New England BioLabs) were added, and incubated at 37°C for 30 min. The choice for α-^{32}P-nucleotides is dependent on the type of nucleotide next to the phosphorothioate modified position. The excess free α-^{32}P-dNTP was washed from the beads with two applications of 100 μl 1X NEBuffer 2 and magnetic collection of DNA-bound beads.

The full-length extension was performed by incubated radiolabeled probes with 5U of Klenow Fragment (3'→ 5' exo-), 1.3 mM dNTP mix, in 30 μl of 1X NEBuffer 2 at 37°C for 30 min. The extension reaction was stopped by washing off Klenow enzyme and free dNTP by centrifugation and resuspension in 1X NEBuffer 2. Fifty μl of the 1X NEBuffer 2 containing 10 U of *Hae*III (New England BioLabs) was added to the DNA-bound beads. Cleavage with *Hae*III at the site near the biotin tag was conducted at 37°C for at least 3 hr, resulting in the release of the radiolabelled DNA from the streptavidin beads.

After cleavage, brief centrifugation and immobilization of the beads on magnetic rack, the supernatant was collected, and the beads were washed twice with 75 μl of water to obtain a total 200 μl of DNA solution. The radiolabeled DNA was subsequently extracted with phenol-chloroform-isoamyl alcohol (PCI) solution and precipitated overnight with ethanol in the presence of NH_4OAc and 1mg of glycogen. DNA fragement was dissolved in 27 μl of water.

2.4.1.3 Derivatization of phosphorothioate-containing DNA with azidophenacyl bromide (APB)

The promoter DNA released from the beads was derivatized with 45 μl of 100 mM *p*-azidophenacylbromide (APB) in 100 mM triethylammonium bicarbonate buffer (TEAB, pH 8.0) in the dark at room temperature for overnight. The derivatized products were then PCI-extracted twice, ethanol-precipitated, and dissolved in 50 μl of distilled water. The c.p.m. (count per minute) of each probe was measured by scintillation counter, and the concentration of DNA was diluted to 10,000 c.p.m. per μl.

2.4.2 Template activity of phosphorothioate and APB-derivatized probes in transcription reactions

To test whether the phosphorothioate modification and APB-derivatization of the DNA probe affected binding of RNAP and Spx to the promoter DNA, in vitro transcription was performed by using non-radioactive phosphorothioate probes and APB-

derivatized probes as transcription templates. To generate non-radioactive probes, dNTP, instead of α-^{32}P-dNTP, was incorporated next to the phosphorothiate modified nucleotide, and followed by normal extension reaction described above. For phosporothioate probes, APB-derivatization step was omitted, but all other procedures were followed. The control promoter template was generated by PCR amplification with oligonucleotides oDYR06-02 and oDYR06-03.

The in vitro transcription reaction was conducted as described above by using modified *trxB* promoter DNA probes, -36, -38, -40, -44. Both phosphorothioate probes and APB-derivatized probes can serve as template for Spx-dependent *trxB* transcription (Fig. 2.5A, B).

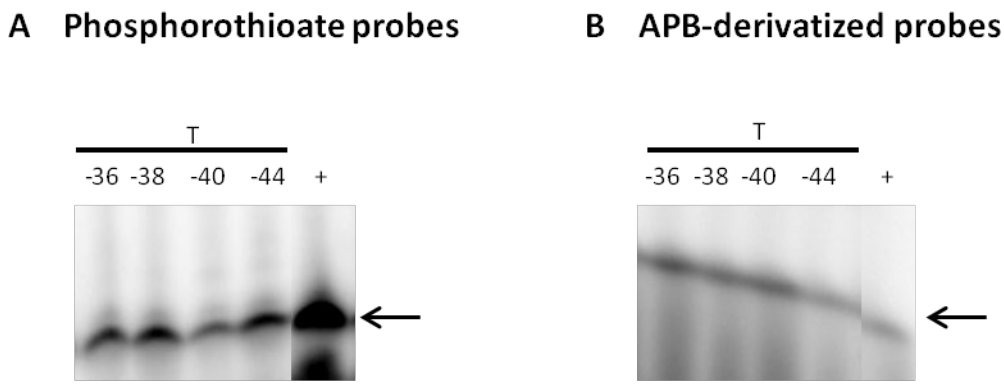

Figure 2.5. In vitro transcription with *trxB* phosphorothioate modified probes (A) or APB-derivatized probes (B). The modified *trxB* promoter templates at position -36, -38, -40 and -44, were incubated with 25 nM of *B. subtilis* SAd-RNAP, 25 nM σ^A, and 75 nM Spx for 10 min and the transcription reaction was performed for 10 min. Symbol + represent reaction using *trxB* control promoter fragment generated by PCR. The arrow indicated the *trxB* transcript.

2.4.3 Photochemical crosslinking reaction

For the cross-linking reaction, 0.25 μM RNAP with 2.5 μM Spx or Spx variants were incubated with radiolabelled probes (20,000 c.p.m.) at 37°C for 30 min in the dark in 10 μl buffer containing 20 mM Tris-HCl (pH 8.0), 50 mM KCl, 5 mM $MgCl_2$, 0.1 mg/ml BSA and 5% glycerol. Cross-linking was carried out by UV irradiation (UV Stratalinker 1800, Stratagene) for 10 seconds, and then samples were immediately transferred to ice.

Samples were next treated with 80U DNase I at 37°C for 1 hr in a 15-μl reaction, and the reaction was stopped by adding SDS-PAGE sample buffer with DTT. After heating at 90°C for 5 min, crosslinked products were resolved on an 18% SDS-PAGE gel (Laemmli, 1970). The dried gels were scanned on a Typhoon Trio+ variable imager (GE Healthcare).

CHAPTER 3

EFFECTS OF RESIDUE SUBSTITUTIONS IN RNA POLYMERASE αCTD ON SPX-DEPENDENT TRANSCRIPTONAL ACTIVATION

3.1 INTRODUCTION

Many mutations in Spx protein have been identified that affect Spx-dependent transcriptional activation, and the role of these residues in Spx was investigated and evaluated in previous studies as well as in studies presented herein (chapters 4 and 5). In order to better understand structural requirements for Spx activated transcription, mutations in RNAP αCTD, the interacting partner of Spx, and mutations in Spx-activated target promoters were examined for their effects on Spx-activated transcription. Here, I introduce a study with unpublished data of the effects of RNAP αCTD mutants.

In previous studies, a *B. subtilis* RNAP αCTD alanine-scanning mutant library was built (Zhang *et al.*, 2006, Nakano *et al.*, 2000). In brief, a PCR fragment of the *rpoA-rplQ* region from the *B. subtilis* chromosome was inserted into vector pAG58-ble-1 to yield pSN108 as a PCR template. A single alanine codon substitution at each position of αCTD-coding part of the *rpoA* gene was introduced by using PCR-based site-directed mutagenesis and confirmed by nucleotide sequencing. The pSN108 derivative bearing the alanine codon substitution was used to transform strain JH642. The plasmid integrated into the *rpoA* locus of the chromosome by a Campbell recombination. By loop-out

recombination, the plasmids were cured from the transformants and the alanine codon substitution in the *rpoA* gene of the plasmid-cured strain was confirmed by PCR amplification followed by nucleotide sequencing (Nakano *et al.*, 2000).

Spx-dependent regulation, both positive and negative, requires interaction with αCTD of RNAP. In a previous study, Y263 residue in αCTD was identified as being required for the interaction between Spx and αCTD(Newberry *et al.*, 2005). Spx-dependent transcriptional repression and activation in the *rpoA(Y263C)* mutant were abolished (Newberry *et al.*, 2005, Nakano *et al.*, 2000).

To investigate whether any other amino acid residue in RNAP αCTD is involved in Spx-activated *trxB* transcription, the RNAP αCTD alanine-scanning mutant library was utilized (Zhang *et al.*, 2006).

3.2 RESULTS

3.2.1 The *rpoA*(*E254A*) mutant affects Spx-dependent transcription

The *trxB-lacZ* fusion and an IPTG-inducible *spx* allele encoding Spx^{DD} (protease resistant) were introduced, respectively, into the *thrC* locus and the *amyE* locus of *B. subtilis* strains containing alanine codon substitution in *rpoA.* All of the strains are listed in Table.3.1.

Table 3.1 *B. subtilis* strains and plasmids for alanine-scanning mutagenesis

Strain or plasmid	Relevant genotype or characteristics	Source or reference
***B. subtilis* strains**		
JH642	*trpC2 pheA1* (parental strain)	James Hoch
ORB7608	*trpC2 pheA1 rpoA(M251A) amyE*::pSN56 *thrC*::pSN78	This study
ORB7609	*trpC2 pheA1 rpoA(T252A) amyE*::pSN56 *thrC*::pSN78	This study
ORB7610	*trpC2 pheA1 rpoA(I253A) amyE*::pSN56 *thrC*::pSN78	This study
ORB7611	*trpC2 pheA1 rpoA(E254A) amyE*::pSN56 *thrC*::pSN78	This study
ORB7612	*trpC2 pheA1 rpoA(L256A) amyE*::pSN56 *thrC*::pSN78	This study
ORB7613	*trpC2 pheA1 rpoA(V260A) amyE*::pSN56 *thrC*::pSN78	This study
ORB7614	*trpC2 pheA1 rpoA(Y263C) amyE*::pSN56 *thrC*::pSN78	This study
ORB7617	*trpC2 pheA1 rpoA(D257A) amyE*::pSN56 *thrC*::pSN78	This study
ORB7618	*trpC2 pheA1 rpoA(L258A) amyE*::pSN56 *thrC*::pSN78	This study
ORB7619	*trpC2 pheA1 rpoA(N264A) amyE*::pSN56 *thrC*::pSN78	This study
ORB7620	*trpC2 pheA1 rpoA(C265A) amyE*::pSN56 *thrC*::pSN78	This study
ORB7623	*trpC2 pheA1 rpoA(V274A) amyE*::pSN56 *thrC*::pSN78	This study
ORB7624	*trpC2 pheA1 rpoA(Q275A) amyE*::pSN56 *thrC*::pSN78	This study
ORB7625	*trpC2 pheA1 rpoA(E276A) amyE*::pSN56 *thrC*::pSN78	This study
ORB7626	*trpC2 pheA1 rpoA(L277A) amyE*::pSN56 *thrC*::pSN78	This study
ORB7627	*trpC2 pheA1 rpoA(G270A) amyE*::pSN56 *thrC*::pSN78	This study
ORB7628	*trpC2 pheA1 rpoA(N272A) amyE*::pSN56 *thrC*::pSN78	This study
ORB7629	*trpC2 pheA1 rpoA(T273A) amyE*::pSN56 *thrC*::pSN78	This study
ORB7630	*trpC2 pheA1 rpoA(K280A) amyE*::pSN56 *thrC*::pSN78	This study
ORB7631	*trpC2 pheA1 rpoA(T281A) amyE*::pSN56 *thrC*::pSN78	This study
ORB7632	*trpC2 pheA1 rpoA(L291A) amyE*::pSN56 *thrC*::pSN78	This study
ORB7633	*trpC2 pheA1 rpoA(R293A) amyE*::pSN56 *thrC*::pSN78	This study
ORB7634	*trpC2 pheA1 rpoA(K300A) amyE*::pSN56 *thrC*::pSN78	This study
ORB7635	*trpC2 pheA1 rpoA(N279A) amyE*::pSN56 *thrC*::pSN78	This study
ORB7636	*trpC2 pheA1 rpoA(L303A) amyE*::pSN56 *thrC*::pSN78	This study
ORB7637	*trpC2 pheA1 rpoA(E304A) amyE*::pSN56 *thrC*::pSN78	This study
ORB7638	*trpC2 pheA1 rpoA(E305A) amyE*::pSN56 *thrC*::pSN78	This study
ORB7639	*trpC2 pheA1 rpoA(L306A) amyE*::pSN56 *thrC*::pSN78	This study
ORB7640	*trpC2 pheA1 rpoA(G307A) amyE*::pSN56 *thrC*::pSN78	This study
ORB7641	*trpC2 pheA1 rpoA(L308A) amyE*::pSN56 *thrC*::pSN78	This study
ORB7642	*trpC2 pheA1 rpoA(G309A) amyE*::pSN56 *thrC*::pSN78	This study
ORB7643	*trpC2 pheA1 rpoA(G310A) amyE*::pSN56 *thrC*::pSN78	This study
ORB7658	*trpC2 pheA1 rpoA(V288A) amyE*::pSN56 *thrC*::pSN78	This study
ORB7659	*trpC2 pheA1 rpoA(E297A) amyE*::pSN56 *thrC*::pSN78	This study
ORB7662	*trpC2 pheA1 rpoA(A269A) amyE*::pSN56 *thrC*::pSN78	This study
ORB7663	*trpC2 pheA1 rpoA(N290A) amyE*::pSN56 *thrC*::pSN78	This study
ORB7670	*trpC2 pheA1 rpoA(E282A) amyE*::pSN56 *thrC*::pSN78	This study
ORB7671	*trpC2 pheA1 rpoA(E283A) amyE*::pSN56 *thrC*::pSN78	This study
ORB7674	*trpC2 pheA1 rpoA(I271A) amyE*::pSN56 *thrC*::pSN78	This study
ORB7675	*trpC2 pheA1 rpoA(D284A) amyE*::pSN56 *thrC*::pSN78	This study
ORB7691	*trpC2 pheA1 rpoA(M285A) amyE*::pSN56 *thrC*::pSN78	This study
ORB7692	*trpC2 pheA1 rpoA(M286A) amyE*::pSN56 *thrC*::pSN78	This study
ORB7693	*trpC2 pheA1 rpoA(K287A) amyE*::pSN56 *thrC*::pSN78	This study
ORB7694	*trpC2 pheA1 rpoA(S295A) amyE*::pSN56 *thrC*::pSN78	This study
ORB7695	*trpC2 pheA1 rpoA(V299A) amyE*::pSN56 *thrC*::pSN78	This study

ORB7696	*trpC2 pheA1 rpoA(R311A) amyE*::pSN56 *thrC*::pSN78	This study
ORB7697	*trpC2 pheA1 rpoA(K312A) amyE*::pSN56 *thrC*::pSN78	This study
ORB7702	*trpC2 pheA1 rpoA(S262A) amyE*::pSN56 *thrC*::pSN78	This study
ORB7703	*trpC2 pheA1 rpoA(K267A) amyE*::pSN56 *thrC*::pSN78	This study
ORB7704	*trpC2 pheA1 rpoA(D313A) amyE*::pSN56 *thrC*::pSN78	This study
ORB7705	*trpC2 pheA1 rpoA(D314A) amyE*::pSN56 *thrC*::pSN78	This study
ORB7712	*trpC2 pheA1 rpoA(Y263A) amyE*::pSN56 *thrC*::pSN78	This study
ORB7713	*trpC2 pheA1 rpoA(L296A) amyE*::pSN56 *thrC*::pSN78	This study
ORB7723	*trpC2 pheA1 rpoA(S259A) amyE*::pSN56 *thrC*::pSN78	This study
ORB7724	*trpC2 pheA1 rpoA(L266A) amyE*::pSN56 *thrC*::pSN78	This study
ORB7725	*trpC2 pheA1 rpoA(E298A) amyE*::pSN56 *thrC*::pSN78	This study
ORB7767	*trpC2 pheA1 rpoA(K302A) amyE*::pSN56 *thrC*::pSN78	This study
ORB7796	*trpC2 pheA1 rpoA(E254A) amyE*::pSN56 *thrC*::pSN78	This study
ORB7797	*trpC2 pheA1 rpoA(V260A) amyE*::pSN56 *thrC*::pSN78	This study
ORB7798	*trpC2 pheA1 rpoA(L266A) amyE*::pSN56 *thrC*::pSN78	This study
ORB8093	*trpC2 pheA1 rpoA(E254A) rpoC-his10-cat sigA(L366A)*	This study
ORB8094	*trpC2 pheA1 rpoA(Y263C) rpoC-his10-cat sigA(L366A)*	This study
RNAP αCTD alanine-scanning mutant library		(Zhang *et al.*, 2006)
UDB283	*trpC2 pheA1 sigA(L366A)*	a gift from C. P. Moran, Jr., Emory University
Plasmids		
pSN56	pDR111 with *spx*^{DD}	(Nakano *et al.*, 2003a)
pSN78	pDG793 with *trxB*(-510~+47)-*lacZ*	(Nakano *et al.*, 2003a)

By overexpressing the Spx^{DD} protein and measuring *trxB*-directed β-galactosidase activity, the effect of the αCTD mutants on the transcription activation was examined. As expected, the *rpoA* Y263A mutant, which disrupts αCTD/Spx interaction, almost abolished *trxB* transcription (Fig. 3.1). In all mutants screened, only two mutations at E254A and L266A in *rpoA* reduced the *trxB* transcription activity by half (Fig. 3.1, 3.2A, C). The effect of these two mutants was also examined on another Spx-dependent promoter, *trxA*, and only the *rpoA*(*E254A*) mutant affected transcription activation (Fig. 3.2B, D). Since the effect of *rpoA*(*L266A*) mutant was only observed on *trxB* transcription, but not have a general effect on Spx-dependent promoters, the further analysis for *rpoA*(*L266A*) was not conducted in this study.

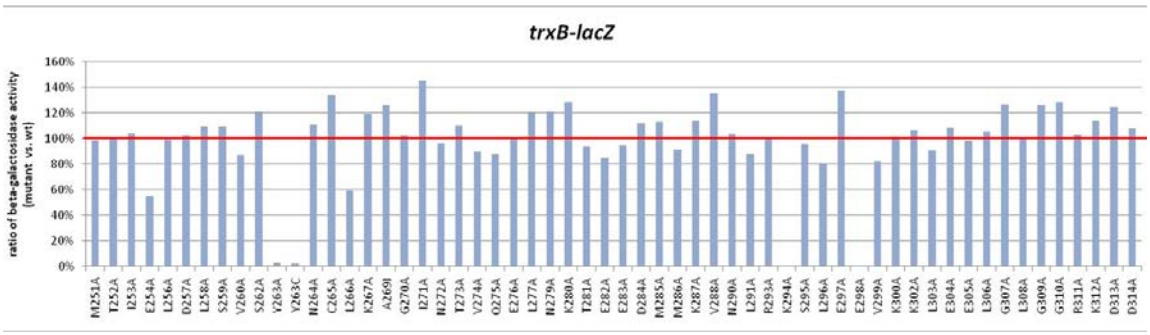

Figure 3.1. Effect of RNAP αCTD mutant on *trxB-lacZ* transcription. Alanine codon substitutions in the αCTD-coding region of the *rpoA* gene are listed in order in the x-axis. β-galactosidase activity is present as a percentage of the average activity measured in *rpoA*$^{+}$ strain in the y-axis. *B. subtilis* strains bearing either K294A or E298A mutation in RNAP αCTD could not be established. The red line across all of the columns represents the β-galactosidase activity of mutant comparable to the activity of wild-type.

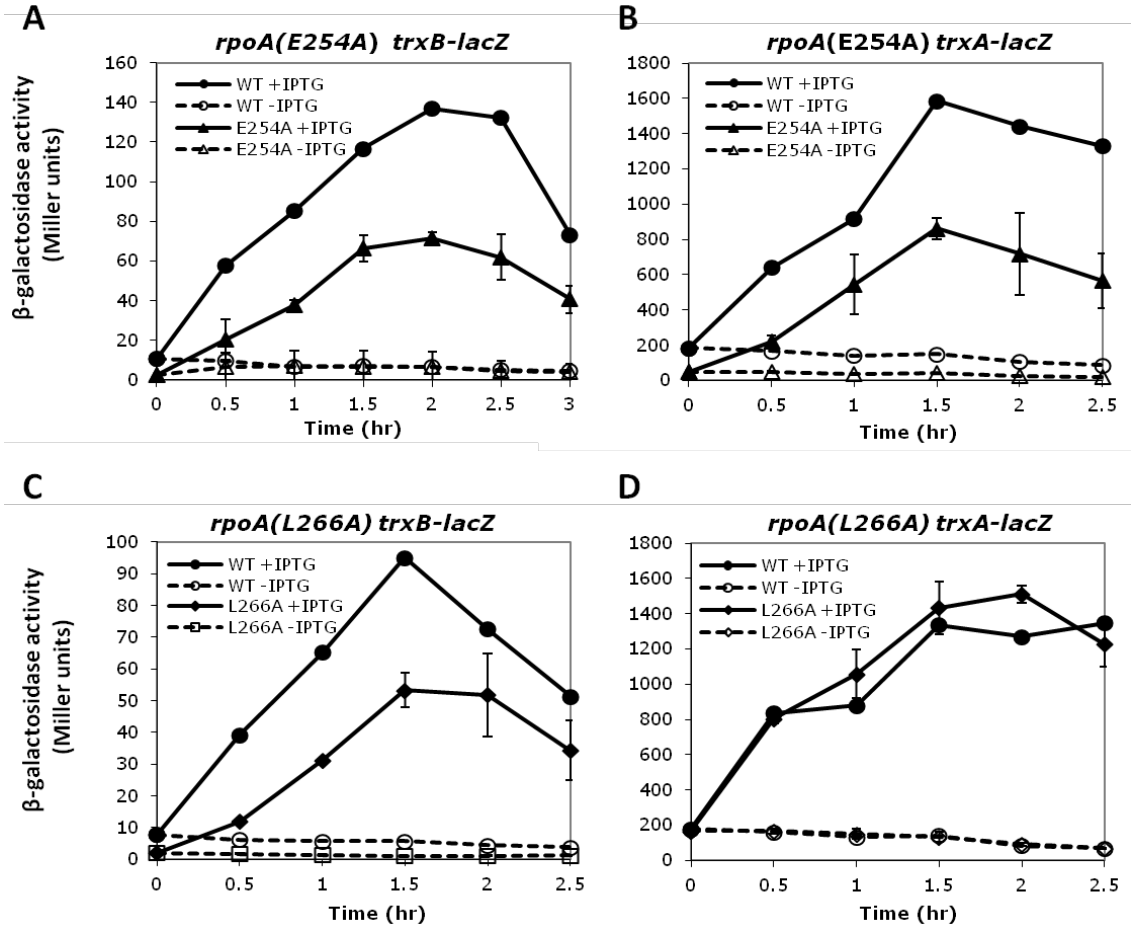

Figure 3.2. Effect of *rpoA*(*E254A*) and *rpoA*(*L266A*) on Spx-dependent transcription activation in vivo. The *trxB-lacZ* (A, C) or t*rxA-lacZ* (B, D) fusion was introduced into wildtype, *rpoA*(*E254A*) (A, B) or *rpoA*(*L266A*) (C, D) mutant strains bearing an IPTG-inducible *spx* allele encoding Spx^{DD} (protease resistant). Strains (listed in Table 3.1) were grown in DS medium. When the OD_{600} reached 0.4, each culture was divided into two flasks, and 1 mM IPTG was added to one flask to induce Spx^{DD} expression. Samples were taken at time intervals and β-galactosidase activities were measured. Symbols: circles, WT; triangles, *rpoA*(*E254A*), and diamonds, *rpoA*(*L266A*). Open symbols with broken lines represent cells cultured without IPTG, and closed symbols with solid lines represent cell culture with IPTG.

3.2.2 Phenotype screening with sodium selenite and diamide

Spx is a global transcriptional regulator for the response to many stress conditions. Besides diamide, *spx* null mutant is also sensitive to other toxic agents, such as paraquat, selenite, electrophiles, hypochlorite and methylglyoxal (Zuber *et al.*, 2011). The interaction of Spx with RNAP is necessary for its function, whether any alanine substitution in RNAP αCTD affects Spx function in response to some toxic agents was tested. To screen for growth phenotype of *rpoA* mutants to selenite sensitivity, strains were grown on DSM agar plats containing 1.5 mM sodium selenite (Na_2SeO_3) and incubated at 37°C for overnight. In the presence of sodium selenite, the defective growth of *rpoA*(*Y263A*) and *rpoA*(*Y263C*) was observed as expected for their importance in Spx binding. Only one other mutant, *rpoA*(*E254A*), showed defective growth on sodium selenite plate (Fig. 3.3). When the concentration of sodium selenite increased to 2 mM, the growth of the *rpoA*(*Y263A*), *rpoA*(*Y263C*) and *rpoA*(*E254A*) mutants was more severely affected. The growth defect of *rpoA*(*V288A*) and *rpoA*(*E297A*) mutants was also observed, but these two mutants did not show an effect on *trxB-lacZ* transcription, and the effects of these two mutants are needed to be confirmed.

The sensitivity of *rpoA*(*E254A*) to diamide, the oxidant which induces Spx-dependent response, was also investigated. The *rpoA*(*E254A*) mutant was sensitive to diamide, but not to the extent shown by *rpoA*(*Y263C*) mutant, which could not grow on a DSM plate containing 50 μM diamide (Fig. 3.4). This indicates that the E254 residue in RNAP αCTD is important for Spx function.

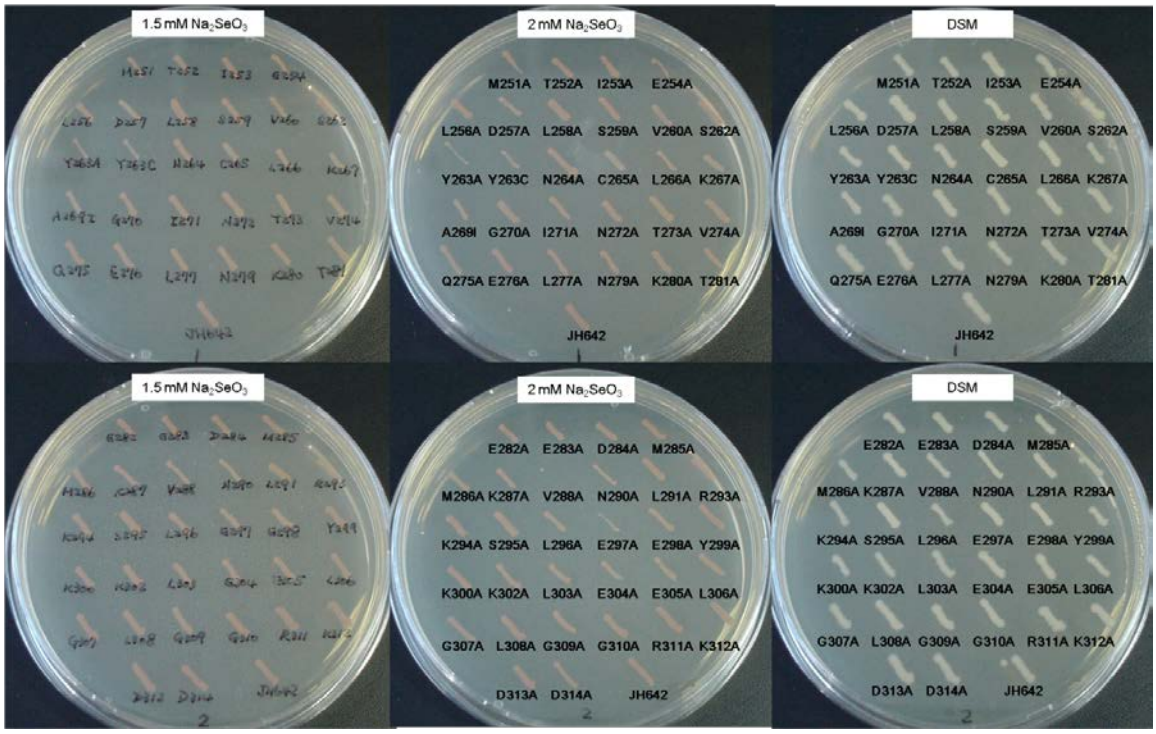

Figure 3.3. Sensitivity of *B. subtilis rpoA* mutants to sodium selenite. All of the *rpoA* mutant strains together with wildtype strain, JH642 were streaked on DSM agar plates, with or without 1.5mM, or 2mM sodium selenite, and incubated at 37°C for overnight.

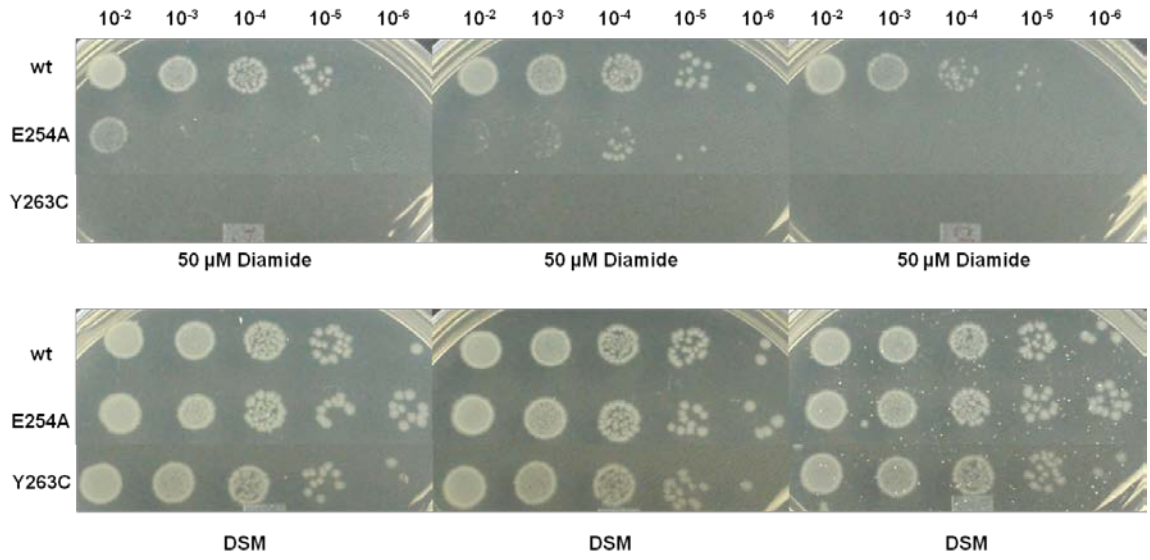

Figure 3.4. Sensitivity of selected *B. subtilis rpoA* mutants to diamide. WT, *rpoA*(*E254A*), and *rpoA*(*Y263C*) mutant strains was serially diluted and spotted on DSM agar plates, with or without 50 µM diamide and incubated at 37°C for overnight. The growth of three isolates from each stain was tested.

3.2.3 Mutant RNAP purification and in vitro transcription

To examine the effect of *rpoA*(*E254*) on Spx-dependent transcription in vitro, His-tagged *rpoA*(*E254A*) RNA polymerase was constructed and purified. The in vitro transcription of *trxB* and *rpsD* was performed with wild-type and mutant RNAP. To evaluate the activity of mutant RNAP, the transcription of *B. subtilis* housekeeping gene, *rpsD* was examined. Both *rpoA*(*Y263C*) and *rpoA*(*E254A*) RNAP can activate *rpsD* transcription to the same extent as wild-type RNAP (Fig. 3.5, lane 7-9). The *rpoA*(*Y263C*) RNAP failed to activate *trxB* transcription in vitro (Fig. 3.5, lane 4), and the *trxB* transcription with *rpoA*(*E254A*) RNAP was reduced by more than half (Fig.3.5, lane 6). It

suggests that E254 residue in RNAP αCTD is required for optimal Spx-dependent transcriptional activation.

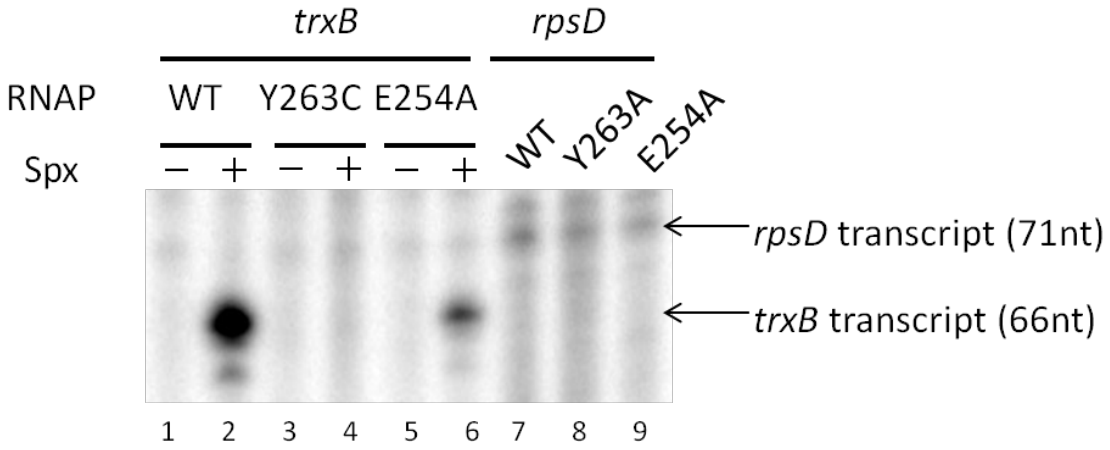

Figure 3.5. The effect of mutant *rpoA*(*Y263C*) and *rpoA*(*E254*) RNAP on in vitro transcription. The linear *trxB* (lane 1-6) or *rpsD* (lane 7-9) promoter template (10 nM) was incubated with wild-type, *rpoA*(*Y263C*), or *rpoA*(*E254*) SAd-RNAP (25 nM) together with σ^A (25 nM) in the abcence or presence of Spx (75 nM) and transcription reaction was performed for 10min.

3.3 CONCLUSION

Previous study showed *rpoA*(*E254A*) mutant affected ComA-activated *srfA* transcription (Zhang *et al.*, 2006). It seems that the E254 residue in αCTD of RNAP is involved in both Spx-dependent transcriptional activation and repression. Since both regulatory mechanisms require Spx and αCTD interaction, it is possible E254 residue plays a role for the contact to Spx. The requirement of the E254 residue for optimal

RNAP interaction with Spx is supported by the location of the Glu254 side chain in the *B. subtilis* αCTD structure. (Fig. 3.6) The E254 side chain turns toward the α1 helix in the vicinity of the Y263 aromatic side chain. The two residues likely form part of the binding surface that contacts the central domain of Spx.

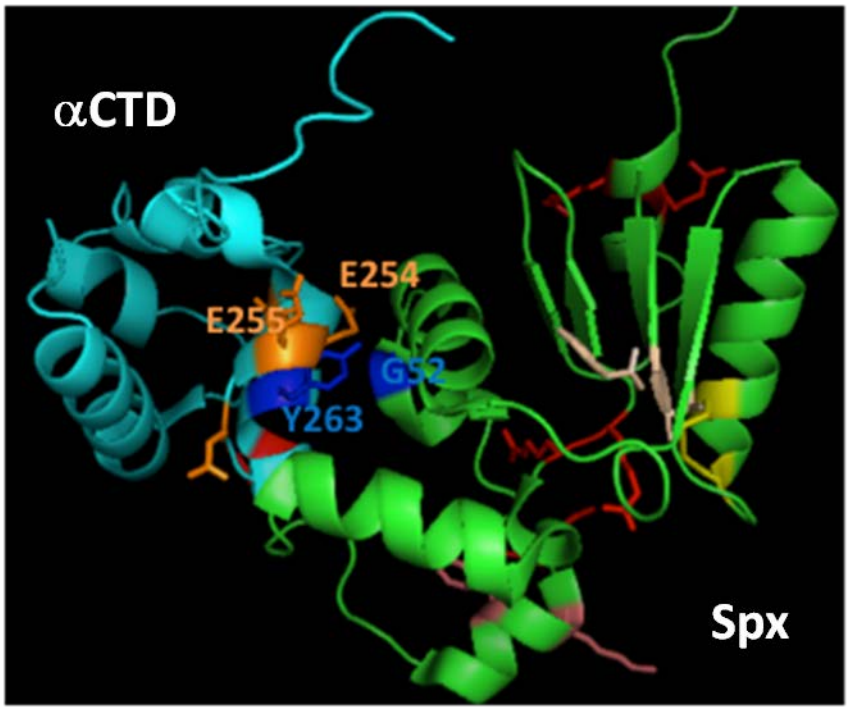

Figure 3.6. Structure of *B. subtilis* RNAP αCTD showing the locations of the Y263 and E254 side chains. Their close proximity to each other suggests that they constitute a part of the Spx-binding surface. The αCTD is shown in cyan, and Spx is shown in green (PDB accession number 3GFK).

CHAPTER 4

EVIDENCE THAT A SINGLE MONOMER OF SPX CAN PRODUCTIVELY INTERACT WITH RNA POLYMERASE IN *BACILLUS SUBTILIS*

4.1 INTRODUCTION

Throughout phylogeny, positive transcriptional control plays an important role in cellular decision-making (Rhodius & Busby, 1998). The mechanisms that activate transcription initiation in response to environmental and metabolic signal inputs are varied and involve complex sensory functions linked to specific macromolecular interactions conducted at targeted chromosomal loci. For many regulatory systems, these interactions involve contacts between transcriptional regulators and RNA polymerase (RNAP). In prokaryotes, RNA polymerase, composed of β,β', σ, 2α and ω subunits, contains multiple target surfaces that can engage positive regulatory proteins, which function to direct RNAP to the specific regulatory regions of genes that are under their control (Ishihama, 2000). The α subunit, bearing two domains that occupy the protein's N- and C-termini (NTD and CTD, respectively) is a common target for regulatory protein interaction (Ishihama, 1992). A classic example is the class I and II positive control exerted by the cAMP receptor protein, CRP-cAMP, which interacts with a specific cis-acting element upstream of promoter DNA as a dimeric complex that recruits RNAP by direct interaction with RNAP αCTD (Busby & Ebright, 1999).

While direct interaction between DNA-bound regulator and RNAP is a common mechanism of positive transcriptional control, mechanisms of RNAP appropriation and "pre-recruitment" have been reported that involve initial RNAP-regulator interaction prior to promoter engagement (Beck *et al.*, 2007). Proteins encoded in bacteriophage genomes, such as NS_4SSB of phage N4 (Miller *et al.*, 1997) and AsiA of phage T4 (Hinton *et al.*, 2005), target RNAP without contacting DNA, yet participate in gene-specific transcriptional activation. The SoxS protein that mediates the bacterial response to superoxide, and the MarA protein that functions in control of multi-drug resistance mechanisms, first contact RNAP α subunit prior to sequence-specific DNA interaction (Griffith & Wolf, 2004, Martin *et al.*, 2002). Spx, a protein of low GC Gram-positive bacteria that serves as a transcriptional activator of genes that function in thiol-specific oxidative stress (Griffith & Wolf, 2004, Martin *et al.*, 2002, Zuber, 2004), also exerts control of RNAP through a pre-recruitment mechanism (Nakano *et al.*, 2010b).

Spx governs a large regulon of genes that include those encoding thioredoxin (*trxA*), thioredoxin reductase (*trxB*) (Nakano *et al.*, 2005), methionine sulfoxide reductase (You *et al.*, 2008), and genes whose products function in bacillithiol biosynthesis (Gaballa *et al.*, 2010), cysteine biosynthesis (Nakano *et al.*, 2003b), and iron uptake/metabolism (Zuber *et al.*, 2011). Spx has also been linked to control of biofilm and virulence-related functions (Kajfasz *et al.*, 2010, Pamp *et al.*, 2006). Spx is under multiple levels of control that operate at the transcriptional and post transcriptional level. Multiple forms of RNAP target the operon in which the *spx* gene resides (Eiamphungporn & Helmann, 2008, Qiu & Helmann, 2001). The *spx* gene itself is under negative transcriptional control involving two repressors, YodB and PerR that control the

transcriptional response to toxic electrophiles and peroxide, respectively (Leelakriangsak *et al.*, 2007). Spx protein is under tight proteolytic control involving the ATP-dependent protease, ClpXP (Nakano *et al.*, 2003b, Nakano *et al.*, 2003c) and a cognate proteolysis-enhancing factor, YjbH (Garg *et al.*, 2009, Larsson *et al.*, 2007). Encounters with any one of a variety of toxic agents can result in elevated Spx concentration and Spx activation (Antelmann *et al.*, 2008, Chi *et al.*, 2011, Eiamphungporn & Helmann, 2008, Nguyen *et al.*, 2009, You *et al.*, 2008).

Spx protein bears a CXXC disulfide redox center that controls its transcription stimulating activity (Nakano *et al.*, 2005). Spx in its oxidized, disulfide form productively interacts with RNAP, forming a complex that contacts promoters bearing a cis-acting element (having the sequence a/tGCA followed by an AT-rich sequence) located immediately upstream of the promoter -35 region (Nakano *et al.*, 2010b, Reyes & Zuber, 2008). While Spx cannot by itself interact with DNA, a complex consisting of Spx and αCTD will interact with DNA that bears the cis-acting element of the Spx-controlled promoter (Nakano *et al.*, 2010b). From mutational analysis of promoter DNA and studies of Spx/ αCTD-DNA interaction, evidence was obtained suggesting that two Spx/ αCTD complexes might participate in Spx-controlled promoter recognition (Nakano *et al.*, 2010b). The notion of two Spx proteins, each binding an α subunit, engaging RNAP has significant implications when considering the roles of multiple Spx paralogs that are encoded within the genomes of several low-GC Gram-positive species (Kajfasz *et al.*, 2010, Reder *et al.*, 2008, Turlan *et al.*, 2009), including pathogenic streptococci. Could two paralogous forms of Spx engage RNAP, thus expanding the promoter recognition and sensory capabilities of the Spx/RNAP complex?

In the study reported herein, the composition of the Spx/RNAP complex was examined using differentially affinity-tagged Spx proteins. Affinity interaction chromatography experiments of in vitro assembled complexes of epitope-tagged Spx and RNAP, as well as complexes collected from extracts of cells expressing tagged Spx derivatives indicate that the Spx/RNAP complex bears a single Spx monomer.

4.2 RESULTS

4.2.1 Epitope-tagged versions of Spx are active in vivo and in vitro

Allelic variants of *spx* were constructed that specified modifications to the C-terminal ends of each product. Oligonucleotide PCR primers specifying the HA and c-Myc epitopes were used to create alleles encoding C-terminal epitope-tagged versions of Spx, and a deletion variant that is missing the C-terminal 12 amino acid residues. Previous studies had shown that the deletion of 12 C-terminal residues created an active, protease-resistant version of Spx (SpxΔC, see below, C. M. Chan and P. Z., unpublished). The epitope-tagged variants included HA-tagged SpxΔC (SpxΔCHA), as well as c-Myc-tagged, full-length Spx protein (Spxc-Myc). SpxΔCHA and Spxc-Myc were tested in vivo by ectopic expression from an IPTG-inducible promoter at the *amyE* locus within a strain bearing the *trxB-lacZ* fusion (Fig. 4.1A and B), expression of which is stimulated by Spx (Reyes & Zuber, 2008). A construct bearing an allele of *spx* encoding the protease-resistant form of Spx [Spx^{DD}, (Nakano *et al.*, 2003b)] was used in parallel as a positive control. Both of the epitope-tagged variants showed activity in vivo, based on

the level of *trxB-lacZ* expression after IPTG addition, but activity was lower by around 50% of the Spx^{DD} control. This reduction in activity was not due to a defect in Spx protein in terms of its ability to activate *trxB* expression, but was due to residual proteolytic control that reduced HA- and c-Myc-tagged Spx concentration. The activity of the epitope-tagged derivatives was examined in a *yjbH* null mutant background (Fig. 4.1A and B), which showed that activity of the two epitope-tagged Spx variants was the same as Spx^{DD}. This indicated that the reduced activity of the two epitope-tagged Spx variants was due to the sensitivity of the proteins to YjbH-mediated proteolysis catalyzed by ClpXP.

To confirm that the SpxΔCHA and Spxc-Myc proteins were active, the proteins were produced as intein-chitin binding domain fusions and purified by chitin column affinity chromatography and intein cleavage (Fig. 4.2A). After further purification by anion exchange chromatography, each protein was applied to a transcription reaction containing trxB promoter DNA and purified RNAP holoenzyme (Fig. 4.2B). Both epitope-tagged versions of Spx stimulated *trxB* transcription in vitro, using the same transcriptional start site as the wild-type Spx/RNAP complex.

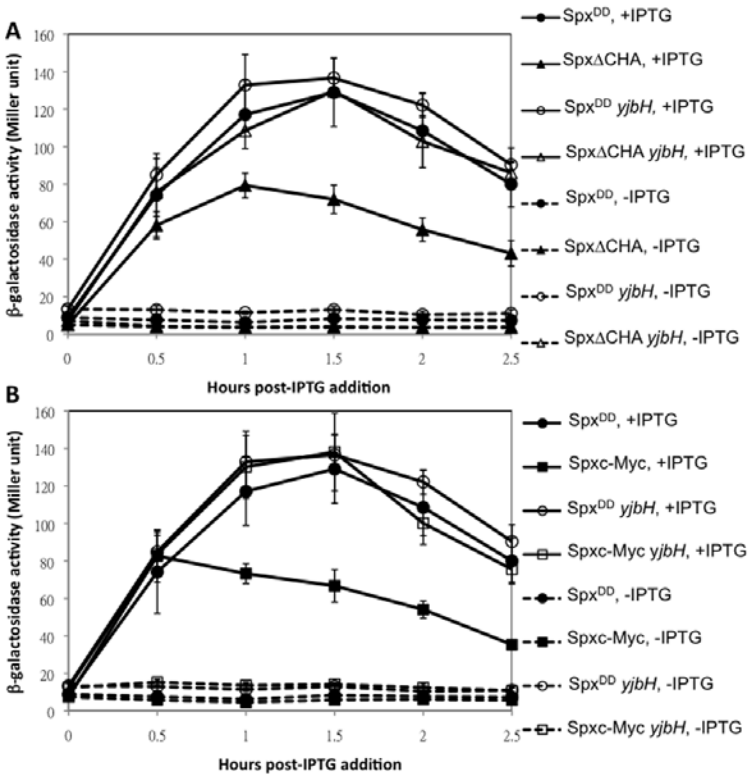

Figure 4.1. Effect of epitope-tagged Spx on *trxB-lacZ* expression in wild type and *yjbH* strains. Alleles of *spx* encoding epitope-tagged Spx, SpxΔHA (A) or Spxc-Myc (B) were introduced into the *amyE* locus of the wildtype or *yjbH*- strain lacking of *spx* allele and bearing a *trxB-lacZ* fusion in the *thrC* locus. The expression of ectopic Spx proteins is IPTG-inducible. Strains were grown in DS medium until OD_{600} reached 0.4, when 1mM IPTG was added to induce Spx expression. Samples were collected at 30min-intervals and β-galactosidase activity was measured and presented in Miller units. Spx^{DD} is resistant to YjbH-mediated proteolysis and used as the positive control. Symbols: circles, Spx^{DD}; triangles, SpxΔCHA; squares, Spxc-Myc; closed symbols, $yjbH^{+}$ strains; open symbols, *yjbH* strains; solid and dashed lines, in the presence and absence of IPTG, respectively.

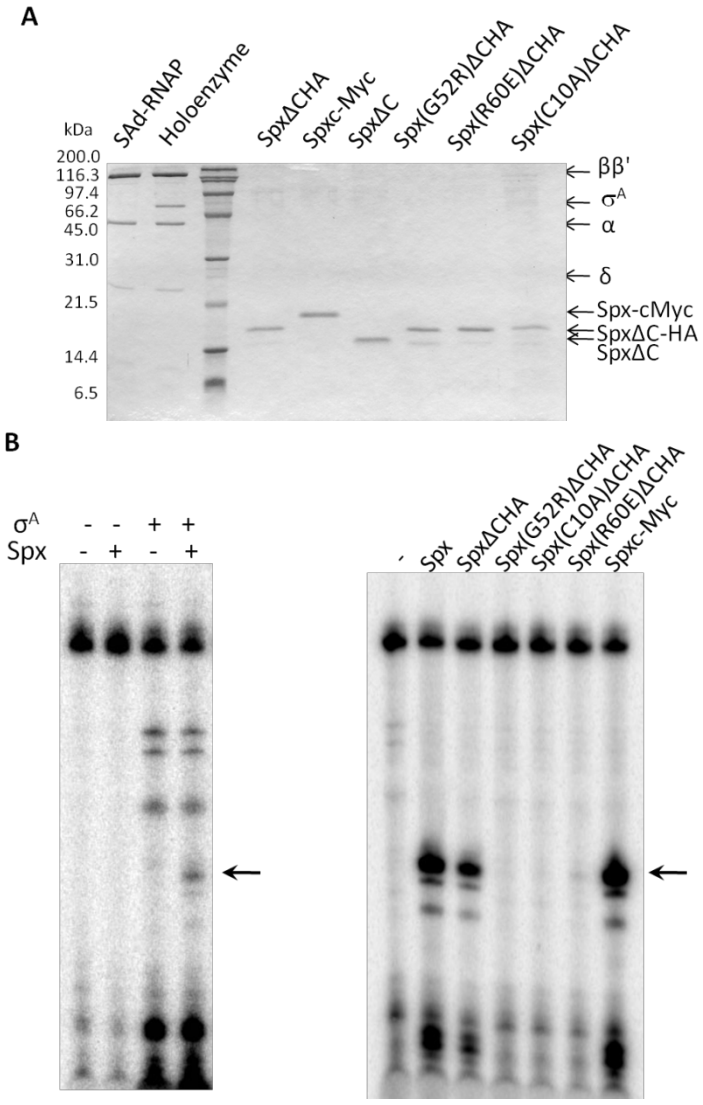

Figure 4.2. Purified RNAP and Spx proteins and their activities on *trxB* transcription. (A) Purified proteins used in pull-down assay. His tagged SAd-RNAP was purified from ORB5853 by Ni-NTA affinity chromatography, heparin-agarose chromatography, and Hi-Q anion exchange chromatography. Spx, its derivatives, and σ^A were purified by intein-tag mediated purification and appropriate ion exchange chromatography. For RNAP holoenzyme assembly, SAd-RNAP and σ^A were incubated at equal molar ratio. (B) In vitro transcription from the *trxB* (–115-+47) promoter by

using purified proteins. The activity of SAd-RNAP was validated in the absence and presence of σ^A (Left figure) on activation of *trxB* promoter with Spx. Different versions of Spx were incubated with RNAP and *trxB* promoter DNA to examine transcriptional activity. The detailed method was described in Materials and Methods. A 66-nt transcript was indicated by an arrow.

4.2.2 SpxΔCHA and Spxc-Myc interaction with RNAP confirmed by affinity chromatography

To examine the composition of Spx/RNAP, affinity chromatography designed to capture Spx bound to RNAP was undertaken. RNAP and SpxΔCHA were combined in 1:10 molar ratio in a binding reaction that was applied to an anti-HA affinity column that had been blocked with buffer containing milk to prevent non-specific protein binding. Elution of SpxΔCHA with associated RNAP was accomplished with a high pH buffer and confirmed by SDS-PAGE (Fig. 4.3A). RNAP did not interact with the anti-HA column (Fig. 4.3B). Spxc-Myc bound to RNAP could also be captured by an anti c-Myc affinity column, and eluted fractions could be resolved by SDS-PAGE, showing Spxc-Myc and bound RNAP (Fig. 4.3D), while RNAP showed weak interaction with the anti-c-Myc column. Using the sigAL366A *B. subtilis* mutant, a σ^A defect in RNAP core enzyme interaction (Zuber *et al.*, 2011) a preparation of RNAP depleted of σ^A (SAd-RNAP) was obtained (Fig. 4.2A). As shown in Fig. 4.2B, RNAP from the sigAL366A mutant did not transcribe the *trxB* template, but transcripts were detected after purified σ^A protein was applied to the reaction. Further addition of Spx stimulated transcription from

the Spx-controlled *trxB* promoter. Binding of σ^A –depleted RNAP with SpxΔCHA was observed by anti-HA affinity chromatography, although binding affinity of SpxΔCHA with RNAP was higher when σ^A was present (Fig. 4.3A and C). Repeat binding reactions containing SAd-RNAP and SpxΔCHA were applied to the anti-HA affigel column. SAd-RNAP co-eluted with SpxΔCHA, however the amount of bound enzyme was less than reactions using holo-RNAP (Fig. 4.4A and B). The result suggested that σ^A is required for optimal Spx-RNAP interaction. Note that RNAP holoenzyme and SAd-RNAP showed no affinity for the anti-HA affigel column (Fig. 4.5).

To test the interaction of RNAP with Spx mutants that show defects in transcriptional activation, anti-HA affigel interaction reactions were assembled with proteins having substitutions at residue positions known to be required for Spx activity. An SpxΔCHA variant bearing a G52R mutation, shown previously to disrupt Spx-αCTD interaction, was combined with RNAP holoenzyme or SAd-RNAP. After incubation the mixture was applied to the anti-HA affinity column. Immobilized complexes were eluted at high pH and analyzed by SDS-PAGE (Fig. 4.6A and B). The Spx-RNAP interaction was quantified by calculating the ratio of Spx band intensity to large subunit (β, β´) band intensity. The SpxΔCHAG52R mutant showed significantly reduced affinity for RNAP holoenzyme, and was in line with previous results (Nakano *et al.*, 2010b, Newberry *et al.*, 2005). A similar result was obtained for reactions containing a mutant form of RNAP holoenzyme bearing an α subunit with a Y263C substitution that does not interact efficiently with Spx (Fig. 4.7). These experiments confirmed that *spx* and *rpoA* mutations that compromise Spx-α interaction disrupt Spx-RNAP complex formation. In contrast, the SpxR60E and SpxC10A mutants were expected to interact with RNAP. The

Spx(R60E)ΔCHA and Spx(C10A)ΔCHA mutant proteins interacted with RNAP holoenzyme with an affinity only slightly less than that of the parent SpxΔCHA, but showed noticeably reduced affinity for SAd-RNAP (Fig. 4.6C and D). SpxR60E and SpxC10A exert negative transcriptional control in vivo by direct interaction with RNAP, but are severely defective in transcriptional activation, which is the result of poor binding to their DNA target when complexed with αCTD (Nakano *et al.*, 2010b, Nakano *et al.*, 2005, Zhang *et al.*, 2006).

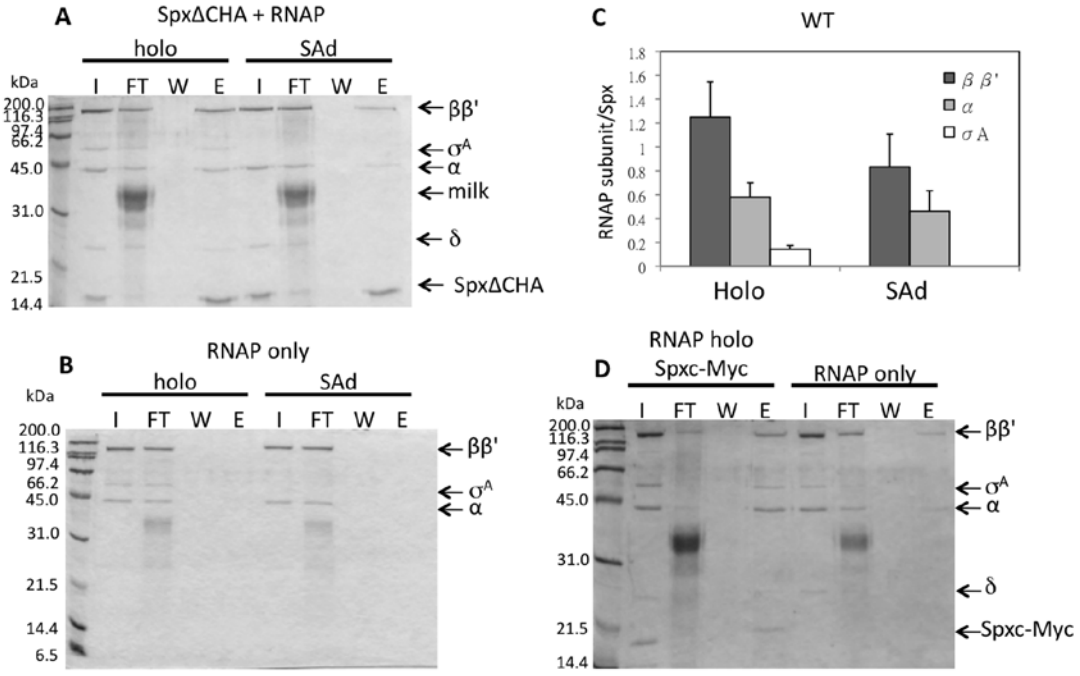

Figure 4.3. In vitro SpxΔCHA binding to RNAP holoenzyme and SAd-RNAP. RNAP holoenzyme (holo) or σ^A-depleted RNAP (SAd) was incubated with (A) or without (B) SpxΔCHA in reaction buffer (RB, 10mM Tris-HCl pH8.0, 100mM KCl, 5mM MgCl2) and applied to an anti-HA affinity column that was blocked with 5% milk. After washing, Spx/RNAP complex was eluted from the column with 100 mM triethylamine. Input (I), flow-through (FT), wash (W) and elution (E) from each column

were collected and the composition of Spx/RNAP complex was analyzed by SDS-PAGE. (C) The intensity of each RNAP subunit protein band on the gel was quantified by image analysis software ImageJ, and presented as a ratio to the intensity of SpxΔCHA. (D) The ability of Spxc-Myc to interact with RNAP was confirmed with anti-c-Myc affigel affinity chromatography and SDS-PAGE. Image of stained, dried gel is shown. Reactions of holo-RNAP with (left four lanes) and without (right four lanes) Spxc-Myc were applied to anti-c-Myc affigel and fractions indicated were analysed by SDS-PAGE.

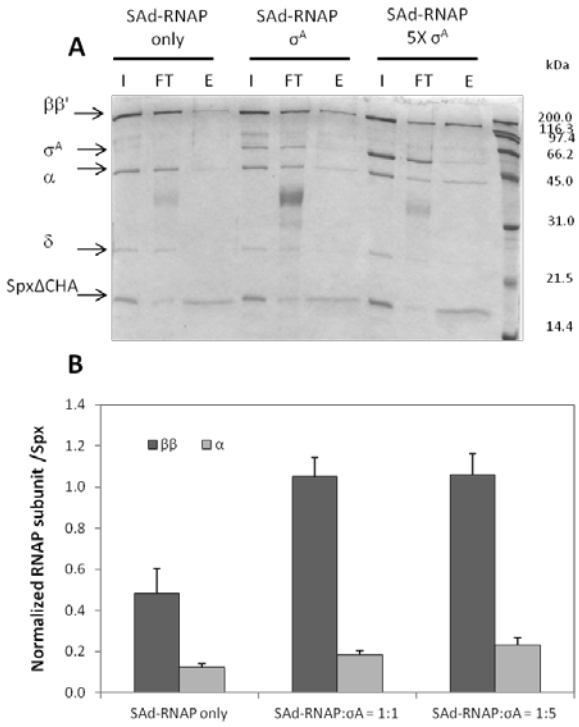

Figure 4.4. The effect of σ^A addition on Spx/RNAP binding in vitro. (A) σ^A was added at the equal or 5-fold excess molar ratio to SAd-RNAP in the binding reaction with SpxΔCHA for anti-HA affinity pull-down. For core RNAP binding, only SAd-RNAP

was incubated with Spx in the binding reaction. The protein complex was then eluted at high-pH and analyzed on SDS-PAGE gel (B) The ratio of RNAP subunit band to Spx band in the absence of σ^A was given the value 1.0. The ratio of RNAP subunit to Spx in the presence of σ^A was normalized against the SAd-RNAP only values.

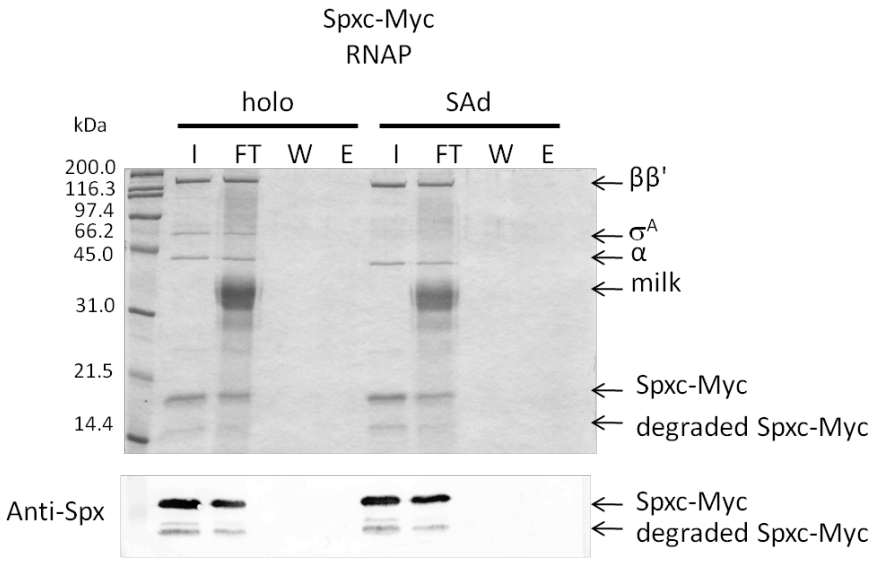

Figure 4.5. Control for competition pull-down assay. To verify that there is no non-specific binding of Spxc-Myc/RNAP complex to antibody-affinity columns, an anti-HA affinity experiment was performed with Spxc-Myc and RNAP holoenzyme or SAd-RNAP in the absence of SpxΔC-HA. The column fractions were analyzed by SDS-PAGE and Western blot with Spx antiserum. I: input, FT: flow-through, W: wash, E: elution.

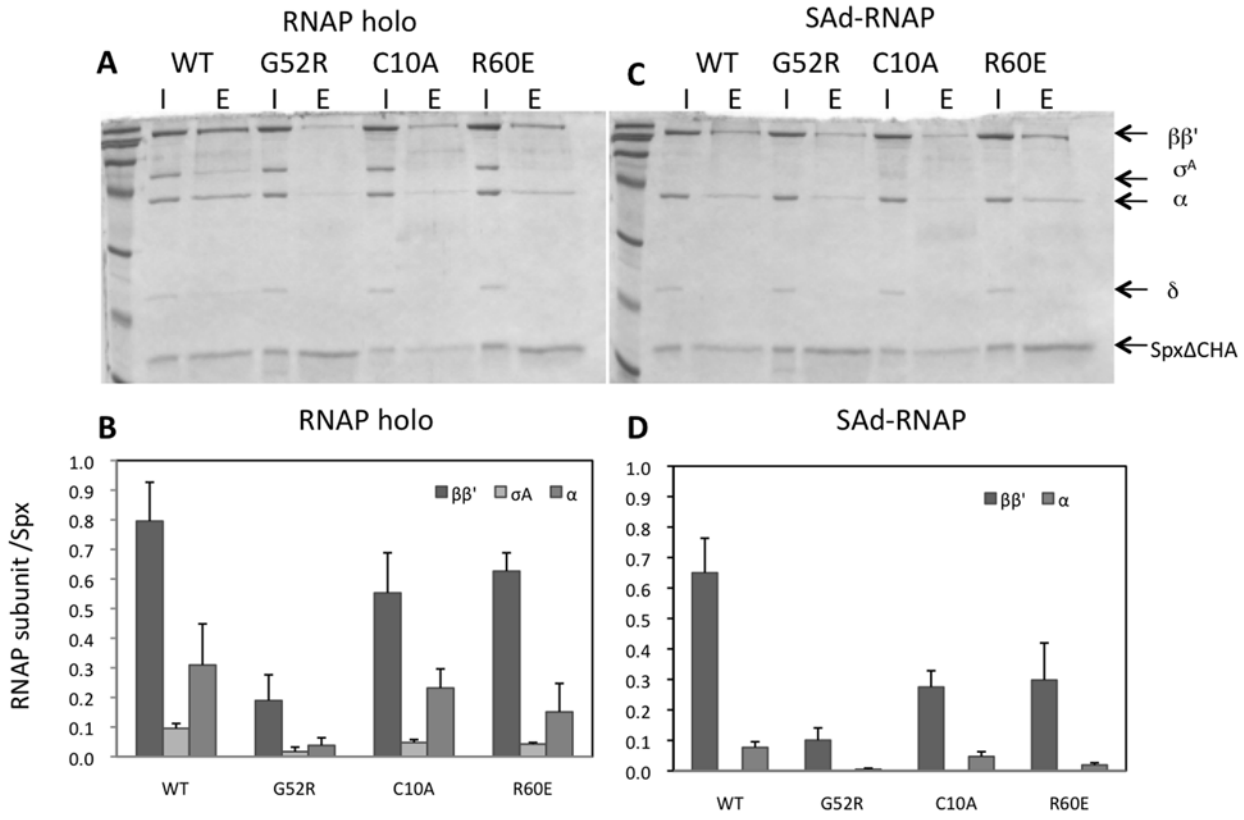

Figure 4.6. Effect of Spx mutants on RNAP interaction in vitro. Interaction assay was carried out with anti-HA affinity chromatography. Interaction between Spx mutants and RNAP holo (A) or SAd-RNAP (C) was analyzed by SDS-PAGE, and the intensity of each subunit of RNAP holo (B) or SAd-RNAP (D) was quantified, and presented as a ratio to the intensity of SpxΔCHA. Abbreviation: WT, SpxΔCHA; G52R, Spx(G52R) ΔCHA; C10A, Spx(C10A)ΔCHA; R60E, Spx(R60E)ΔCHA; I, input and E, elution. Only input and elution are shown.

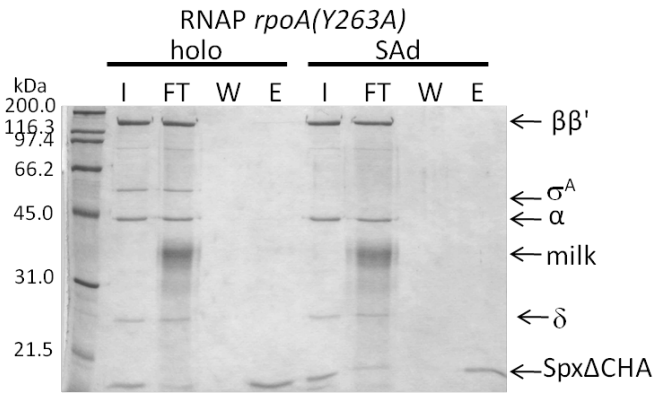

Figure 4.7. In vitro anti-HA interaction assay with RNAP *rpoA(Y263A).* The Y263A residue in RNAP α subunit was previously reported to affect Spx/α interaction (Zhang *et al.*, 2006). SAd-RNAP *rpoA(Y263A)* was purified from ORB8094 and incubated with SpxΔC-HA in the presence or absence of σ^A. An anti-HA affigel interaction assay was performed to examine the effect of the *rpoA* mutation on Spx/RNAP interaction. I, input; FT, flow-through; W, wash; E, elution.

4.2.3 SpxΔCHA and Spxc-Myc compete for RNAP interaction.

One view of Spx/RNAP composition is that two Spx proteins, one bound to each α subunit, would associate with RNAP and generate a transcription activation complex in which two cis-acting, Spx response elements would be utilized to stimulate transcription from an Spx-controlled promoter (Nakano *et al.*, 2010b). Experiments were conducted with epitope-tagged Spx variants to determine if Spx/RNAP contains two Spx monomers. A reaction was assembled in which SpxΔCHA and Spxc-Myc were combined with holo RNAP then applied to the anti-HA affinity column. As shown in Fig. 4.2, the two Spx

variants can be distinguished by SDS-PAGE according to the differences in their molecular weights. Elution of the complex from the anti-HA column should result in co-elution of RNAP and Spxc-Myc protein if the transcription complex contains two Spx monomers. The gel profile of the eluted fraction showed that only the HA-tagged Spx variant and associated holo-RNAP (Fig. 4.8A and B) or SAd-RNAP (Fig. 4.8C and D) bound to the anti-HA column, while Spxc-Myc was found in the flow-through and wash fractions. The elution was carried out at high pH, and the fraction collected was not active in an in vitro transcription reaction. However, the immobilized complex on the anti-HA affigel beads was active in transcription reactions when combined with *trxB* promoter DNA and radiolabeled nucleotide mixture (Fig. 4.9). The results indicate that the active Spx/RNAP complex is composed of a single Spx protein. The same result was obtained when the reaction was applied to an anti-c-Myc affigel (Fig. 4.10A). Following elution and gel electrophoresis, Spxc-Myc is found to be associated with RNAP, a protein of lower molecular weight is barely detectable beneath the Spxc-Myc band, which might reflect a small amount of RNAP non-specifically bound to the column (Fig. 4.10B), or a degradation product of Spxc-Myc, which we observed on some of the SDS-PAGE gels and western blots.

The experiment was repeated by first purifying RNAP in the presence of SpxΔCHA and Spxc-Myc protein using a Ni-NTA column; taking advantage of the *rpoC* allele encoding a His-tagged β' subunit (Qi & Hulett, 1998). Fig. 4.11 shows the input of RNAP (I_R) followed by SpxΔCHA and Spxc-Myc input (I_S). Elution with imidazole recovers RNAP bound to the Spx proteins. This was then applied to the affigel anti-HA

column, and the eluted fraction, again, contained only SpxΔCHA and RNAP, while Spxc-Myc was found in the flow-through fraction.

The possibility that promoter DNA was required for the interaction of two Spx monomers with the Spx-activated transcription complex was tested using the two epitope-tagged forms of Spx. A segment of *trxB* promoter DNA used in previous EMSA studies containing sequence from -50 to +20 (Nakano *et al.*, 2010b) was added to the binding reaction containing SpxΔCHA, Spxc-Myc, and RNAP. The reaction was applied to the anti-HA column, and fractions collected from the column were analyzed by SDS-PAGE and western blot using anti-Spx antiserum. The addition of *trxB* promoter DNA had no effect on Spx interaction with RNAP. Again, only the SpxΔCHA protein was found in the elution with RNAP, and no Spxc-Myc protein was detected (Fig. 4.12A). In vitro transcription using the flow-through and beads showed that the Spxc-Myc/RNAP and SpxΔCHA/RNAP complexes were transcriptionally active (Fig. 4.12B), yielding the expected 20 nucleotide transcript.

The finding that only one Spx protein establishes contact with RNAP suggests that other forms of Spx, such as the reported paralogous forms in certain Gram-positive bacteria, could potentially compete for RNAP. The Spx-RNAP pull-down experiment using SpxΔCHA and Spxc-Myc proteins, was repeated with 3-fold higher concentration of Spxc-Myc. As predicted, when excess Spxc-Myc was present in the binding reaction that was applied to the anti-HA affigel column, less RNAP co-eluted with SpxΔCHA (Fig. 4.8A and B). To rule out the possibility that the extended C-terminus of the Spxc-Myc protein inhibited interaction of a second Spx monomer with Spx/RNAP, wild-type Spx protein was added to the binding reaction containing SpxΔCHA and RNAP. The two

Spx proteins are nearly the same molecular weight and cannot be distinguished by SDS-PAGE. However, the same reduction in SpxΔCHA-RNAP interaction was observed when a 3-fold excess of Spx was added to the binding reactions (data not shown). Competition for SAd-RNAP was also observed when Spxc-Myc was added in excess to the binding reaction containing SpxΔCHA and SAd-RNAP (Fig. 4.8C and D).

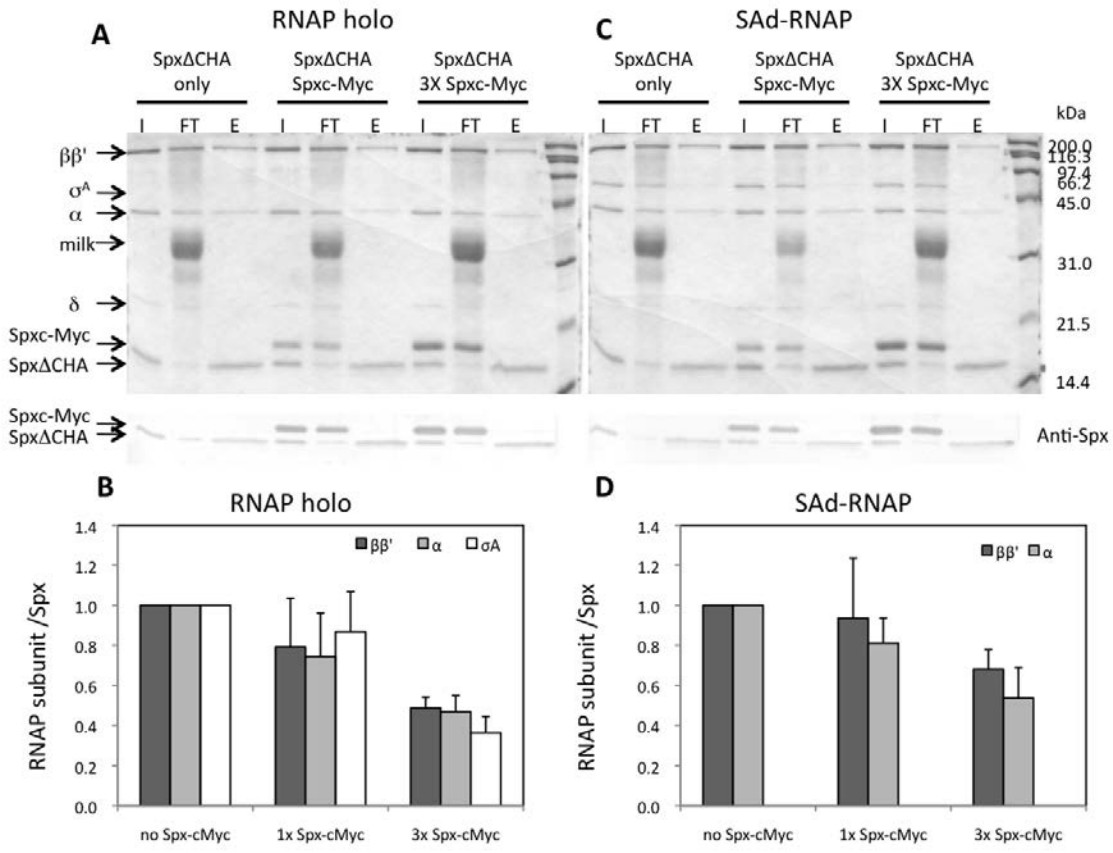

Figure 4.8. In vitro RNAP binding competition between SpxΔCHA and Spxc-Myc. SpxΔCHA and an equal or 3-fold molar excess amount of Spxc-Myc were incubated with RNAP holo- (A) or SAd-RNAP (C) in binding reactions. The complex was captured with anti-HA column and the composition of Spx/RNAP complex was analyzed by SDS-

PAGE and Western blot using antibodies against Spx. (B and D) The relative amount of RNAP subunit binding to SpxΔCHA in the presence of competitor Spxc-Myc was quantified, normalized against the reactions containing no Spxc-Myc (in which the ratio of RNAP subunit to Spx was given the value 1.0) and presented as a RNAP subunit/Spx ratio.

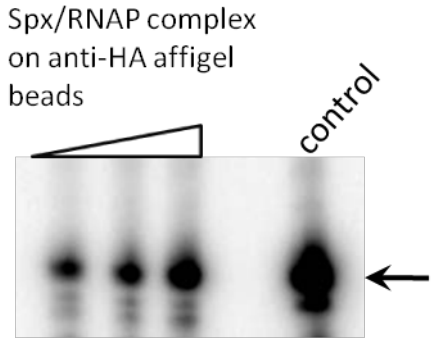

Figure 4.9. In vitro transcription from *trxB* promoter with Spx/RNAP complex immobilized on anti-HA beads. An anti-HA affigel interaction assay was performed as described in Materials and Methods. Instead of eluting Spx/RNAP complex from the column, beads were suspended with reaction buffer and directly applied to a transcription reaction containing *trxB* promoter DNA to confirm the activity of the Spx/RNAP complex. For the control, purified RNAP and Spx were used. The 66-nt transcript was pointed by an arrow. Open triangle at the top of image indicates the increasing volume of bead suspension containing Spx/RNAP complex.

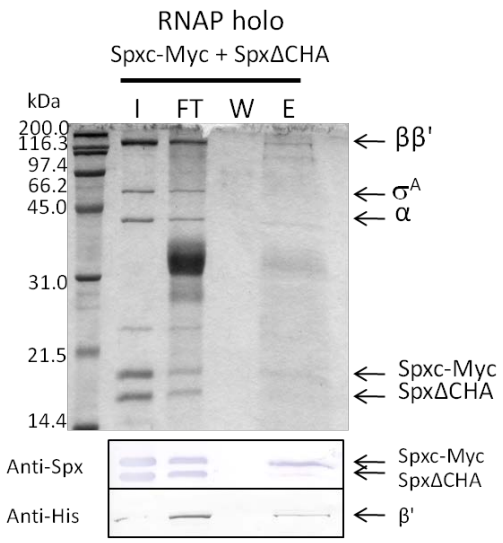

Figure 4.10. In vitro anti-c-Myc affigel pull-down competition. The composition of Spx/RNAP complex was confirmed with anti-c-Myc affigel interaction assay. An equimolar ratio of Spxc-Myc and SpxΔCHA was incubated with RNAP holoenzyme and applied to an anti-c-Myc affigel, followed by the same washing and elution procedure used for operation of anti-HA affigel chromatography. Due to the low binding capacity of anti-c-Myc affigel, the elution fraction was concentrated to appropriate volume for SDS-PAGE using a contricon filter (Millipore). The result was analyzed by Western Blot using Spx and His antibodies to detect Spx proteins and RNAP β' subunit. I, input; FT, flow-through; W, wash; E, elution

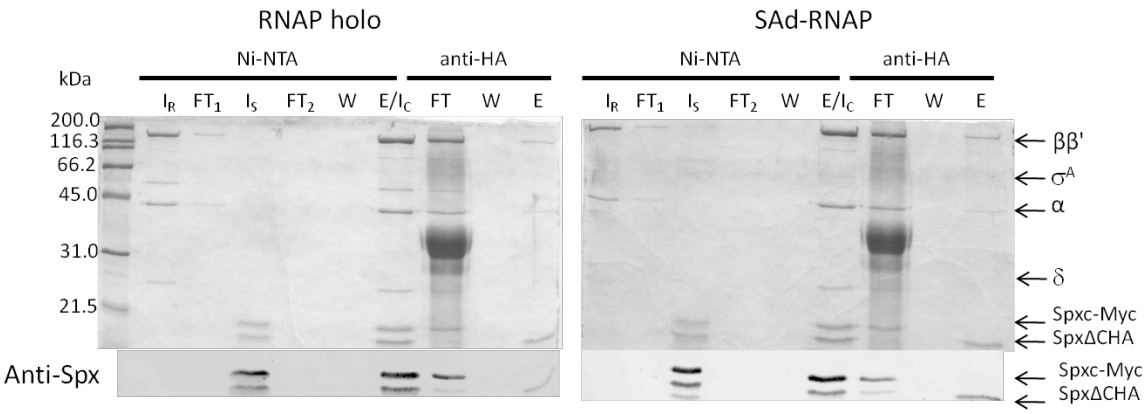

Figure 4.11. In vitro two-column interaction assay of Spx/RNAP complex. The His-tagged RNAP holo or SAd-RNAP was immobilized onto a Ni-NTA column and a mixture of SpxΔC-HA and Spxc-Myc at 1:1 molar ratio was applied to the RNAP pre-bound Ni-column. The Spx/RNAP complex was eluted with buffer containing 200 mM imidazole, and the elution fraction was directly applied to an anti-HA affinity column. The Spx/RNAP complex was captured through the SpxΔCHA interaction and eluted at high-pH. All the fractions from the two columns were collected and analyzed by SDS-PAGE and Western blot using Spx antibodies. Abbreviations: I_R, RNAP input; FT_1, RNAP flow-through; I_s, Spx input; FT_2, Spx flow-through; W, wash; E/I_c, elution from Ni-column and input for anti-HA column; FT, complex flow-through; E, elution.

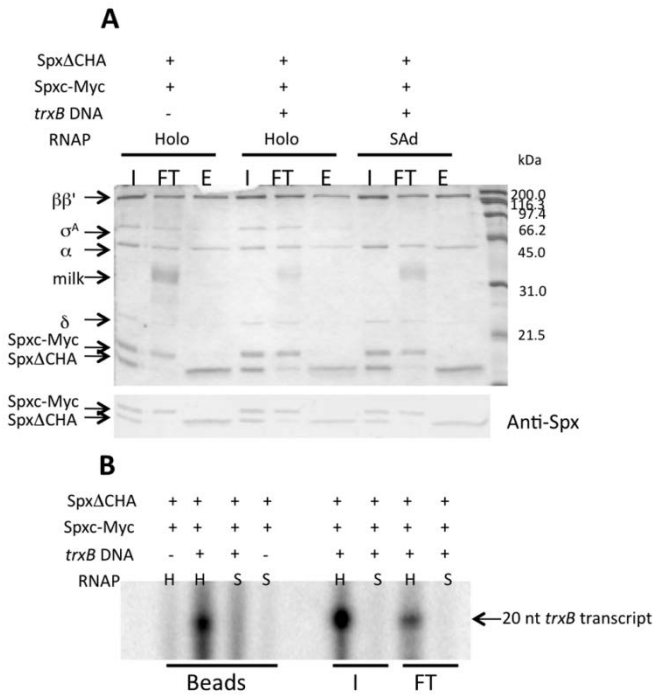

Figure 4.12. Composition of Spx/RNAP complex in the presence of *trxB* promoter DNA. (A) The affinity interaction assay reaction was performed by incubation of 2.5 μM SpxΔCHA, 2.5 μM Spxc-Myc and 0.25 μM RNAP holo or SAd-RNAP with or without 0.2 μM *trxB* promoter DNA fragment from position –50-+20 on promoter region in the presence of 20 μM initiating rATP at 37°C for 30 min. The protein mixture was applied to an anti-HA column, and the composition of Spx/RNAP/*trxB* complex was analyzed by SDS-PAGE and Western blot using Spx antibodies. (B) The activity of Spx/RNAP/DNA complex was examined by in vitro transcription. Instead of eluting from anti-HA column at high-pH, the complex-bound beads from each column were suspended with reaction buffer and directly used in the reaction without adding extra *trxB* DNA template. Abbreviations: I, input; FT, flow-through; E, elution; H, RNAP holoenzyme, S, SAd-RNAP.

4.2.4 Evidence that Spx is a monomer in solution

A possible explanation for why two differentially tagged versions of Spx do not engage RNAP simultaneously might be that Spx forms a dimer in solution, and the dimer of SpxΔCHA is in contact with the two α subunits of Spx. Previous reports argue against this possibility. The crystal structure of an in vivo assembled Spx/αCTD complex shows no interaction between Spx monomers (Lamour *et al.*, 2009) and no Spx in dimeric form was generated in the Spx/αCTD complex assembled in vitro (Newberry *et al.*, 2005). Secondly, ArsC, the structural homolog of Spx functions as a monomer (Martin *et al.*, 2001). We performed a glutaraldehyde crosslinking experiment (Fig. 4.13), using Spx/αCTD and α protein alone as positive controls, indicating that the majority of SpxΔCHA and wild-type Spx protein in solution is monomeric, while crosslinked versions of Spx/αCTD and α/α complexes can be detected. Notably, the Spx/αCTD crosslinked product is the size predicted if one monomer of Spx interacted with αCTD. Size exclusion chromatography with molecular weight markers showed that SpxΔCHA elutes from the column between MW 13kDa and 29kDa, indicating a monomeric form of the protein (Fig. 4.13B).

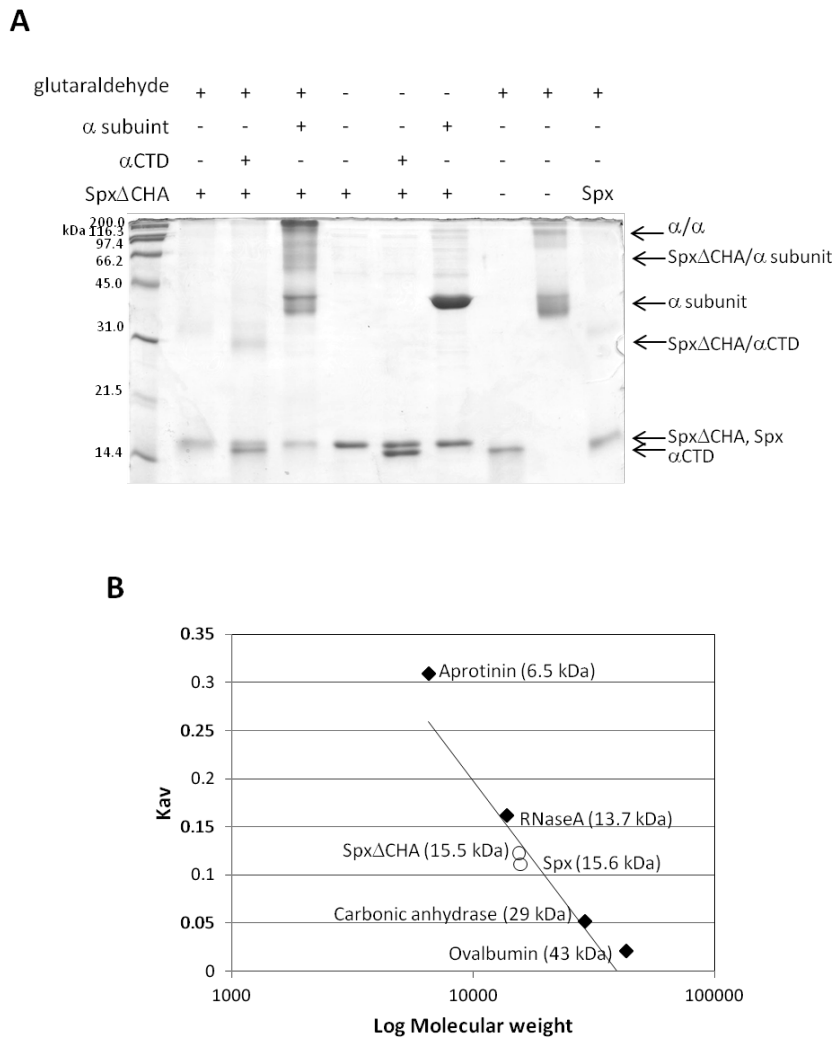

Figure 4.13. Glutaraldehyde crosslinking of Spx, αCTD, and α proteins and Gel fitration chromatography. (A) Glutaraldehyde cross-linking of SpxΔCHA with αCTD or α subunit. Ten μM of SpxΔCHA was incubated with ΔCTD or α subunit in 25mM Na-phosphate buffer, pH 8.0, 100 mM KCl, 5% glycerol at room temperature. After 15 min incubation, 150 μM of glutaraldehyde was added into reaction and incubated at room temperature for 90 min. The cross-linked complex was analyzed by 15% SDS-PAGE and Coomassie Blue G-250 staining. Purified wildtype Spx was used in the cross-linking reaction as a negative control in the last line. (B) Plot of K_{av} versus the logarithm of

molecular weight from gel filtration chromatography. The K_{av} values of proteins with known molecular weight (solid diamond symbols) were calculated to determine the calibration curve (solid line). Based on the elution volume of Spx or SpxΔCHA, the K_{av} value of Spx was also calculated and correlated to the standard curve. The estimated molecular weights of Spx proteins by gel filtration chromatography were in agreement with the molecular weight of a single monomer.

4.2.5 Wild-type Spx does not confer activity to a Spx(R60E)ΔCHA/RNAP complex

Evidence from affinity interaction experiments indicate that a single Spx protein interacts with RNAP to form the transcription activation complex, although it was possible that a small, undetectable amount of RNAP bound to two Spx proteins was captured on the anti-HA column. The possibility that two Spx proteins are capable of binding RNAP, but only one is active was tested by the following experiment. A binding reaction was assembled that contained Spxc-Myc, RNAP, and Spx(R60E)ΔCHA and was applied to the anti-HA affigel column. Affigel beads were retrieved to determine transcriptional activity of the complex. As was observed in the previous experiments, only the HA tagged form of Spx was detected in the elution fraction as determined by SDS-PAGE and western blot (Fig. 4.14A). The anti-HA beads containing immobilized Spx(R60E)ΔCHA –RNAP complex had no activity when *trxB* promoter DNA was added to immobilized mutant Spx/RNAP complexes on anti-HA resin in the presence of NTPs and radiolabeled UTP (Fig. 4.14B). No transcriptional activity was detected in the resin bound Spx/RNAP complex when *trxB* promoter DNA was added to the binding reaction

with RNAP, Spxc-Myc, and Spx(R60E)ΔCHA prior to column chromatography (Fig. 4.14C). These results indicate that active Spx does not productively associate with the RNAP complex bearing an inactive Spx variant.

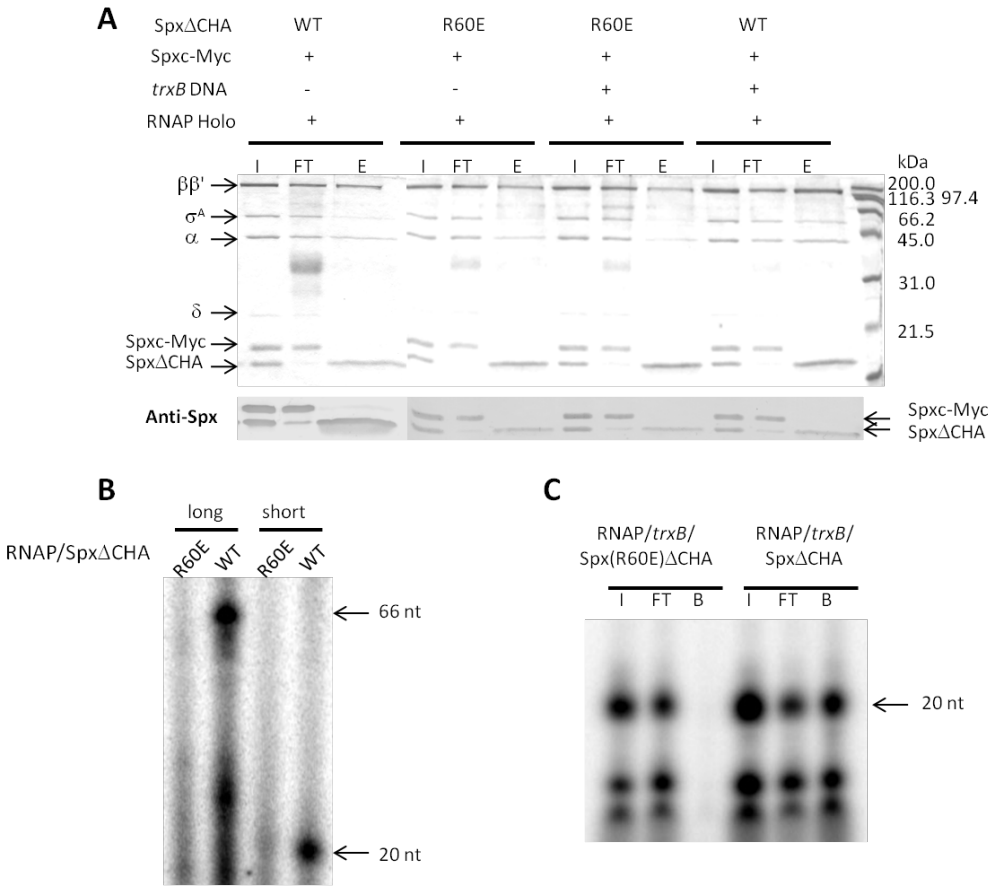

Figure 4.14. Binding reactions of RNAP with Spxc-Myc and mutant Spx(R60E)ΔCHA do not yield active Spx/RNAP complex bound to anti-HA column. (A) Anti-HA affigel interaction assay conducted in the presence of *trxB* promoter DNA. RNAP was incubated with SpxΔCHA or Spx(R60E)ΔCHA in the absence/presence of *trxB* (-50-+20)DNA, and protein mixture was applied to anti-HA affigel column. After washing and elution, the complex was analyzed by SDS-PAGE and Western blot with Spx antibodies. For in vitro transcription by using complex-bound beads, the beads were

resuspended with reaction buffer and directly added into transcription reaction. (B) Spx/RNAP-complex-bound beads were added into transcription containing *trxB* long (-118-+47) or short (-50-+20) promoter template. (C) Spx/RNAP/*trxB*-complex-bound beads were added to an in vitro transcription reaction. The *trxB* transcripts were marked by arrow. I, input; FT, flow-through; E, elution; B, complex-bound anti-HA beads.

4.2.6 A single Spx monomer interacts with RNAP in vivo

The data of Fig 4.2- 4.6 were generated in experiments using purified Spx and RNAP to assemble complexes in vitro. To gain an understanding of Spx/RNAP complex composition in vivo, an experiment was conducted to recover RNAP from cells in which Spx variants with differentially modified C-termini were produced. Two *spx* alleles were expressed, one resided in the *spx* locus and encoded SpxΔC, which is active but missing the C-terminal 12 amino acids; while at the *amyE* locus, a version of *spx* encoding SpxΔCHA was expressed from an IPTG-inducible promoter. SpxΔCHA could be distinguished from the SpxΔC protein on SDS-PAGE by its higher molecular weight. The strain bearing the two spx alleles also contained an allele of rpoC (β') whose product has a C-terminal His-tag designed for RNAP purification (40).

Cells of the *spx* diploid strain were grown in DSM to OD_{600} of 0.4 then treated with IPTG. Cells were harvested after 30 min and lysed by French press. The lysate was applied to an anti-HA column, which was washed and finally treated with high pH elution buffer. Western analysis of the column fractions showed that only the SpxΔCHA protein was eluted from the column (Fig. 4.15A), while the ΔC product was found in the

flow-through fraction. This result supported previous structural data and the experiment of Fig. 4.13, indicating that Spx does not form a homo-multimer (31). Western analysis of the fractions using anti-His-tag showed that RNAP copurified with SpxΔCHA in the affinity interaction assay reaction.

A sample of lysate, prepared in the same manner as described above, was applied to a Ni-chelate chromatography column. SDS-PAGE of the eluted RNAP showed that both Spx products co-eluted (Fig. 4.15B, showing replicate results), indicating that both are capable of interacting with RNAP in vivo. The eluted fraction was then applied to the anti-HA affigel column, which was washed and then treated with high pH elution buffer. The fractions were applied to two SDS-PAG and the resolved proteins were blotted onto nylon filters for western analysis using anti-Spx and anti-His-tag antibody. The RNAP and SpxΔHA were detected in the eluted fraction of the affigel anti-HA column. SpxΔC, which co-eluted with RNAP from the Ni-chelate column, was observed in the flow through fraction but was not detectable in the eluted fraction. The results show that both in vivo produced Spx derivatives are able to interact with RNA polymerase, but only one Spx protein is observed within an Spx/RNAP complex.

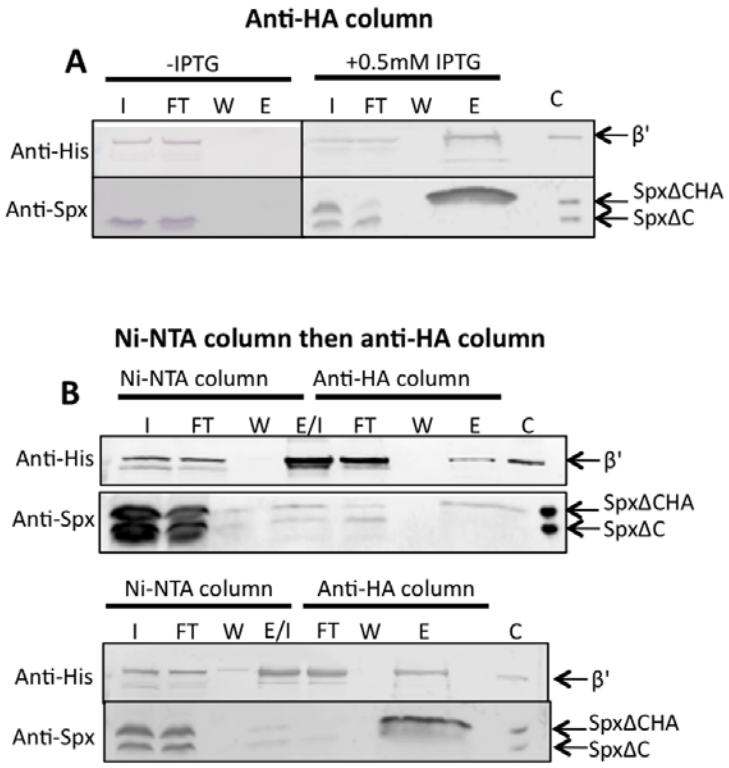

Figure 4.15. In vivo pull-down assay. The *B. subtilis* strain ORB8130 bearing the two *spx* alleles encoding SpxΔC and SpxΔCHA, and *rpoC-His* (β') was grown in DSM at 37°C to OD_{600} of 0.4, and treated with 0.5mM IPTG to induce SpxΔCHA expression for 30min. Cells were harvested and lysed, and the cleared lysate was directly applied to an anti-HA column (A). Replicate experiments were conducted with lysate applied first to a Ni-NTA column followed by anti-HA affinity chromatography (B). Shown are the stained SDS-PAG of fractions and Western blot analysis of fractions using anti-His-tag and anti-Spx antibodies to detect RNAP β' subunit and Spx proteins respectively. I, input; FT, flow-through; W, wash; E, elution, C, control lane containing RNAP, SpxΔC, and SpxΔCHA.

4.3 DISCUSSION

Previous studies have shown that Spx contacts RNAP αCTD to form a complex that can interact with a cis-acting element of Spx-controlled promoters (Nakano *et al.*, 2010b, Newberry *et al.*, 2005). The report of these studies posed a hypothesis that two Spx monomers could contact RNAP, forming a complex that could recognize promoters bearing either one or two Spx-responsive sequence elements. Such Spx-responsive elements have been found in the *trxA*, *trxB*, *nfrA*, and *ytpQ* genes, all of which are transcriptionally activated by Spx. The sequence resides immediately upstream of the -35 region of the core promoter in all four promoters, while in the *trxB* and *trxA* genes, a second element was thought to be located in a sequence overlapping with the -35 element (Nakano *et al.*, 2010b). Several scenarios could be envisioned to explain the mechanism of Spx/RNAP-promoter interaction. Two Spx monomers, each occupying a binding surface on the RNAP α subunit, might be required for optimal activation, or two Spx monomers bind to RNAP but only one functions in stimulating transcription. A third possibility is that a single Spx monomer engages RNAP and generates the DNA-binding SpxαCTD complex for promoter recognition. The evidence reported herein strongly supports the third scenario, that a single Spx monomer interacts RNAP holoenzyme to form the active Spx-stimulated transcription complex.

In this third scenario, one of the two α subunits, αI bound to β or αII to β', is the target of Spx interaction, and binding to either one could result in formation of a transcriptionally active complex. Alternatively, Spx must bind to only one of the two α subunits to productively engage RNAP. In this case, interaction between Spx and RNAP might involve multiple contacts, not only with αI or αII, but with another subunit, as

binding to one or the other would position Spx to contact another specific interaction surface on one of the RNAP subunits. In the affigel experiments, more RNAP co-eluted with Spx when holoenzyme was present in the binding reactions than when SAd-RNAP was applied to the reaction, suggesting that σ^A enhances Spx-RNAP interaction, and that the σ subunit might contribute an interaction surface. However, the exact basis of this effect remains to be investigated.

An excess of Spx protein was applied to each RNAP binding reaction, yet a significant amount of RNAP remained unbound to Spx. This might be due, in part, to the aforementioned preference of Spx for σ^A-bearing RNAP holoenzyme, but could also be due to the blocking conditions used to prevent non-specific binding of protein to the affigel column. Adding σ^A in 5X molar excess did not improve significantly the proportion of RNAP that could bind Spx. Recently reported proteomic analysis provided evidence that approximately 60% of holoenzyme RNAP is bound to σ^A (Delumeau *et al.*, 2011). While the RNAP preparation used in our studies appears quite pure after a 3-column purification, we cannot rule out the presence of RNAP-associated proteins, such as alternative sigma subunits, that might weaken Spx-RNAP interaction. At present, we do not know if Spx can engage alternative holoenzyme forms or if Spx can associate with elongating RNAP.

CRP-cAMP is capable of interacting with either α subunit as part of its mechanism for stimulating transcription initiation (Busby & Ebright, 1999). In class I transcriptional activation, the target promoter bears a CAP site centered at position -61 and is followed by an AT-rich sequence upstream of the -35 core promoter element. It is estimated that 3 in 4 class I activated complexes involve contact between a CRP dimer

and αI subunit (Hudson *et al.*, 2009, Lawson *et al.*, 2004). The αI CTD that binds CRP interacts with the upstream AT-rich region and contacts σ^{70} region 4 positioned at the -35 promoter sequence. The organization of the class I CRP-activated promoter is similar to the promoter sequence targeted by Spx, in that *trxB*, *trxA*, *ytpQ*, and *nfrA* all contain an upstream AT-rich sequence near the -35 element (Nakano *et al.*, 2010b, Reyes & Zuber, 2008). This suggests that productive interaction between a single monomer of Spx and RNAP might require contact between Spx and the CTD of αI (Fig. 4.16). That only a single monomer binds RNAP suggests further that α may not be the only binding partner of Spx and another subunit of RNAP might also serve as an Spx contact site, as suggested above. Further investigation of the Spx-activated transcription initiation complex is required to uncover the RNAP binding surfaces and cis-acting element directly targeted by Spx, and the organization of Spx-activated promoters.

The genomes of several low GC Gram-positive bacteria encode multiple paralogs of Spx; *B. anthracis* has two, SpxA1 and SpxA2, both of which are close homologs of *B. subtilis* Spx (Read *et al.*, 2003), and *L. lactis* has as many as 7 paralogs (Veiga *et al.*, 2007). With the established target of Spx being the αCTD, one could envision that two paralogous Spx forms could engage RNAP and refine the target recognition capabilities of the Spx-RNAP complex. Optimal transcriptional activation would involve interaction of a regulatory region with tandemly arranged sequences specific for each Spx/αCTD complex. In light of the evidence presented herein, which supports a model whereby a single Spx monomer engages RNAP, a more likely possibility is competition among Spx paralogs for RNAP interaction. Thus, synthesis of paralogous forms could be the result of differential expression of individual *spx* genes, with each product produced under distinct

environmental/metabolic conditions. Each Spx paralog could exert control over its own unique regulon, or paralogous Spx forms might occupy overlapping realms of control, directing the expression of common sets of genes.

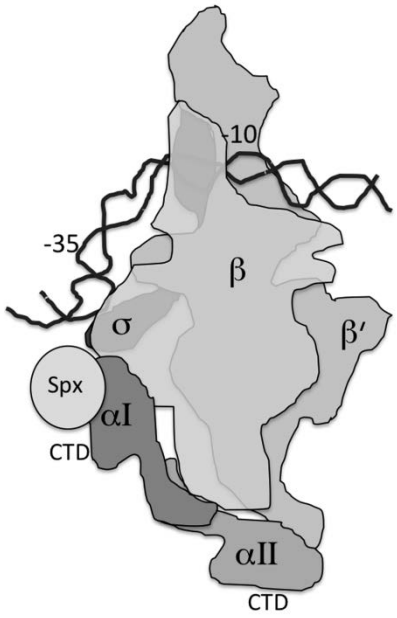

Figure 4.16. Model of Spx/RNAP/DNA complex. Interaction studies provide evidence that only a single Spx monomer binds RNAP. A proposed model of Spx interaction with RNAP is shown based on previous studies and data reported herein, as well as interaction between RNAP, CRP-cAMP and its class I promoter (Hudson *et al.*, 2009, Lawson *et al.*, 2004). Similar to CRP, single Spx might interact with αI CTD and form a productive complex with RNAP. The result of our experiments also suggests that not only αCTD, but other RNAP subunits, such as β subunit, may be involved in the interaction with Spx.

4.4 MATERIALS AND METHODS

4.4.1 Bacterial strains and culture conditions

All bacterial strains and plasmids are listed in Table 4.1. The *B. subtilis* strains used in this study are derivatives of JH642 and were grown at 37°C in 2× yeast extract-tryptone (2×YT) or Difco sporulation medium (DSM) (Harwood & Cutting, 1990). *E. coli* DH5α was used for plasmid construction and were grown at 37°C in 2×YT liquid or on Luria-Bertani (LB) solid medium containing 1.2% agar (Difco). For over-production and purification of Spx proteins in *E. coli*, ER2566 strains (New England Biolabs) bearing *spx* overexpressing plasmids were grown at 37°C in LB liquid medium. Antibiotic concentrations used were as previously reported (Choi *et al.*, 2006).

Table 4.1. *B. subtilis* strains and plasmids for Chapter 4

Strain or plasmid	Relevant genotype or characteristics	Source or reference
***B. subtilis* strains**		
JH642	*trpC2 pheA1*(parental strain)	James Hoch
MH5636	*trpC2 pheA1 rpoC*-His_{10} *cat*	Marion Hulett
ORB3834	*trpC2 pheA1* Δ*spx*::*neo*	Nakano, Hajarizadeh *et al.*, 2001
ORB5853	*trpC2 pheA1 sigA*(L366A) *neo rpoC*-His_{10} *cat*	This study
ORB6122	*trpC2 pheA1 rpoA*(Y263A) *rpoC*-His_{10} *cat*	This study
ORB7276	*trpC2 pheA1* Δ*spx*::*neo thrC*::pDYR9(*trxB-lacZ*) *amyE*::pSN56(P*spankhy-spx*^{DD})	Nakano, Lin, *et al.*, 2010
ORB7843	*trpC2 pheA1* Δ*spx*::*neo thrC*::pDYR9(*trxB-lacZ*) *amyE*::pAL45(P*spankhy-spx*Δ*CHA*)	This study
ORB7844	*trpC2 pheA1* Δ*spx*::*neo thrC*::pDYR9(*trxB-lacZ*) *amyE*::pAL50 (P*spankhy-spxcMyc*)	This study
ORB7850	*trpC2 pheA1* Δ*spx*::*neo amyE*::pDR111	This study
ORB7852	*trpC2 pheA1* Δ*spx*::*neo* Δ*yjbH*::*tet*$_{forward}$	This study
ORB7857	*trpC2 pheA1* Δ*spx*::*neo* *amyE*::pAL45(P*spankhy-spx*Δ*CHA*)	This study
ORB7858	*trpC2 pheA1* Δ*spx*::*neo* *amyE*::pAL50(P*spankhy-spxcMyc*)	This study
ORB7865	*trpC2 pheA1* Δ*spx*::*neo* Δ*yjbH*::*tet*$_{forward}$ *thrC*::pDYR9(*trxB-lacZ*) *amyE*::pSN56(P*spankhy-spx*^{DD})	This study
ORB7868	*trpC2 pheA1* Δ*spx*::*neo* Δ*yjbH*::*tet*$_{forward}$ *thrC*::pDYR9(*trxB-lacZ*) *amyE*::pAL45(P*spankhy-spx*Δ*CHA*)	This study
ORB7869	*trpC2 pheA1* Δ*spx*::*neo* Δ*yjbH*::*tet*$_{forward}$	This study

	thrC::pDYR9(*trxB-lacZ*) *amyE*::pAL50(P*spankhy-spxcMyc*)	
ORB8094	*trpC2 pheA1 rpoA*(Y263A) *rpoC*-His_{10} *cat sigA*(L366A)	This study
ORB8121	*trpC2 pheA1 amyE*::pAL45(P*spankhy-spx*Δ*CHA*)	This study
ORB8129	*trpC2 pheA1 rpoC*-His10 *cat amyE*::pAL45(P*spankhy-spx*Δ*CHA*)	This study
ORB8130	*trpC2 pheA1 rpoC*-His10 *cat spx*::pAL81 (*spx*Δ*C-neo*) *amyE*::pAL45(P*spankhy-spx*Δ*CHA*)	This study
Plasmids		
pAL39	pUC18 with *cMyc* tag	This study
pAL40	pUC18 with *HA* tag	This study
pAL42	pUC18 with *spx*Δ*CHA*	This study
pAL45	pDR111 with *spx*Δ*CHA*	This study
pAL46	pTYB4 with *spx*Δ*CHA*	This study
pAL47	pUC18 with *spxcMyc*	This study
pAL50	pDR111 with *spxcMyc*	This study
pAL51	pTYB4 with *spxcMyc*	This study
pAL73	pTYB4 with spx^{C10A}Δ*CHA*	This study
pAL74	pTYB4 with spx^{G52R}Δ*CHA*	This study
pAL75	pTYB4 with spx^{R60E}Δ*CHA*	This study
pAL78	pUC19 with *spx* upstream chromosomal region and *spx*Δ*C*	This study
pAL79	pUC19 with *spx* downstream chromosomal region	This study
pAL80	pUC19 with *spx* upstream chromosomal region, *spx*Δ*C*, and *neo*	This study
pAL81	pUC19 with *spx* upstream chromosomal region, *spx*Δ*C*, *neo*, and downstream sequence	This study
PDG783(ECE94)	vector with Km^R(Neo^R) cassette	Guérot-Fleury *et al*., 1995
pDG793	*thrC* integration vector with promoter-less *lacZ* reporter	Guérout-Fleury *et al.*, 1996
pDR111	*amyE* integration vector with P*spankhy* promoter	Britton *et al.*, 2002
pDYR9	pDG793 with *trxB*(-115~+47)-*lacZ*	Reyes and Zuber, 2008
pMMN470	pTYB4 with *spx*	Nakano *et al.*, 2007
pSN56	pDR111 with with spx^{DD}	Nakano, Kuster-Schock, *et al.*, 2003
pSN64	pTYB4 with *sigA*	Nakano, *et al*., 2006
pTYB4	*E. coli* expression vector for IMPACT™ system	New England BioRads
pUC18	cloning vector	
pUC19	cloning vector	

4.4.2 Construction of epitope-tagged Spx derivatives

To construct the expression plasmids producing epitope HA- or c-Myc-tagged Spx proteins, DNA fragments encoding HA and c-Myc tags were generated by annealing the forward and reverse oligonucleotides whose sequences correspond to HA or c-Myc codons (oAL29/oAL30 for c-Myc tag; oAL33/oAL34 for HA tag, oligonucleotide sequences are listed in Table 4.2), followed by PCR. The fragments generated were

cleaved with BamHI and SalI and inserted into pUC18 that was cleaved with BamHI and SalI to create pAL39 and pAL40 carrying cMyc and HA tag, respectively. In order to distinguish Spx variants by molecular weight, a truncated *spx* lacking codons specifying the carboxyl-terminal 12 amino acids (*spxΔC*) was generated by PCR using oligonucleotides oMMN01-135 and oAL35. PCR-amplified full-length and truncated *spx* fragments were then cloned into pAL39 and pAL40 to create pAL47 and pAL42 containing *spxc-Myc* and *spxΔCHA*, respectively. These constructs served as PCR templates for the following constructions.

Table 4.2. oligonucleotides used in the study (Chapter 4)

oligonucleotide	sequence	purpose
oAL29	CGCGGATCCGAGCAGAAATTAATATCAGAAGAGGATTTGTAG GTCGACATTG	*c-Myc* forward
oAL30	CAATGTCGACCTACAAATCCTCTTCTGATATTAATTTCTGCTC GGATCCGCG	*c-Myc* reverse
oAL31	TCCCCCGGGCAAATCCTCTTCTGATAT	*cMyc* reverse (pTYB4)
oAL32	CAATGTCGACCTACAAATCCTCTTCTGA	*c-Myc* reverse (pDR111)
oAL33	CGCGGATCCTATCCTTATGATGTTCCCTGATTATGCTTAGGTC GACATTG	*HA* forward
oAL34	CAATGTCGACCTAAGCATAATCAGGAACATCATAAGGATAGG ATCCGCG	*HA* reverse
oAL35	TCCCCCGGGAGCATAATCAGGAACATC	*HA* reverse (pTYB4)
oAL36	CAATGTCGACCTAAGCATAATCAGGAAC	*HA* reverse (pDR111)
oAL37	CGCGGATCCGCGAACTTTTCTTGGCAG	*spx*ΔC reverse
oAL38	CTGAGGACCGAACAGATG	*spx* G52R forward
oAL39	CATCTGTTCGGTCCTCAG	*spx* G52R reverse
oAL43	GCAGGATCCTAGATCGTATCATCAAAAGAAGG	*downstream of spx* forward
oAL44	TGTGAATTCCTTTGTATTTCTATTTTATG	*downstream of spx* reverse
oDYR06-03	ATCCCCATCAAACGTATTCCTTAC	*trxB* (-50~+20) forward
oDYR06-032	TAAACCATCTTTAAGCTTTTGGGCTCTTTC	*trxB* (-115~+47) reverse
oDYR07-052	GCGAATTCGGCCTTCTATAAACAGAAGGC	*trxB* (-115~+47) forward
oKE09	GGAATTCTGTTGAGCAAAAAAATAGCGTATC	*trxB* (-50~+20) reverse
oML02-07	CCCAAGCTTGCATTTCAAGCATGCTCAG	*upstream of spx* forward

oMMN01-135	AGAGGAGTGAAGATCCATGGTTACACTATAC	*spx* forward (pTYB4)
oMMN01-137	TAACTCCCGGGGTTTGCCAAACGCTGTGCTT	*spx* reverse (pTYB4)
oMMN01-173	CGAGGAAGCTTAGATGTTCATCCTACTA	*spx* forward (pDR111)
oMMN01-174	TACCAGCAGGTCGACAAATAAAAGAAGG	*Spx* reverse (pdR111)
oMMN07-351	GAAATCATCTCAACCGAGTCAAAAGTATTCCAA	*spx* R60E forward
oMMN07-352	TTGGAATACTTTTGACTCGGTTGAGATGATTTC	*spx* R60E reverse
oMN07-357	GAAAATCAGGTCGACTTAGCGAACTTTTCTTGGCAG	*spxΔC* reverse
oSG09-3	ATATGGATCCGTTTGCCAAACGCTGTGAAC	*Spx* reverse
oSN03-66	CACATCACCAAGCGCGACTTCATGCAGAA	*spx* C10A forward
oSN03-67	TTCTGCATGAAGTCGCGCTTGGTGATGTG	*spx* C10A reverse

To evaluate the activity of epitope-tagged Spx variants in *B. subtilis*, the alleles specifying the variants were integrated into the *amyE* locus using the pDR111 integration vector (Busby & Ebright, 1999) and expressed from an IPTG-inducible P*spankhy* promoter. The construction of pDR111 derivatives was described in a previous study (Nakano *et al.*, 2003b). Briefly, the *spx* fragments were amplified from plasmids carrying *spx*c-Myc or *spx*ΔCHA with upstream oligonucleotide oMMN01-173 and downstream oAL32 or oAL36 specifying the cMyc or HA tag, respectively. DNA fragments were digested with *Hin*dIII and *Sal*I, and cloned into pDR111 that was digested with the same enzymes. The recombinant plasmids were introduced by transformation into *B. subtilis* strains carrying *trxB-lacZ* fusion at the *thrC* locus (Reyes & Zuber, 2008). For the HA-tagged Spx mutants, two-step PCR-based mutagenesis was performed to generate the desired amino acid substitution as detailed in a previous study (Nakano *et al.*, 2010b). The previously constructed pSN56 bearing C-terminal amino acid substitutions (AN to DD) of Spx, which renders Spx resistant to ClpXP proteolysis (Nakano *et al.*, 2003b), was used as positive control. To express epitope-tagged Spx protein in *E. coli* for protein purification, the epitope-tagged *spx* fragments were

amplified from pAL47 or pAL42 with forward oligonucleotide oMMN01-135 and reverse oAL31 or oAL35 for cMyc or HA tag, respectively. DNA fragments were digested with *Nco*I and *Sma*I and then cloned into pTYB4, which is an *E. coli* expression vector used in the IMPACTTM Kit (New England BioLabs). The recombinant plasmids were introduced by transformation into E. coli strain ER2566.

To investigate Spx and RNAP interaction in vivo, two forms of ClpXP-resistant Spx with distinguishable molecular weights were produced in *B. subtilis*. To replace native spx gene with *spxΔC* by double crossover, *spx* with upstream and downstream flanking regions was PCR amplified with oligonucleotide oML02-07/oMMN07-357 and oAL43/oAL44 respectively, and the resultant PCR products were cloned into pUC19 to create pAL78 and pAL79. For antibiotic selection, a kanamycin-resistant (Km^R) cassette isolated from pDG783 (Guerout-Fleury *et al.*, 1996) was inserted immediately downstream of the *spx* sequence in pAL78 to create pAL80. To create a clone containing spx::km for integration into the *spx* locus, downstream sequence was cut from pAL79 with *BamH*I and *EcoR*I and inserted into pAL80 to create pAL81, which was used for *B. subtilis* transformation. For ectopic, IPTG-inducible *spxΔCHA* expression from the amyE locus, pAL45 mentioned above was used to transform *B. subtilis*.

4.4.3 β-galactosidase assays

Strains bearing a *trxB-lacZ* fusion were grown at 37°C overnight on DSM agar plates supplemented with appropriate antibiotics. The overnight cultures were used to inoculate the same liquid medium at a starting optical density at 600 nm of 0.02. When the OD_{600}

of the cultures reached 0.4, the cultures were divided into two flasks and 1 mM IPTG was added to one of the flasks. Samples were collected every 30 min, and β-galactosidase activity was assayed as previously described (Nakano *et al.*, 1998) and data is presented as Miller units (Miller, 1972).

4.4.4 Protein purification

His-tagged, σ^A-depleted RNAP (SAd-RNAP) was purified from σ^A mutant *B. subtilis* strain ORB5853 (*rpoC-His10*, *sigAL366A*), in which the Leu366 substitution in σ^A weakens the interaction to RNAP core enzyme (Zuber *et al.*, 2011). *B. subtilis* cells were grown in 2×YT liquid containing chloramphenicol and neomycin at 37°C until the OD_{600} of the culture reached 0.8-0.9, and then harvested by centrifugation at 2,000 xg. The pellets were frozen at −80°C prior to purification. Ni-NTA (PerfectPro, 5prime) affinity column, heparin column and Bio-Rad High Q column chromatography was performed as previously described (Nakano *et al.*, 2010b, Reyes & Zuber, 2008). (Note: Spx was previously reported to interact with Ni-NTA resin (Nakano *et al.*, 2002a), but the resin used in this study did not bind native Spx protein). RNAP was purified and stored at −20°C in buffer containing 10 mM Tris-HCl pH7.8, 100 mM KCl, 5 mM $MgCl_2$, 0.1 mM EDTA, and 50% glycerol.

The genes specifying σ^A and Spx variants were cloned in plasmid pTYB4 (terminus IMPACTTM-CN system, New England Biolabs). The products of the recombinant plasmids bear a self-cleavable intein and chitin-binding domains positioned at the C-termini. σ^A was overproduced from plasmid pSN64 (Nakano *et al.*, 2006) in *E.*

coli ER2566 and purified by using chitin resins (New England Biolabs) followed by BioRad High Q column. Purified protein was dialyzed and stored at −80°C in buffer containing 25 mM Tris-HCl pH8.0, 100 mM KCl, 0.1 mM EDTA, 1 mM MgCl2, and 10% glycerol. Spx variants were expressed from pTYB4 derivatives listed in Table 4.1. As previously described, Spx proteins were purified by using chitin column followed by BioRad High S column (Nakano *et al.*, 2001). For the affinity interaction assay, all of the Spx proteins were concentrated to 10 μM and stored at −80°C in buffer containing 10 mM Tris-HCl pH 8.0, 100 mM KCl, and 5% glycerol.

4.4.5 In vitro transcription.

A linear *trxB* promoter DNA template was generated by PCR with oligonucleotides oDYR07-32 and oDYR07-52, to yield a fragment that will direct the synthesis of a 66-nt transcript. For the reaction, 10 nM of the template and 25 nM of RNAP together with 25 nM σ^A were incubated without or with 75 nM Spx protein in 17.8 μl of 10 mM Tris-HCl pH 8.0, 50 mM NaCl, 5 mM MgCl2, and 50 mg/ml BSA. After 10-min incubation at 37°C, 2.2 μl of nucleotide mixture (200 mM ATP, GTP and CTP, 10 mM UTP, 5 mCi α-^{32}P-UTP) was added. After incubation at 37°C for 8 min, 10 μl of stop solution (1 M ammonium acetate, 0.1 mg/ml yeast RNA, and 0.03 M EDTA) was added to the reaction. The mixture was precipitated with ethanol and the pellet was dissolved with 5 ml of formamide-dye (0.3% xylene cyanol, 0.3% bromophenol blue, and 12 mM EDTA dissolved in formamide). The samples were heated at 90°C for 2 min and were applied to

an 8% polyacrylamide-urea gel. The dried gels were scanned on a Typhoon Trio+ variable imager (GE Healthcare).

To confirm that pull-down complexes were active, the RNAP/Spx complex-bound anti-HA resin was directly used in transcription reactions. An in vitro anti-HA affinity interaction assay was performed on a reaction containing 0.25 μM SAd-RNAP, 0.25 μM σ^A, and 2.5 μM SpxΔCHA. After washing, instead of eluting protein with triethylamine, resin was suspended in 40 μl of Reaction Buffer (RB, 10 mM Tris-HCl, pH8.0, 50 mM NaCl, 5 mM $MgCl_2$). Ten μl of resin suspension was directly added in the transcription reaction buffer with 10 nM of *trxB* (-115~+47) promoter DNA, and the reaction was performed as outlined above.

For the in vitro transcription with RNAP/Spx/DNA complex-bound resins, an in vitro anti-HA affinity interaction assay was performed with a reaction containing 0.25 μM SAd-RNAP, 0.25 μM σ^A, 2.5 μM SpxΔCHA, and 0.2 μM *trxB* (-50~+20) promoter DNA in the presence of 1 mM rATP. Ten μl of resin suspension, or 1 μl of input or flow-through from the column was added to separate reaction tubes and the in vitro transcription was performed as above.

4.4.6 In vitro affinity interaction assay

To detect proteins interacting with HA-tagged Spx in vitro, 40 μl of the anti-HA affinity matrix was pre-equilibrated with 10 column volumes (CV) of RB and blocked with 4 CV of Blocking Buffer (5% skim milk in RB) followed by washing with 8 CV of RB. For the reaction, 0.25 μM His-tagged SAd-RNAP and 2.5 μM SpxΔCHA were

incubated with or without 0.25 μM σ^A in 150 μl of RB at room temperature. After 20 min, protein mixture was then applied to the anti-HA affinity column followed by washing with 10 CV of Washing Buffer (0.05% Tween 20 in RB) and with 10 CV of RB. The protein complex was eluted from the column with 80 μl of 100 mM triethylamine, pH 11.5, and neutralized with 1/10 volume of 1 M Tris-HCl, pH6.8. The composition of protein complex was analyzed on the 15% SDS-polyacrylamide gel followed by Coomassie Blue G250 staining.

For the competition experiments, 2.5 or 7.5 μM Spxc-Myc was incubated together with RNAP and SpxΔC-HA in RB. To confirm the stoichiometry of Spx in the complex, the 2-column pull-down was also performed. After protein mixture was prepared, instead of directly being applied to anti-HA column, it was applied to a 40-μl Ni-NTA column, followed by washing with 20 CV of RB containing 30 mM imidazole. Complexes were eluted with 80 μl of RB containing 200 mM imidazole. The elution from the Ni-column was next applied to a 40-μl anti-HA column and the same procedure described above was followed.

For the interaction assay reaction carried out in the presence of promoter DNA, a *trxB* promoter fragment from position –50-+22 was PCR amplified with oligonucleotides oKE-9 and oDYR06-3 and purified from a low-melting agarose gel. In the reaction containing 0.25 μM SAd-RNAP, 2.5 μM SpxΔCHA, 2.5 μM Spxc-Myc, with or without 0.25 μM σA, 0.2 μM trxB DNA was added in the presence of 20 μM of initiating rATP in RB. The protein mixture was incubated at 37°C for 30 min and applied to a 40-μl anti-HA column. The same affinity pull-down procedure as detailed above was then conducted.

4.4.7 In vivo affinity interaction assay

To investigate the RNAP-Spx complex generated in vivo, a *B. subtilis* strain, ORB8130, which produces a His-tagged RNAP, and bears the *spx*Δ*C* allele in the *spx* locus, and an IPTG inducible *spx*Δ*CHA* allele in the *amyE* locus was generated. Briefly, the *B. subtilis* strain JH642 was first transformed with pAL45 with selection for spectinomycin resistance to create strain ORB8121. To express His-tagged *rpoC* in *B. subtilis*, ORB8121 was transformed with chromosomal DNA of strain MH3656 (Qi & Hulett, 1998) with selection for chloramphenicol resistance to create ORB8129. Because over-expression of Spx affects competence, the last step involved replacing the *spx* gene with the *spxΔC* allele by transforming ORB8129 with pAL81 with selection for neomycin resistance. The resultant strain ORB8030 was grown at 37°C overnight on LB agar plate supplemented with chloramphenicol, neomycin, and spectinomycin. The overnight cultures were used to inoculate 1 L of the DSM liquid medium supplemented only with chloramphenicol and spectinomycin. When the OD_{600} of the cultures reached 0.4, 0.5 mM IPTG was added. After 30 min incubation at 37°C, when the OD_{600} reached 0.8, cells were harvested by centrifugation at 2,000xg, and the pellets were frozen at –80°C. Cell pellet was suspended in 10 ml of RB containing 1 protease inhibitor cocktail tablet (Complete Mini, EDTA-free, Roche) and lysed by 2x passage through a French Press. The crude lysate was then centrifuged at 26,800xg, 4°C for 30 min, and the supernatant was filtered through a 0.22μm MILLEX-GP filter (Millipore). For affinity interaction assay with anti-HA resins, 500 μl of the clear lysate (10 mg/ml) was applied

to 40-μl anti-HA affinity column, and the same procedure as described above for the in vitro pull-down reaction was conducted. The flow-through, wash, and elution fractions were analyzed by SDS-polyacrylamide gel, and by Western blot using anti-Spx or anti-His antiserum.

For two-column pull-down, the cleared lysate (around 9.5 ml) was applied to 1-ml Ni-NTA column and incubated at 4°C for 1 hr. The Ni-column was washed with 20 CV of RB containing 30 mM imidazole and the protein complex was eluted with 2 ml of RB containing 200 mM imidazole. The elution fraction from the Ni-column was applied to a 0.5-ml anti-HA column. The anti-HA resin was washed with 10 CV of washing buffer and 10 CV of RB as described above. The protein complex was eluted with 2 ml of 100 mM triethylamine, pH 11.5, neutralized with 1 M Tris-HCl, pH6.8, followed by concentration with a 3-KDa Amicon ultra-centrifugal filter (Millipore) to an appropriate volume for loading onto the SDS-polyacrylamide gel (less than 30 μl per lane). The composition of protein complex was analyzed by SDS-polyacrylamide gel, and by Western blot using anti-Spx or anti-His serum.

4.4.8 Gel fitration chromatography

To determine whether Spx proteins form homodimers in solution, gel filtration chromatography was performed. Purified Spx or SpxΔCHA was applied to the column packed with Bio-Gel® P-60 polyacrylamide gel (Bio-Rad) and run with buffer containing 10 mM Tris-HCl pH8.0, 100 mM KCl, and 2% glycerol. The void volume and the calibration curve were determined by using the Gel filtration LMW Calibration Kit (GE

healthcare) and ploting a standard K_{av}-logMW graph. The partition coefficient, K_{av}, of each protein was calculated by using the equation: $K_{av} = (Ve-Vo)/(Vc-Vo)$, where Vo = void volume, Ve = elution volume, and Vc = geometric column volume. By correlating the Kav value of Spx protein to the calibration curve, the composition of Spx protein in solution was determined.

CHAPTER 5

RESIDUE SUBSTITUTIONS NEAR THE REDOX CENTER OF BACILLUS SUBTILIS SPX AFFECT RNA POLYMERASE INTERACTION, REDOX CONTROL AND SPX-DNA CONTACT AT A CONSERVED CIS-ACTING ELEMENT

5.1 INTRODUCTION

Bacterial responses to environmental and metabolic changes often involve gene regulation at the level of transcription initiation. The essential enzyme catalyzing this first step of gene expression, RNA polymerase (RNAP), is targeted by a variety of regulatory factors that direct RNAP activity to specific transcription units (Lee *et al.*, 2012). The core RNAP, bearing the catalytic component, is composed of large subunits, β and β', the α subunit dimer, and the ω subunit. Interaction of core RNAP with the σ subunit gives rise to the holoenzyme endowed with gene promoter specificity (Murakami & Darst, 2003, Murakami *et al.*, 2003). Regulatory factors that are controlled by signal sensing/transducing systems that mediate stress responses can target one or more of the RNAP subunits to modulate activity and promoter specificity. Some regulatory factors exert positive control by engaging promoter DNA and recruiting RNAP through direct protein-RNAP subunit interaction (Lee *et al.*, 2012). There is a growing list of regulatory proteins that pre-recruit or appropriate RNAP by first contacting holoenzyme before

mediating DNA target recognition (Haugen *et al.*, 2008). One of them, AsiA of phage T4, serves to mediate contact between RNAP σ subunit and a phage-encoded DNA-bound factor, MotA, which triggers prereplicative phage gene transcription (Pineda *et al.*, 2004). The DksA/Gre family proteins target the RNAP active site to affect transcription initation and elongation at specific promoters (Paul *et al.*, 2004). SoxS and related proteins engage in pre-recruitment by interacting with holoenzyme before contacting specific cis-acting promoter elements (Griffith *et al.*, 2002). Other factors, such as Crl and 6S RNA, stabilize or inhibit specific holoenzyme forms bearing distinct σ subunits (Barrick *et al.*, 2005, Bougdour *et al.*, 2004).

In low GC Gram-positive bacteria, the Spx family of proteins control transcription initiation in response to thiol reactive agents (Zuber, 2004). A variety of genes/operons are activated by Spx, including those whose products function in thiol homeostasis, in low molecular weight redox buffer biosynthesis, and in cysteine biosynthesis/uptake (Chi *et al.*, 2011, Gaballa *et al.*, 2010, Nakano *et al.*, 2003b, Rochat *et al.*, 2012). Spx is often encoded by paralogous genes within certain bacterial species (Turlan *et al.*, 2009), and in some cases the genes are essential and/or required for bacterial virulence in pathogenic species (Chen *et al.*, 2012, Kajfasz *et al.*, 2012, Kajfasz *et al.*, 2010). Spx is a monomer in solution, and a single monomer engages RNAP by contacting the α dimer (Lin & Zuber, 2012). Spx has higher affinity for holoenzyme bearing the σ^A subunit than for core RNAP, although there is little evidence that Spx directly contacts sigma (Lin & Zuber, 2012, Newberry *et al.*, 2005). Free Spx protein of *B. subtilis* does not bind to DNA, although when it interacts with holoenzyme it directs RNAP to promoter regions that bear a conserved upstream sequence motif, which is usually AGCA, centered

approximately at position -44 with respect to the transcription start site (Nakano *et al.*, 2005, Reyes & Zuber, 2008). This sequence assignment was supported by recent ChIP-chip analysis, which also showed that Spx/RNAP complex targeted 144 operons in the *B. subtilis* genome (Rochat *et al.*, 2012).

The expression of *spx* in *B. subtilis* is under multilevel control. Transcription is catalyzed by four different RNAP holoenzyme forms and is under negative control by PerR and YodB, which are sensitive to peroxide and thiol-reactive agents, respectively (Antelmann *et al.*, 2000, Eiamphungporn & Helmann, 2008, Jarvis, 1967, Leelakriangsak *et al.*, 2007, Thackray & Moir, 2003). The activity of Spx is controlled by a redox switch involving an N-terminal CXXC thiol/disulfide center. Spx mediates RNAP-promoter interaction when in the oxidized, disulfide form, as Spx/RNAP contact with promoter DNA is abolished in the presence of reductant (Nakano *et al.*, 2005). Lastly, Spx is under proteolytic control mediated by the ATP-dependent protease, ClpXP and a substrate recognition factor, YjbH (Garg *et al.*, 2009, Larsson *et al.*, 2007). Proteolytic control is responsive to oxidative stress, as Spx protein accumulates to elevated concentrations in cells that encounter toxic, thiol-reactive oxidants (Engman *et al.*, 2012, Nakano *et al.*, 2003c).

Many questions remain to be answered with respect to the mechanism of Spx-activated transcription. It is not known why Spx has higher affinity for holoenzyme than for RNAP lacking σ^A. It is not known if Spx contacts promoter DNA. It is not known why the oxidized form of Spx promotes RNAP-promoter DNA contact. It is not clear why only one Spx monomer contacts the α dimer. Previous structural studies showed that Spx contacts the C-terminal domain of the α subunit (αCTD) and that an α helix, α4 (see

Fig. 1) in Spx becomes unfolded upon reduction of the Spx disulfide center (Nakano *et al.*, 2010b). An amino acid substitution, R60E, in this region of the protein affects Spx-dependent activation and prevents a complex of Spx and αCTD from binding to promoter DNA.

The structural analysis of the Spx protein uncovered two domains: A redox domain consisting of the N- and C-terminal regions and containing the redox disulfide center (C10TSC13), and the central domain that contains the αCTD binding surface (defined by the *spx* codon substitution G52R (Nakano *et al.*, 2000, Newberry *et al.*, 2005)) and the α4 helix (residue R60 to V69, (Nakano *et al.*, 2010b)). The two domains are separated by a linker of two coils bearing residues, which in ArsC function in catalysis (Martin *et al.*, 2001). In this report, a study is presented in which residue substitutions in the linker and a4 of Spx were generated that affect RNAP and α subunit interaction. Together, the data suggest the presence of an additional site on Spx required for α subunit contact. Data is also presented that demonstrates Spx direct contact with the conserved upstream AGCA element, and defects in DNA contact are conferred by Spx residue substitutions that affect Spx-activated transcription. DNA-protein crosslinking data shows that Spx interaction with RNAP and the AGCA upstream element results in a re-positioning of the σ^A subunit resulting in its contact with the core promoter.

5.2 RESULTS

5.2.1 Mutational analysis identified residues near the redox switch and within the helix α4 that are important for *trxB* transcriptional activation

Optimal Spx-stimulated transcription requires the formation of a disulfide bond between C10 and C13 in Spx. The structures of the oxidized Spx and reduced C10S Spx in complex with RNAP αCTD have been resolved (Lamour *et al.*, 2009, Nakano *et al.*, 2010b, Newberry *et al.*, 2005). A significant conformational change was found between the oxidized and reduced forms of Spx (Fig. 5.1), whereby the helix α4 in mutant C10S Spx was unfolded when the disulfide bond could not be formed. It is likely that the formation of disulfide bond may lead to the structural change in helix α4 of Spx, and further enable Spx to activate transcription by facilitating target promoter or RNAP contact. To investigate whether the residues within helix α4 are necessary for the function of Spx, and whether residues in the vicinity of the redox center conserved in ArsC are involved in transcriptional activation, single amino acid substitutions were introduced within the helix α4 region and near the redox disulfide center in the linker region separating the redox and central domains of the Spx protein to examine their effects on Spx activity. To prevent the degradation of Spx by ClpXP protease under non-stress conditions, we expressed the ClpXP-resistant forms (Spx^{DD}) of the wild-type and mutant proteins from an IPTG-inducible promoter and evaluated the effect of Spx amino acid substitutions on Spx-dependent *trxB-lacZ* transcription *in vivo* in the presence of IPTG. The relative activity of mutant to the wild-type Spx product and production of each Spx protein, as observed by western blot analysis, are shown in Fig. 5.2. Previous

mutational analyses showed that the residue C10 in the redox disulfide center and R60 and K62 residues in the helix α4 region are important for the transcriptional activation of *trxB* (Nakano *et al.*, 2010b, Nakano *et al.*, 2005). The Spx R60E mutant markedly reduced transcriptional activation *in vivo* and in vitro, and the Spx(R60E)/αCTD complex could not interact with DNA (Nakano *et al.*, 2010b). As shown in a previous study, Spx C10A and R60E mutants significantly reduced the *trxB* transcription, and the K62E mutant was also moderately defective in transcription activation (Fig. 5.2A). This confirmed that the R60 residue plays an important role in the interaction between Spx/RNAP and promoter DNA. The F64A mutant showed a similar effect as K62E. When F64 was substituted with tryptophan, another amino acid bearing an aromatic side chain, the activity of Spx was restored, which implied that the aromatic ring at this position in α4 might be involved in forming a proper structure for Spx function. The other three mutants, Q65A, N68A, and N70A in helix α4 region, showed no effect on transcription activation. We also investigated the effect of residues around the redox disulfide center required for *trxB* transcriptional activation. The Y5 in the N-terminal sheet β1 near the redox center was substituted with alanine, but the production of mutant protein was not detected by western blot analysis (Fig. 5.2B), hence the decreased transcriptional activity is due to low levels of Spx (Fig. 5.2A). However, the Y5F mutant protein is stable and the activity is similar to wild-type Spx, indicating that and aromatic side chain is required at this position. The function of Y5 is apparently structural and is not directly involved in Spx-dependent transcriptional activation.

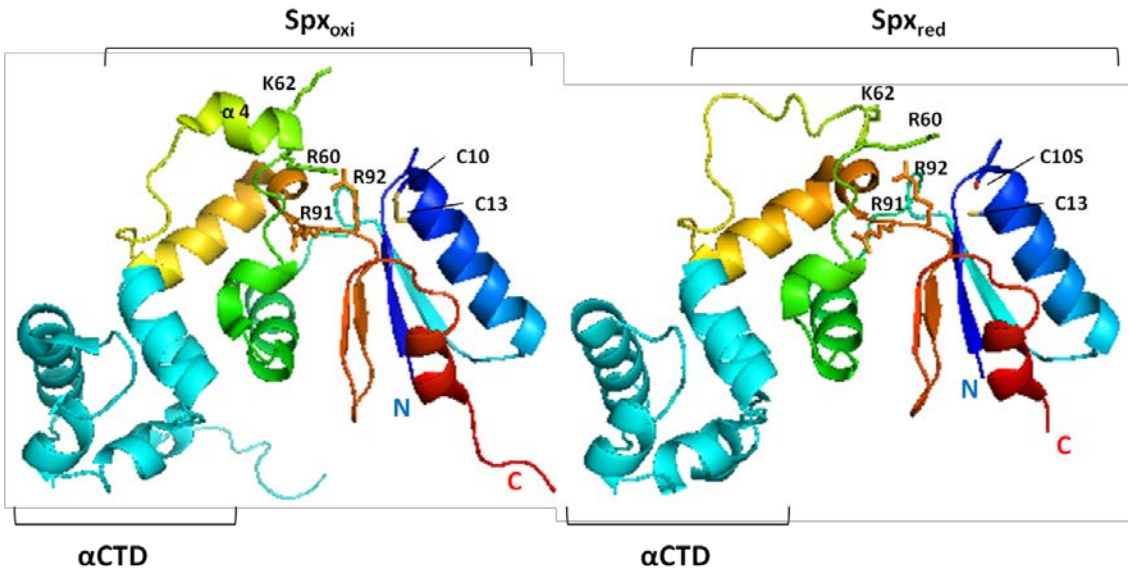

Figure 5.1. Structures of oxidized Spx (A) and reduced C10S Spx (B) in complex with αCTD. The crystal structures of *B. subtilis* oxidized Spx (PDB accession number 3GFK) (Lamour *et al.*, 2009) and reduced C10S Spx (PDB accession number 3IHQ) (Nakano *et al.*, 2010b) /αCTD complexes were visualized by using the software PyMOL. The αCTD and Spx are shown as cyan and rainbow color ribbons, respectively. The side-chains of C10, C13, R60, K62, R91, and R92 are shown and labeled.

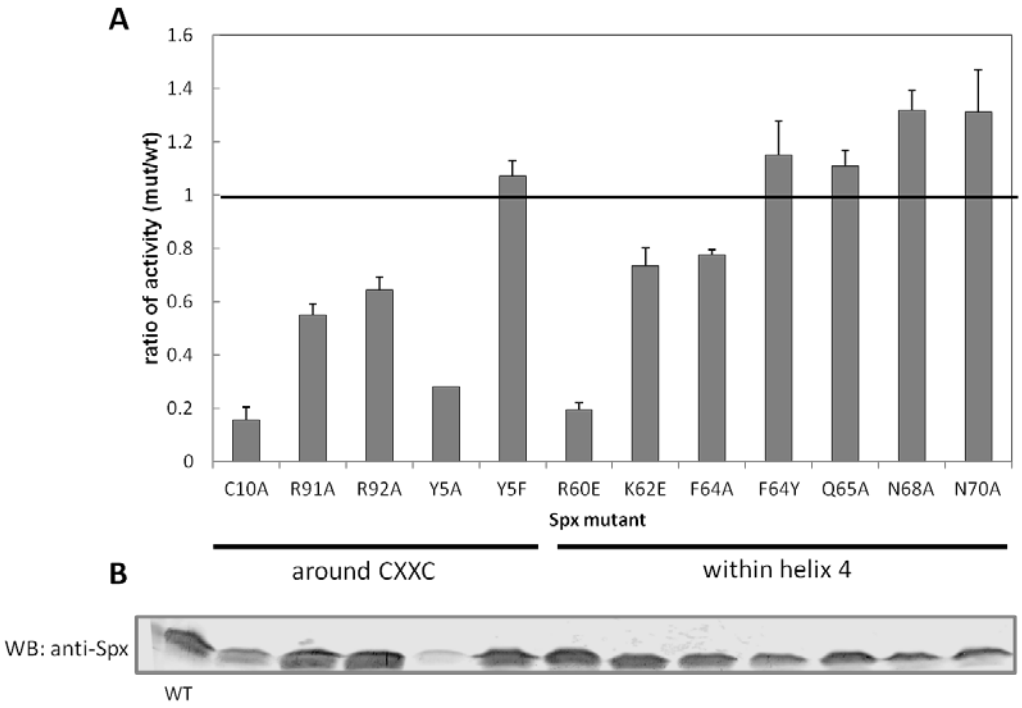

Figure 5.2. Effect of amino acid substitutions near the redox switch and within helix α4 of Spx on *trxB-lacZ* transcription. (A) The IPTG- inducible alleles encoding proteolysis-resistant form of Spx^{DD} or Spx^{DD} with other amino acid substitutions was introduced into the *amyE* locus of the Spx null mutant strain bearing a *trxB-lacZ* fusion. Strains were grown in DS medium and when the OD_{600} was 0.4, 1 mM IPTG was added to induce the spx^{DD} transcription. Samples were taken at time intervals and β-galactosidase activities were measured. The highest activities in each Spx mutant during growth were selected and used to calculate the ratio of Spx activity relative to the wildtype. (B) Cells of each strain were harvested 1.5 h after IPTG addition and lysed with bead-beating method to extract total cellular protein. Spx protein levels in these strains were determined by Western blot analysis using anti-Spx antibody.

The R92 residue is conserved in arsenate reductase and thought to heighten the C10 thiolate reactivity (Shi *et al.*, 2003). The side chain of R92, which is in the vicinity of the C10 and the helix α4 region in Spx, turns away from the disulfide upon Spx oxidation [Fig. 5.1,(Nakano *et al.*, 2010b, Newberry *et al.*, 2005)]. Next to the R92 is another conserved arginine, R91, which in some Spx orthologs is replaced with a lysine. Both Spx mutants, R91A and R92A, reduced the *trxB*-lacZ expression up to 30% to 40% (Fig. 5.2). However, the R91A R92A double mutant, showed synergistic effects on the *trxB* transcription and almost abolished transcription (Fig. 5.3A). This result implies that the two arginine residues play different roles in Spx-dependent transcription regulation. To determine whether the effect of these two arginine mutants is specific to Spx-dependent transcription activation, the involvement of the two substitutions in negative control was examined by measuring the expression of a *srfA-lacZ* construct. As reported previously, ComA-dependent transcriptional activation of *srfA* is repressed by Spx in vivo and in vitro (Nakano *et al.*, 2003c). The R92A mutant form of Spx produced in the presence of IPTG could still repress *srfA* transcription as well as the wild-type Spx, but the R91A mutant lost the ability to repress *srfA* transcription (Fig. 5.3B). This result indicated that Spx R92A mutation affected transcription activation but was able to engage RNAP. In contrast, R91A mutant Spx is defective in RNAP interaction, since neither Spx-dependent positive or negative control was fully operational. For the R92 residue, the crystal structure of Spx in the sulfate-free condition showed movement of the R92 residue when the disulfide formed, but a conformational change in helix α4 region was not detected (Fig. 5.1A) (Lamour *et al.*, 2009). To examine whether the structure of the side chain of R92 is important for the transcriptional activation, the R92 residue was

substituted with glutamine residue, which has a similar side chain geometry but is uncharged. However, Lac assay results showed that Spx R92Q mutant also had 30% reduction of *trxB* transcription, which was similar to the defect conferred by the R92A mutation (Fig. 5.4). To test if the positive charge of the Arg side-chain is required for optimal activity, R92 was replaced with a lysine, but this did not restore Spx activity in vivo to that of the wild- type parent protein (Fig. 5.4). This suggests that the role of R92 is not to contribute a positive charge for the electrostatic interaction of Spx with DNA, which its interaction with a sulfate ion within the crystal structure was thought to imply (Lamour *et al.*, 2009, Newberry *et al.*, 2005).

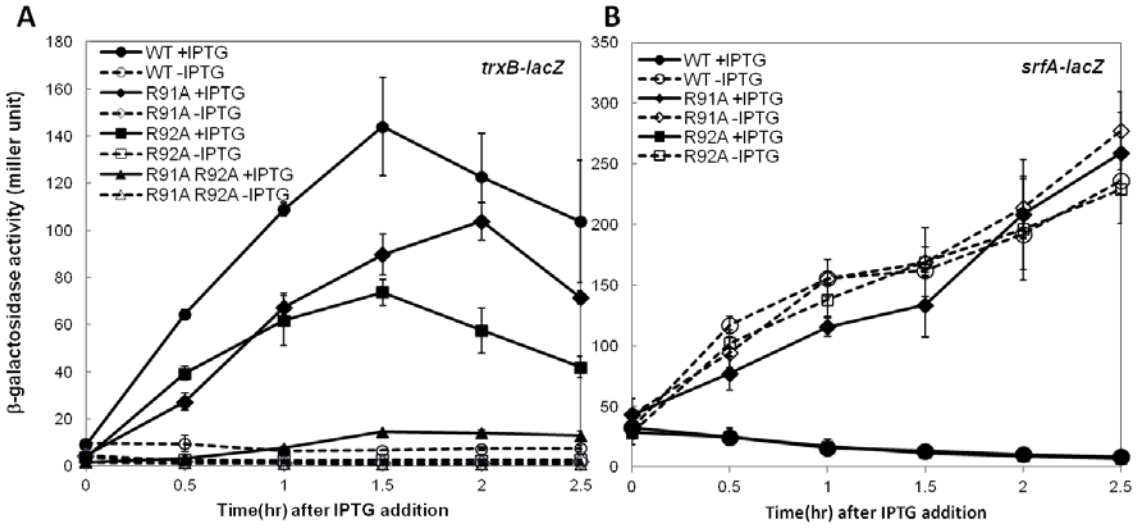

Figure 5.3. Effect of Spx R91A and R92A mutations on the transcription of *trxB-lacZ* and *srfA-lacZ*. Strains bearing *trxB-lacZ* (A) or *srfA-lacZ* (B) were grown in DS medium as mentioned above. When the OD_{600} reached 0.4, each culture was divided into two flasks, and 1 mM IPTG was added to one flask to induce Spx^{DD} expression. Samples were taken at time intervals and β-galactosidase activities were measured. Symbols:

circles, Spx^{DD}; diamonds, Spx(R91A)^{DD}; squares, Spx(R92A)^{DD}; triangles, Spx(R91A, R92A)^{DD}. Open symbols with broken lines represent cells cultured without IPTG, and closed symbols with solid lines represent cell culture with IPTG.

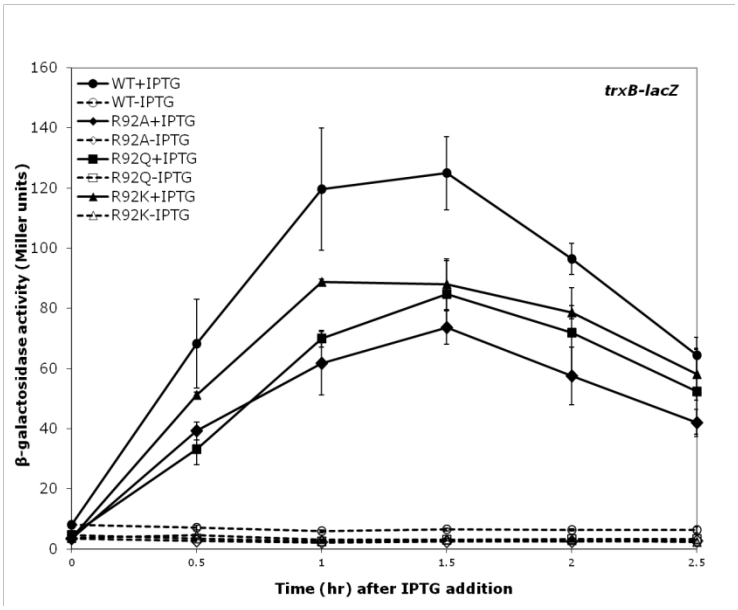

Figure 5.4. Effect of R92 substitutions in Spx on the transcription of *trxB-lacZ*. Spx R92 residue was substituted with alanine (R92A), glutamine (R92Q), or lysine (R92K), and the resulting mutant alleles were introduced under IPTG control at the *amyE* locus in *spx* null mutant strain bearing *trxB-lacZ*. Strains were grown in DS medium until the OD_{600} reached 0.4. Then, each culture was divided into two flasks, and 1 mM IPTG was added to one flask to induce Spx^{DD} expression. Samples were taken at time intervals and β-galactosidase activities were measured. Symbols: circles, Spx^{DD}; diamonds, Spx(R92A)^{DD}; squares, Spx(R92Q)^{DD}; triangles, Spx(R92K)^{DD}. Open symbols with broken lines represent cells cultured without IPTG, and closed symbols with solid lines represent cell culture with IPTG.

5.2.2 The phenotype of double mutants suggests a role of R92 in redox control of Spx

Several additional residue substitutions were introduced in the *spxR92A* mutant to create a series of double mutants, including Spx(C10A, R92A), Spx(R60E, R92A), and Spx(K62E, R92A), and *trxB-lacZ* activity was examined in these mutant strains. Western blot analysis indicated that mutant Spx proteins were within a 2-fold range of intracellular concentration (Fig. 5.5B). The results indicate that the C10A mutation is epistatic to R92A in the Spx(C10A, R92A)-expressing strain, as the same level of activity as the Spx(C10A) mutant was observed (Fig. 5.5A and B). In contrast, R60E or K62E, together with R92A showed synergistic negative effects on the *trxB* transcription, because Spx(R60E, R92A) nearly abolished *trxB-lacZ* expression (Fig. 5.5A) and Spx(K62E, R92A) reduced transcription to the same extent as Spx(C10A) mutant (Fig. 5.5B). These results indicate that the R92A phenotype cannot be observed in the C10A background and is observed only if the C10-C13 disulfide bond is able to form. It suggests that the effect of the R92A on transcription might be connected to disulfide formation and redox control of Spx. In contrast, combining the R92A mutation with R60E results in an additive effect, suggesting that the two residues perform separate functions that contribute to Spx-activated transcription.

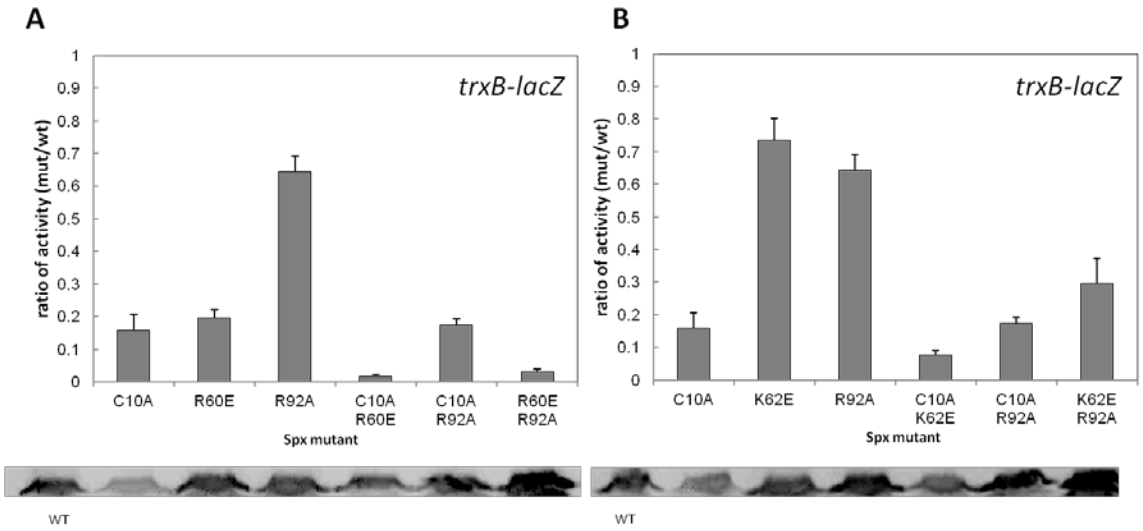

Figure 5.5. Effect of Spx R92A mutant with the amino acid substitutions in redox switch or in helix α4 region on the *trxB-lacZ* transcription. The IPTG-inducible alleles encoding Spx(R92A)^{DD} with amino acid substitutions in either redox switch (C10) or helix α4 region R60(A) or K62(B) were introduced into the *amyE* locus of the Spx null mutant strain bearing *trxB-lacZ*. The β-galactosidase assay was performed as mentioned in Fig. 5.3 and the highest activities of Spx mutants were taken and calculated the ratio to that of Spx^{DD}. Spx levels in these strains were determined by Western blot analysis using anti-Spx antibody and result was shown in the bottom panel.

5.2.3 Residue substitutions at R91 and R92 reduce Spx activity in vitro

To verify the effect of Spx R91A and Spx R92A mutant proteins in vitro, each protein, purified as shown in Materials and Methods, was applied to a transcription reaction with purified RNA polymerase and the supercoiled template (Ross *et al.*, 1990) containing *trxB* promoter DNA. A time-course transcription was performed (Fig. 5.6) and the effect

of Spx mutants was compared to that of wild-type Spx at each time point. The intensity of the transcript was quantified and normalized by using an internal control transcript encoded by plasmid-borne *rna1*. The effect of Spx mutants was presented as percentages on normalized *trxB* transcription relative to that observed in reactions containing wild-type Spx (Fig. 5.6, bottom panel). Both R91A and R92A mutations conferred reduced transcription-stimulating activity, with levels of in vitro-generated transcripts below those synthesized by wild-type Spx/RNAP.

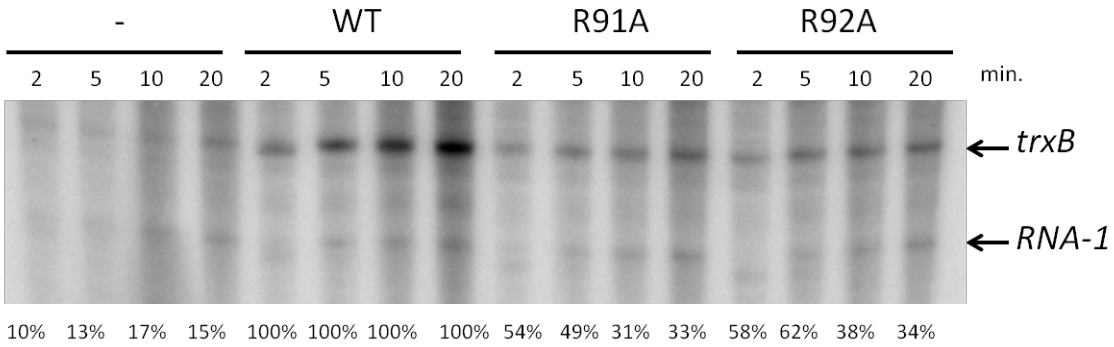

Figure 5.6. *In vitro* transcription from the plasmid carrying the *trxB* promoter in the absence and presence of the wild-type Spx, Spx(R91A), or Spx(R92A). The plasmid DNA containing the *trxB* promoter region (10 nM) was incubated with 10 nM reconstituted *B. subtilis* RNAP (SAd-RNAP: σ^A = 1:3) and 10 nM Spx, Spx(R91A), or Spx(R92A), and the reaction was performed in a time-course manner. Band intensity of each *trxB* transcript was quantified and normalized with that of *RNA-1* transcript. The *trxB* transcription level activated by each Spx mutants was calculated and presented as a percentage compared to that by wild-type Spx.

5.2.4 Spx R91A mutant is defective in RNAP binding

To examine whether the R91 and R92 residue substitutions affect Spx-RNAP interaction, an epitope affinity chromatography system designed to capture Spx bound to RNAP was performed as described previously (Lin & Zuber, 2012). Briefly, epitope-tagged versions of the Spx mutants (SpxΔCHA) were created in which the last 12 C-terminal residues were replaced with a HA (influenza hemaglutinin)-tag. The SpxΔCHA protein is functional in vivo (Lin & Zuber, 2012). The tagged Spx mutant proteins were produced and purified by using a chitin-binding affinity chromatography system, followed by two more column purification steps. His-tagged σ^A-depleted RNAP (SAd-RNAP) was purified from the *sigAL366A B. subtilis* strain as previously described (Lin & Zuber, 2012) and recombinant σ^A protein was purified with chitin-intein affinity column system (Lin & Zuber, 2012). The binding of SAd-RNAP or SAd-RNAP with σ^A subunit (holo-RNAP) to SpxR91AΔCHA and SpxR92AΔCHA was examined by the anti-HA affigel pull-down reaction. After RNAP and HA-tagged Spx were incubated and applied onto an anti-HA affinity column, protein complexes were eluted with high pH buffer and analyzed by SDS-PAGE (Fig. 5.7A, C). The association of each RNAP subunit of the complex to the mutant Spx was quantified and presented as a ratio to the values derived from reactions containing wild-type Spx (Fig. 5.7B, D). Both of the arginine substitutions significantly affected RNAP binding. The SpxR91AΔCHA exhibited severely reduced binding to SAd-RNAP (Fig. 5.7A, B), but the binding was improved in the presence of σ^A subunit (Fig. 5.7C, D). SpxR92AΔCHA showed higher affinity to SAd-RNAP compared with the R91A derivative, but was still lower than that of wild-type Spx. Addition of σ^A subunit improved SpxR92AΔCHA-RNAP interaction (Fig. 5.7B, D).

To examine whether the mutants affect binding of individual RNAP subunits, purified α C-terminal domain (αCTD) and σ^A subunit were applied to the anti-HA affigel pull-down assay. First, the binding of αCTD and σ^A subunit to the SpxΔCHA was tested. As expected, Spx did not interact with σ^A subunit, however, surprisingly, the αCTD showed little affinity for SpxΔCHA (Fig. 5.8A), although interaction was detected with a yeast two-hybrid system (Nakano *et al.*, 2003c) and the crystal structure of the Spx/αCTD complex was solved (Fig. 5.1) (Lamour *et al.*, 2009, Lin & Zuber, 2012, Newberry *et al.*, 2005). This indicates that the interaction between Spx and αCTD may be weak and could be disrupted under the conditions of our pull-down experiment. Hence, we purified intact α subunit to examine whether α/Spx interaction requires the α dimer. The purified α subunit was confirmed as a dimer by gel filtration chromatography (data not shown). The result of the affinity interaction assay showed that Spx interacts with intact α but not αCTD (Fig. 5.8B). Evidence that intact α subunit bears an Spx-binding surface was obtained by far -Western blotting using preincubation of gel-resolved and immobilized RNAP proteins with Spx followed by reaction with anti-Spx antiserum (data not shown). These experiments showed that only intact α subunit but not αCTD or σ^A could interact with Spx . This suggests that the intact α subunit/dimer is required for optimal α/Spx interaction.

To examine the effect of Spx mutant proteins on α/Spx interaction, the affinity of SpxΔCHA and mutant derivatives for the α subunit was examined with anti-HA affigel interaction assay (Lin & Zuber, 2012). The Spx R60E and R92A mutants did not show a significant defect in α binding (Fig.5.9A, lane5, 6; 5.9B), and the C10A mutant only slightly reduced affinity to α subunit (Fig. 5.9A, lane4; 5.9B). It has been known the

G52 residue constitutes part of the αCTD/Spx interaction interface (Nakano *et al.*, 2005, Newberry *et al.*, 2005), and as previous results showed, the α binding to the Spx(G52R)ΔCHA was significantly reduced to 40% compared to that of SpxΔCHA (Fig. 5.9A, lane 2; 5.9B). The SpxR91AΔCHA which is defective in binding to SAd-RNAP (Fig. 5.7A, C), showed a more severe effect on α binding compared to the G52R mutant (Fig. 5.9A, lane 3; 5.9B). The result suggests that the defective SAd-RNAP binding to Spx R91A mutant was attributed to the weakened α/Spx interaction, and indicates that the R91 residue is important for α interaction, and further suggests that Spx might establish multiple contacts with the α subunit dimer.

We reasoned that R91 could be another contact point between Spx and the α dimer, or that the R91A mutation alters indirectly the previously identified α-binding surface of Spx, defined by the G52R substitution. Previous studies showed that the G52R substitution resulted in a 75% reduction in Spx-RNAP interaction according to affinity interaction assay results (Lin & Zuber, 2012). The R91A G52R double mutant was constructed to determine if the phenotype resembled that of the G52R mutant, suggesting that R91 participates in supporting the structure of the αCTD-binding surface of Spx. The SpxG52R,R91A mutant protein was produced in *B. subtilis* in the stable DD form and the effect of its expression was tested by measuring the activity of the *trxB-lacZ* fusion. Introduction of the R91A substitution into the SpxG52R mutant resulted in nearly complete elimination of activity (Fig. 5.10). The affinity interaction assay using a version of SpxG52R,R91A that bears the C-terminal HA tag and using an anti-HA affigel column showed that interaction between R91 or G52R mutant protein with the α dimer is eliminated when the two substitutions are combined in the Spx monomer (Fig. 5.10). This

result, along with the observation of weak interaction of the Spx monomer with αCTD and stable interaction with the α dimer, suggests that the Spx protein has an additional α contact surface, defined by the R91 residue, within the linker region separating the central and redox domains of the Spx protein.

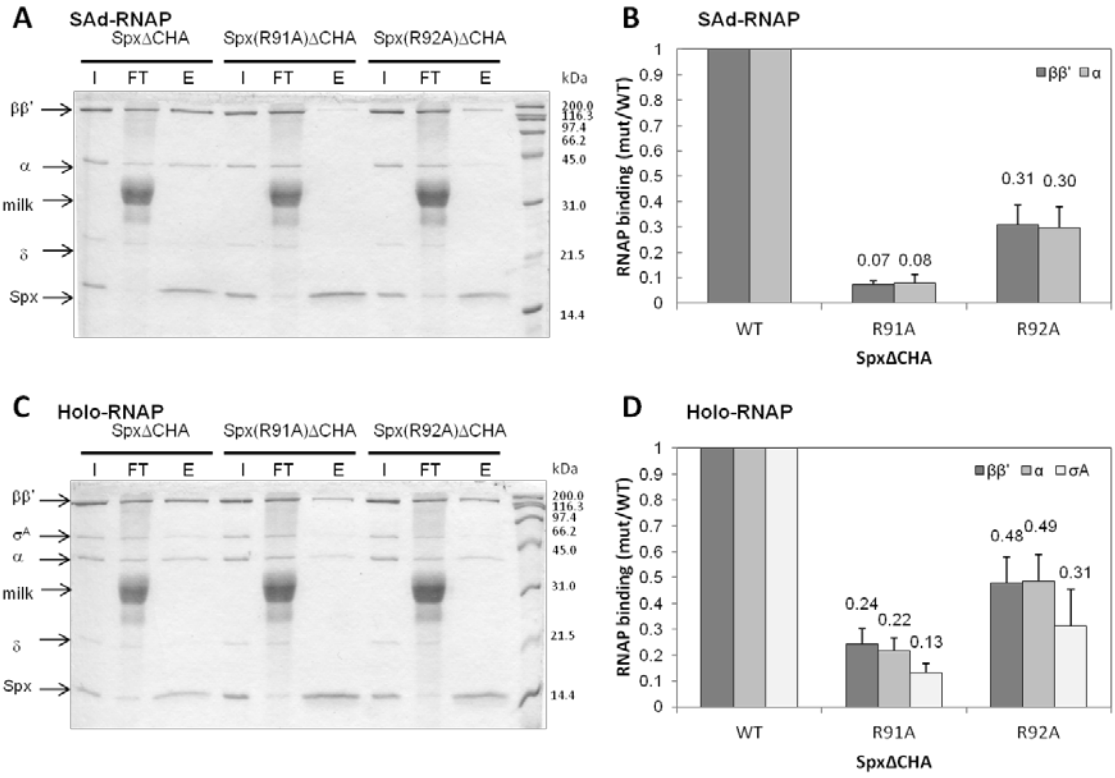

Figure 5.7. The effect of Spx mutants on RNAP interaction *in vitro*. The σ^A-depleted RNAP (SAd-RNAP) or RNAP holoenzyme (Holo-RNAP) was incubated with SpxΔCHA, Spx(R91A)ΔCHA, or Spx(R92A)ΔCHA in binding buffer (10mM Tris-HCl pH8.0, 100mM KCl, 5mM $MgCl_2$). By pull-down assay with anti-HA affinity chromatography, the interaction between Spx mutants and SAd-RNAP (A) or holo-RNAP (C) was analyzed by SDS-PAGE, and the intensity of each subunit of RNAP holo (B) or SAd-RNAP (D) on the gel was quantified, normalized, and presented as a ratio to the intensity

of SpxΔCHA. Abbreviation: I, input and E, eluate. The band labeled milk is protein from the blocking agent (dissolved powdered milk).

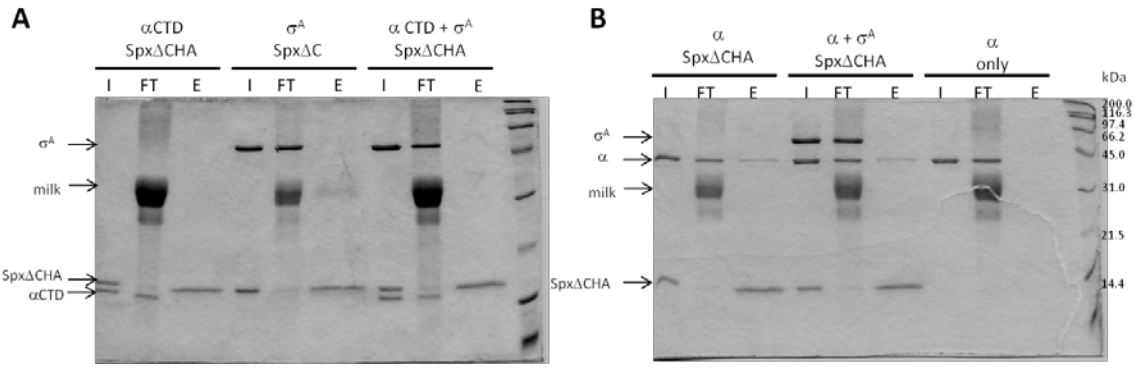

Figure 5.8. ***In vitro*** **interaction of RNAP subunits to Spx.** Spx or Spx mutant proteins was incubated with RNAP subunit, and in vitro affinity interaction assay was performed with anti-HA affinity chromatography. The result was analyzed by SDS-PAGE. (A) Equal molar ratio of αCTD or/and σ^A subunit was incubated with SpxΔCHA. (B) Equal molar ratio of intact α subunit was incubated with SpxΔCHA, or together with σ^A subunit. The α subunit was also applied to the chromatography to confirm that α subunit itself did not bind to anti-HA resin. (Abbreviation: I, input and E, eluate).

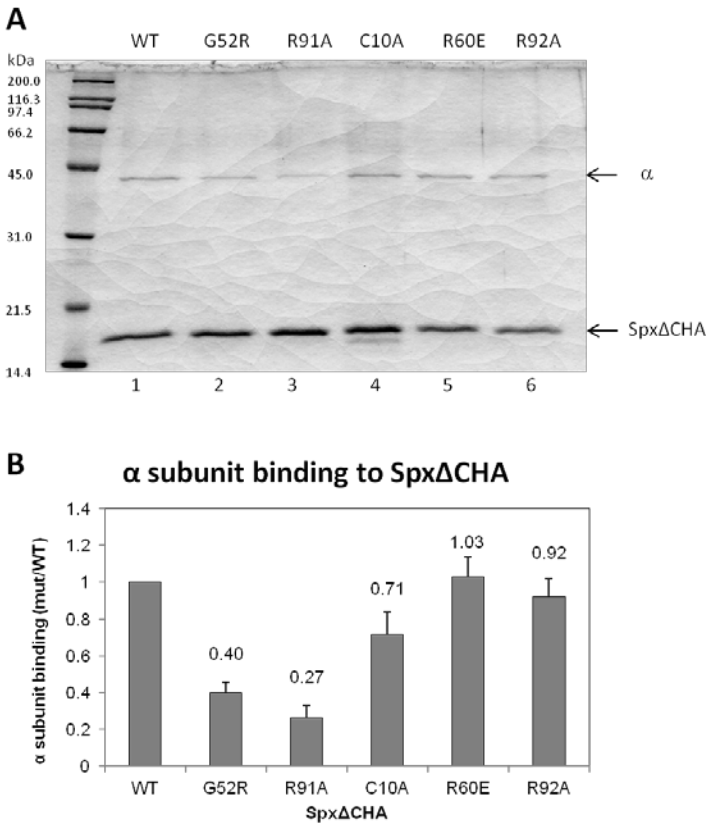

Figure 5.9. The effect of Spx mutants on interaction with α subunit *in vitro*.

SpxΔCHA or SpxΔCHA variants with single amino acid substitution was incubated with α subunit, and in vitro affinity interaction assay was performed with anti-HA affinity chromatography. The result was analyzed by SDS-PAGE (A) and band intensity of α with different Spx mutants on the gel was quantified, normalized, and presented as a ratio to the α binding of SpxΔCHA. Abbreviation: I, input and E, eluate.

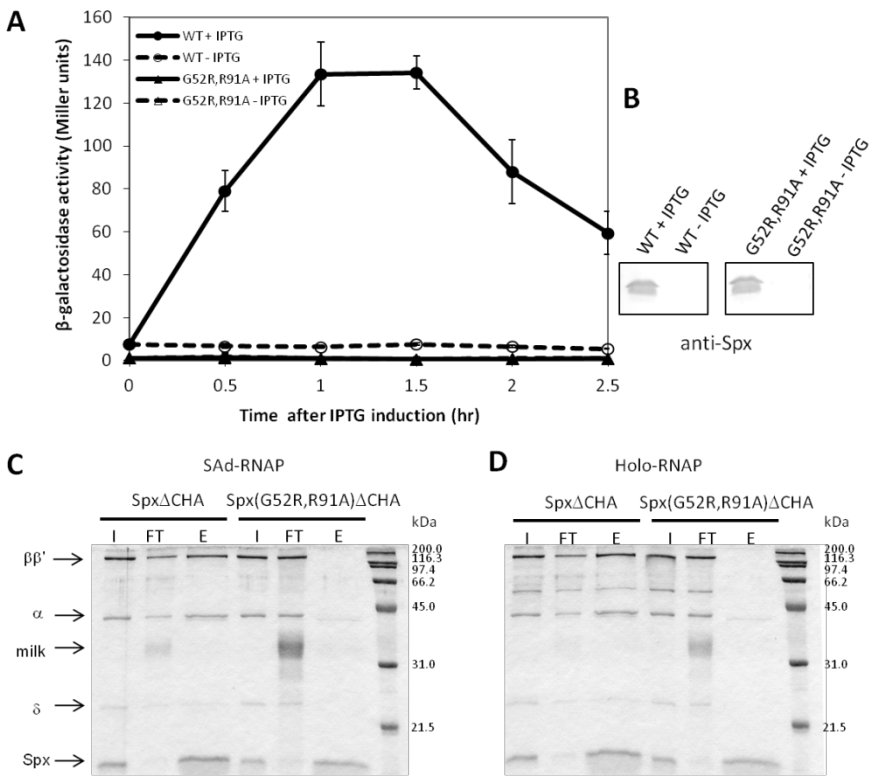

Figure 5.10. Effect of Spx(G52R, R91A) mutant on *trxB-lacZ* transcription and RNAP binding. The IPTG-inducible allele encoding Spx(G52R, R91A)^{DD} was introduced into the *amyE* locus of the Spx null mutant strain bearing *trxB-lacZ*. (A) The β-galactosidase assay was performed as described in Fig. 3 and the highest activities of Spx mutants were selected. The ratio of mutant activity to that of the control Spx^{DD} was calculated. (B) The production of Spx protein in the strains was evaluated by Western blot analysis using anti-Spx antibody. (C, D) Purified Spx(G52R, R91A)ΔCHA protein was used for in vitro RNAP interaction assay. The SAd-RNAP or Holo-RNAP was incubated with SpxΔCHA or Spx(G52R, R91A)ΔCHA and followed by the anti-HA affinity chromatography. The interaction between Spx proteins and SAd-RNAP (C)/Holo-RNAP (D) was analyzed by SDS-PAG. Abbreviation: I, input and E, eluate.

5.2.5 Mutations in -44 element in the *trxB* promoter also affect Spx-dependent transcription in vitro

From the results of footprinting (Nakano *et al.*, 2005), EMSA (Nakano *et al.*, 2010b), and, DNA/promoter cross-linking experiments (Reyes & Zuber, 2008), it suggests that the -44 cis-acting element is responsible for binding of αCTD/Spx complex. In previous published in vitro transcription results, only the effect of A-34T mutation in the *trxB* promoter on in vitro Spx-dependent transcription was examined (Nakano *et al.*, 2010b). Changing the A to a T results in an enhanced -35 promoter element (TAGCGT to TTGCGT), and transcription in the absence of Spx was detected from the *trxBA34T* promoter. Here, the effect of other three mutations in -44 and -33 elements in the *trxB* promoter on in vitro transcription was examined. The transition mutation G-33A in -33 element in *trxB* promoter almost abolished Spx-dependent transcription (Fig. 5.11A). For the transversion mutations in the -44 element, G-44T significantly decreased *trxB* transcription, and C-43T completely abolished Spx-activated transcription (Fig. 5.11B). Spx(R60E) is known to be defective in DNA-binding. Unlike the A-34T mutation, which still can be activated by the Spx(R60E) (Nakano *et al.*, 2010b), both of the *trxB* -44-element mutant promoters were unable to be activated by Spx(R60E) (Fig. 5.11B).

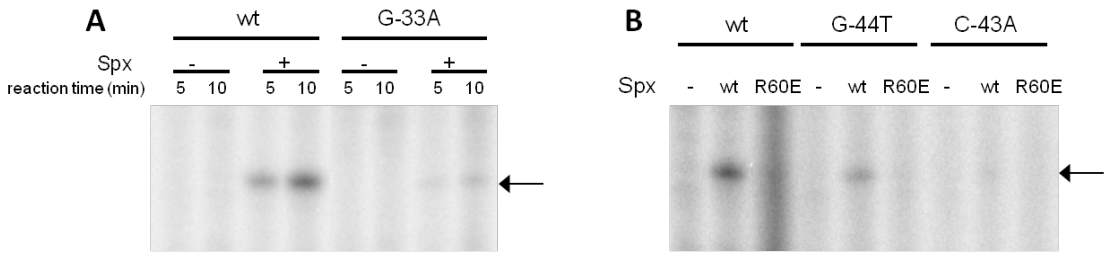

Figure 5.11. Effect of G-33A, G-44T, C-43A in *trxB* promoter on Spx-dependent transcription. In vitro transcription with *trxB* promoter with mutations C-33A (A), G-44T and C-43A (B) was performed. Either the wild-type or mutant template of *trxB* promoter (1 nM) was incubated with 25 nM SAd-RNAP together with 25nM σ^A in the presence of 7.5 nM Spx or Spx(R60E). The transcription reaction was conducted in a time-course manner (A) or for 10min (B). The arrow indicates the 66-base *trxB* transcript.

5.2.6 Spx response cis-acting element of the *nfrA* promoter

Microarray analysis identified the *nfrA* (FMN-containing NADPH-linked nitro/flavin reductase) gene (Moch *et al.*, 2000) as one of the genes activated by Spx (Nakano *et al.*, 2003a). The *nfrA* promoter contains only the AGCA element at the -44 position as in the *trxB* promoter. The same transversion mutations, G-44T and C-43A, were introduced in *nfrA* prmoter, and the effect of the mutant promoter on Spx-dependent transcription was examined in vivo and in vitro.

The result of *nfrA-lacZ* assay confirmed that Spx activates *nfrA* transcription in vivo (Fig. 5.12A), and both of the transversion mutations in *nfrA* promoter substantially reduced Spx-dependent transcription as the effect of these mutations in *trxB* promoter (Fig.5.12A) (Nakano *et al.*, 2010b).

The in vitro transcription by using the mutant *nfrA* promoter was performed. The effect of G-44T and C-43A mutations in *nfrA* promoter on in vitro transcription is also similar to that in *trxB* promoter. The G-44T mutation in *nfrA* reduced Spx-dependent transcription at least by half, and the C-43A mutation almost abolished transcription (Fig.5.12B). Both in vivo and in vitro transcriptional analysis on *nfrA* promoters showed that *nfrA* contains a cis-acting element around positon -44, and mutations this element substantially reduced Spx-dependent transcription.

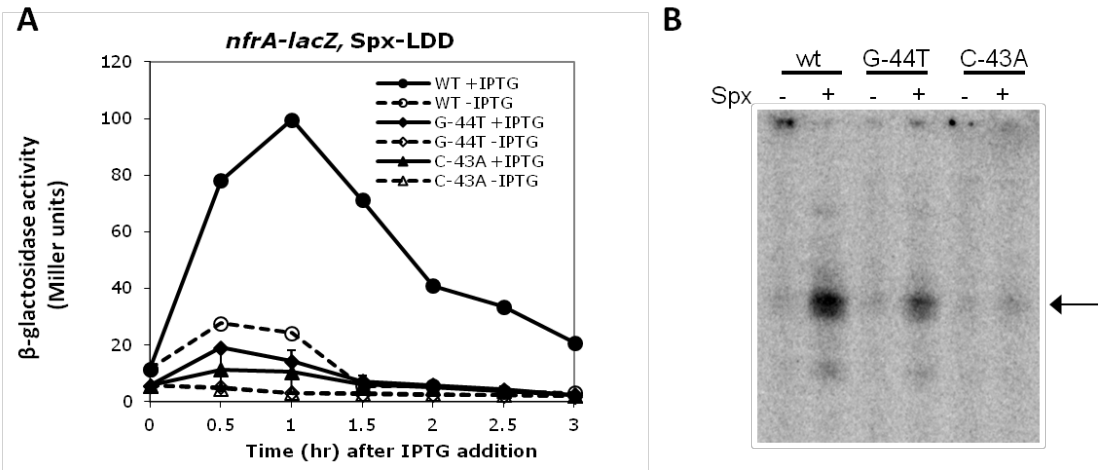

Figure 5.12. Effect of G-44T and C-43A substitutions in *nfrA* promoter on *nfrA* transcription in vivo and in vitro. (A) Strains carrying *nfrA-lacZ* fusions, wild-type or mutants, were grown in DS medium. When the OD_{600} was 0.4, each culture was divided into two flasks, and 1 mM IPTG was added to one flask. Samples were taken at time intervals and β-galactosidase activities were measured. Symbols: circles, wildtype *nfrA* promoter; triangles, C-43A subsititution, and diamonds, C-44A subsititution. Open symbols with broken lines represent cells cultured without IPTG, and closed symbols with solid lines represent cell culture with IPTG. (B) In vitro transcription with *nfrA* promoter with mutations, G-44T and C-43A, was performed. Either the wild-type or mutant template of *nfrA* promoter (1 nM) was incubated with 25 nM SAd-RNAP together with 25nM σ^A in the presence of 7.5 nM Spx. The transcription reaction was conducted for 10 min. The arrow indicates the 66-base *trxB* transcript.

5.2.7 Nucleotide specific DNA-protein cross-linking shows that Spx interacts with conserved AGCA motif and repositions σ^A in the *trxB* promoter region.

Thus far, there is no evidence showing that Spx alone directly interacts with DNA. Our previous work identified two potential *cis*-elements required for Spx-activated *trxB* transcription at position -44 and -33 (Fig. 5.13A, boxes) (Nakano *et al.*, 2010b, Reyes & Zuber, 2008). A sequence in *nfrA*, *trxA*, and *trxB* promoter regions centered at -44 and bearing the sequence AGCA was found to be the location of mutations that reduced Spx-stimulated transcription (Fig. 1.3). These findings were supported by the recently reported ChIP analysis (Rochat *et al.*, 2012). The A/TGCA/T sequence upstream of the -35 core promoter element is conserved in promoters that interact with Spx/RNAP in vivo. The element resides in the DNase I protected region when *trxA* or *trxB* promoter DNA is bound to Spx/RNAP (Nakano *et al.*, 2005, Reyes & Zuber, 2008, Rochat *et al.*, 2012). These results suggest that the upstream -44 *cis*-element could be a site where Spx contacts Spx-activated promoter DNA when bound to RNAP.

The interaction of RNAP and Spx with the *trxB* promoter DNA was examined by nucleotide-specific protein-DNA crosslinking (Reyes & Zuber, 2008). This was conducted by incubating RNAP and Spx with DNA fragments that were APB (*p*-azidophenacyl bromide)-derivatized and radioactively labeled at specific nucleotide positions in the *trxB* promoter, followed by photo-crosslinking and DNase I treatment. Radiolabled, crosslinked proteins were then identified by SDS-PAGE and phosphor imaging. Radiolabeled promoter DNA fragments that were modified with phosphothioate and APB were active as templates for in vitro transcription reactions containing

Spx/RNAP (data not shown). The binding of Spx/RNAP complex to the eight positions, -11, -21, -36, -40, -44, -46, -49 and -51, (Fig. 5.13 and 5.14) on the *trxB* promoter was examined. A previous report showed that in the presence of Spx, a strong σ^A cross-linking signal using a probe labeled at position -11 was generated (Reyes & Zuber, 2008) and no significant crosslinked Spx was detected at -11. Spx also caused elevated generation of a crosslinked product containing the large RNAP subunits and modified position -21 of the *trxB* promter. This result was confirmed in the current study (Fig. 5.13, lane 4). Previously reported results also showed that SpxC10A and SpxG52R mutations failed to induce σ^A contact with -11 crosslinker-modified probe (Reyes & Zuber, 2008). The result suggests that oxidized Spx promotes σ^A contact with the -10 region on the *trxB* promoter during transcription initiation. Among the eight positions tested, there were no significant changes in the interactions of each RNAP subunit to DNA at -46, -49, and -52 when Spx was present in the crosslinking reaction (Fig. 5.13), although at position -46, stronger crosslinked σ^A signal was detected (Fig 5.13, lanes 10 and 12) than at the other two postions.

In the absence of Spx, in a reaction containing only RNAP incubated with DNA, significant cross-linking of ββ' with the -44 probe was detected (Fig. 5.13A, lane 3), especially when compared to the level of crosslinked product at -36 (lane 1). Strong σ^A crosslinking to the -44 probe was also observed, which could be due to the -35-like element located in the -44 region of *trxB* promoter (Fig. 5.13A; 5.13B, lane 3 and Fig. 9B). In the presence of Spx, a strong band representing Spx cross-linked to position -44 was observed, and less cross-linked product was formed in reactions containing DNA modified at position -40 and -36 (Fig. 5.13A, lane 4-6). The -44 position is within the

AGCA motif believed to serve as the Spx-specific cis-acting control element. In the presence of Spx, enhanced crosslinked σ^A protein at position -36 was observed (Fig. 5.13B, lane 4, 10, 19 compared to lane 1). This result indicates that Spx interaction with RNAP repositions the σ^A subunit from the non-productive position, -44 in the *trxB* promoter region to -36 where σ^A protein normally interacts when RNAP contacts the core promoter elements. Higher concentrations of RNAP to 0.5 nM resulted in reduced crosslinking of Spx to -44 and less binding of σ^A to -36 (data not shown). Part of the reason for this result might be heightened competition for the -44 sequence on the part of σ^A, where some σ^A is observed to contact in the overlapping -35-like element.

The effect of Spx residue substitutions on DNA binding was also examined. The R60E mutant, which, when combined with αCTD, showed defective binding to *trxB* DNA in previous EMSA experiments (Nakano *et al.*, 2010b), showed a significantly reduced binding at the position -44 compared to the wild-type Spx (Fig. 5.13A, lane 9). σ^A crosslinking at this position was also reduced. This indicates that SpxR60E mutant is still capable of interacting with RNAP, preventing σ^A contact with DNA at -44, but fails to promote Spx/RNAP interaction with the *trxB* core promoter. The C10A mutant, conferring a defect in redox center, almost abolished the binding ability of Spx to the DNA at -44 (Fig. 5.13A, lane 15), and, as with the R60E mutant, the non-productive σ^A binding was reduced (Fig. 5.13A, lane 15 vs. lane 3). This implies that the C10A mutant still retains some affinity to RNAP, as shown in previous affinity interaction assays; however, since it fails to facilitate a conformational change in helix α4 region under oxidizing conditions, the DNA-binding ability is affected (Nakano *et al.*, 2010b, Nakano *et al.*, 2005), which prevents productive Spx/RNAP-promoter contact. This conclusion is

supported by the previous work showing reduced interaction of σ^A with -11 when SpxC10A mutant protein is complexed with RNAP (Reyes & Zuber, 2008). The residue substitions G52R, R91A, and R92A all caused reductions in the level of contact between RNAP subunits and positions -36, -40, and -44 (Fig. 5.13A, lanes 15-18, 22-27) compared to the pattern of RNAP crosslinking in reactions containing wild type Spx. The two Spx mutants, G52R and R91A, which show defective binding to RNAP α, also showed significant reductions in DNA crosslinking at -44 (Fig. 5.13A, lane 18 and 24). The R92A mutant crosslinked to position-44, and showed a slight defect in σ^A binding to -36 (Fig. 5.13A, lane 27), as the mutation had a modest, albeit reproducible, effect on transcriptional activation (Fig. 5.2 and 5.6).

The enhanced crosslinked σ^A protein observed at position -11 and -36 in the presence of Spx indicates that Spx, when bound to RNAP and contacting the -44 promoter element, redirects σ^A subunit to properly interact with -10 and -35 consensus elements on *trxB* promoter as part of its mode of action during transcriptional activation. Fig. 5.13BC presents a summary of the crosslinking data involving interaction of RNAP subunits with the *trxB* promoter in the absence (B) and presence (C) of Spx.

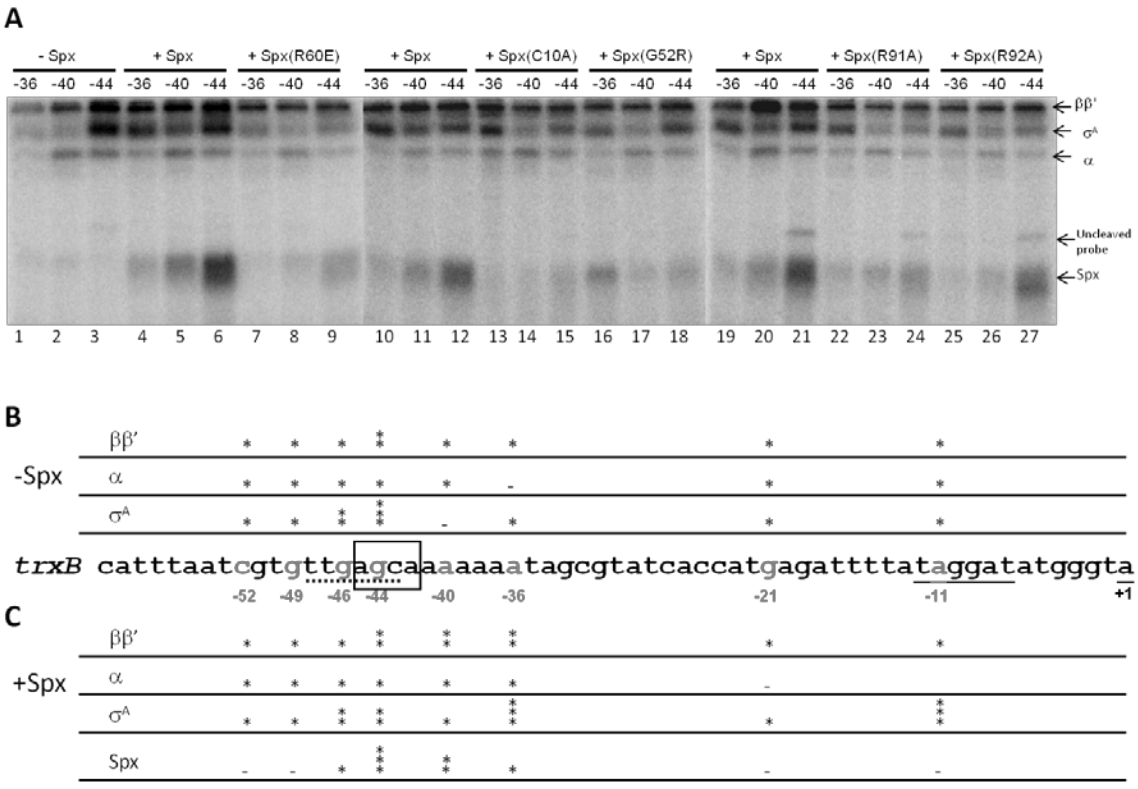

Figure 5.13. Effect of wild-type and mutant Spx on RNAP/*trxB* promoter DNA cross-linking. APB-derivitized and radio-labeled *trxB* promoter DNA was incubated with 0.25 μM RNAP in the absence or presence of 2.5 μM Spx or mutant proteins. After UV irradiation, DNase I treatment, the crossklinking result was analyzed by SDS-PAGE and crosslinked proteins were detected by phosphor-imaging. (A) Crosslinking result at position -36, -40 and -44 on *trxB* promter. (B) and (C) Summary of the result of crosslinking experiment at all positions investigated. The sequence of the *trxB* promoter is showed in the middle and APB (UV-activated cross-linker)-derivitized position was labeled in gray. The binding intensity of each crosslinked proteins in absence (B) and in presence (C) of Spx was presented with aster symbol. More asters represent more binding of the specified protein detected at the position examined on the *trxB* promoter.

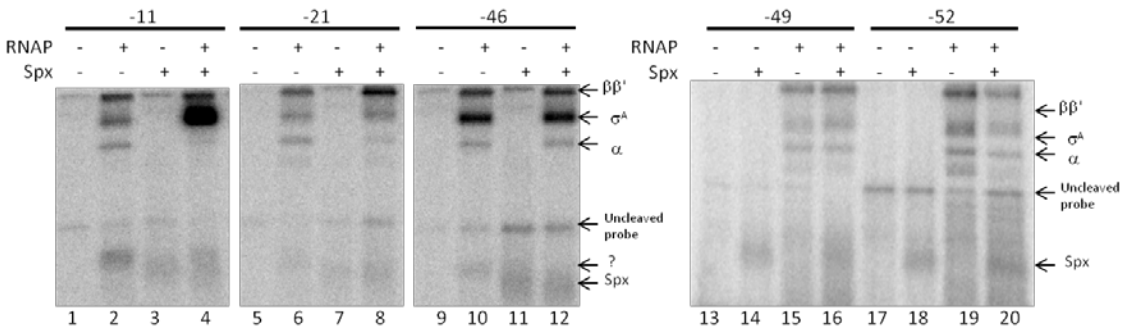

Figure 5.14. Spx/RNAP/*trxB* crosslinking result at position -11, -21, -46, -49, and -52 on *trxB* promoter. Crosslinking reactions were performed as described in Materials and Methods. The nucleotide positions indicated here are crosslinking sites on the *trxB* promoter. Bands of crosslinked products on the gel corresponding to ββ′, σ^A, α and Spx are indicated. The band representing presumed uncleaved radiolabeled DNA substrate is also shown.

5.3 DISCUSSION

Previous studies indicated that the region of Spx that includes the small α4 helix and residues within the linker region separating the redox and central domains undergo conformational changes upon transition from reduced/thiol to oxidized/disulfide states (Nakano *et al.*, 2010b). This transition affects interaction of Spx with αCTD and target promoter DNA. Previous work also showed that a single monomer of Spx engages the RNAP holoenzyme, suggesting that Spx not only targets αCTD, but also another

subunit/domain within the holoenzyme complex (Lin & Zuber, 2012). Evidence presented herein shows that three arginine residues at the end of α4 and within the Spx linker region (R60, R91, and R92) exert effects on: 1) Spx-RNAP interaction, 2) contact of Spx with a conserved cis-acting element in the target promoter of *trxB*, and/or 3) Spx-dependent positioning of the RNAP σ^A subunit with the core promoter elements *trxB*.

One of the questions regarding Spx function is how it interacts with RNAP. In earlier work, Spx was shown to have higher affinity for RNAP holoenzyme than to RNAP depleted in σ^A subunit (Lin & Zuber, 2012). However, several studies have not detected contact between Spx and σ^A (current study, K. J. Newberry, P. Z. R. G. Brennan, unpublished). Affinity interaction assays and far-western blot analysis using Spx and anti-Spx antibody along with gel resolved and filter-immobilized RNAP subunits (data not shown) showed interaction of Spx only with the α subunit and not σ^A or αCTD. The data presented above indicate that Spx targets the α dimer and is shown to have higher affinity for intact α than αCTD, despite the fact that a Spx/αCTD complex has been obtained by co-expression in *E. coli* (Lamour *et al.*, 2009). Mutational analysis suggests that in addition to the αCTD-binding interface in the central domain of Spx, there might also be an α contact point in the linker defined by the R91 residue. The R91A substitution, when in the Spx^{DD} form expressed in vivo, confers a 40% reduction in activity as measured using the Spx-activated *trxB-lacZ* fusion. However, repression of *srfA* expression is abolished by the mutation, indicating a defect in RNAP interaction. SpxR91A shows reduced activity in vitro and diminished α-binding ability, which are in line with in vivo results and the notion that the mutant protein is defective in contacting RNAP. The phenotype of R91 might also relate to the observation that only one Spx

monomer is required to productively interact with RNAP (Lin & Zuber, 2012). The two α contact points defined by G52R and R91A might mediate formation of a bridge between the two α monomers, thus occupying a position in the α dimer that can only accommodate a single Spx monomer. It is not clear why Spx prefers RNAP holoenzyme over interaction with the SAd-RNAP, but the presence of σ^A in the holoenzyme might promote a conformation of the α dimer that maximizes Spx contact. It is also possible that Spx does contact σ^A, but only when the two proteins are incorporated into the holoenyzme complex.

It is known that Spx can undergo oxidation to the disulfide form, a reaction that heightens Spx activity in term of promoting RNAP interaction with the regulatory regions of Spx-activated genes (Nakano *et al.*, 2005). The mechanism behind this process is currently unclear, but evidence provided herein suggests that R92 participates in thiol/disulfide redox control. The C10A mutation eliminates the transcription stimulating activity of Spx in vitro, while $Spx(C10A)^{DD}$ shows an 80% reduction in activity in vivo compared to Spx^{DD}. Introduction of a second substitution at R92 does not change the level of mutant Spx activity in vivo, indicating that the mutant phenotype of R92A is only observed when a disulfide can be generated. Such epistasis experiments using multiple residue substitutions was applied to uncover protein-protein contact surfaces on SoxS and its binding partner, σ^{70} of *E. coli* RNAP (Zafar *et al.*, 2011, Zafar *et al.*, 2010). The epistasis of C10A with respect to R92A is in contrast to mutant combinations in which R92 is pared with R60E or K62A, which results in additive effects on Spx activity inhibition. Likewise, R60E and K62A have additive effects when combined with C10A, indicating that residual activity remaining in the absence of the disulfide switch is

negatively affected by the two substitutions in the α4 helix. As the R60E mutation affects target DNA binding, this result is in keeping with different functions performed by residues C10 and R60. It is not clear how R92 side chain might transduce a redox signal from the disulfide center to the target-interacting surfaces of Spx and ultimately to RNAP. The reduced Spx structure of Lamour *et al.* shows a subtle rotation of the R92 side chain when compared to the structure of oxidized Spx determined by Newberry et al (Lamour *et al.*, 2008, Newberry *et al.*, 2005). On the other hand, the R92 side chain in the structure of the SpxC10S mutant veers away from the C10 position and towards α4 helix.

The presumed cis-acting element within the regulatory region of Spx-activated genes is located in a sequence around -44 with respect to the transcriptional start-site and is usually AGCA followed by an AT-rich sequence. Construction of hybrid promoters, site directed mutagenesis and alignment of sequences that interact with Spx/RNA in vivo (Nakano *et al.*, 2010b, Reyes & Zuber, 2008, Rochat *et al.*, 2012), all indicate that the conserved upstream A/TGCA/T sequence centered at around -44 is required for Spx/RNAP interaction with promoter DNA. This is supported by nucleotide-specific protein-DNA crosslinking, in which wild-type Spx when complexed with RNAP is shown to contact the derivatized -44 nucleotide position. This is accompanied by strong cross-linking signals caused by contact between σ^A and the -10 and -35 regions of the *trxB* promoter. Indications from EMSA analysis that Spx in combination with αCTD could generate a DNA-binding complex were reported previously (Nakano *et al.*, 2010b). Codon substitutions (G52R, R91A) in *spx* that confer defects in RNAP binding also compromised cis-element contact, as shown in the cross-linking data.

In the *trxB* promoter region, there is a -35-like element that overlaps with the AGCA sequence, and cross-linking indicates that this element contacts the σ^A subunit of holoenzyme. In the absence of Spx, the -36 position is poorly contacted by σ^A, but contact between σ^A and -36 is evident in the presence of Spx (Fig. 5.13). Thus, it seems that Spx repositions σ^A when it is bound to RNAP. This does not require contact between Spx and the -44 cis-element, as mutant Spx proteins (SpxR60E for example) also reduce interaction of σ^A with -44 without significant Spx contact with the -44 cis element, suggesting that remodeling of holoenyzme, and σ^A repositioning occurs prior to promoter interaction(Fig. 5.15). As previously reported and presented herein, SpxR60E can form a complex with αCTD and RNAP (Lin & Zuber, 2012, Nakano *et al.*, 2010b), but does not promote transcriptional activation, most likely due to the failure to contact target DNA, which is necessary to induce σ^A binding to core promoter elements. This suggests that remodeling of RNAP by Spx might occur at the pre-DNA-binding stage, but σ^A and promoter interaction involves Spx contact with the -44 element as part of the Spx/RNAP/promoter complex.

Codon substitutions affecting RNAP binding (G52R and R91A) cause a reduction in contact between Spx and-44, as well as σ^A at -36 (Fig. 5.13). The R92A mutation affects interaction of Spx at -44 and σ^A at -36 as well, which could account for its intermediate negative effect on in vivo and in vitro Spx activity. There is little if any specific contact between Spx/RNAP complex and DNA upstream at -49 and -52 (Fig. 5.13).

The current study provides evidence for multiple RNAP-binding surfaces on Spx, the resulting interaction of which causing remodeling of RNAP so that σ^A contacts the -35 and -10 core promoter elements. This is further facilitated by interaction of RNAP-bound

Spx protein with the -44 element that is conserved among the Spx-activated genes. The results reported herein also suggest that redox control is transmitted, in part, through changes in positioning of the R92 side chain, but will likely involve other conformational changes in the important linker region of Spx separating the redox and central domains.

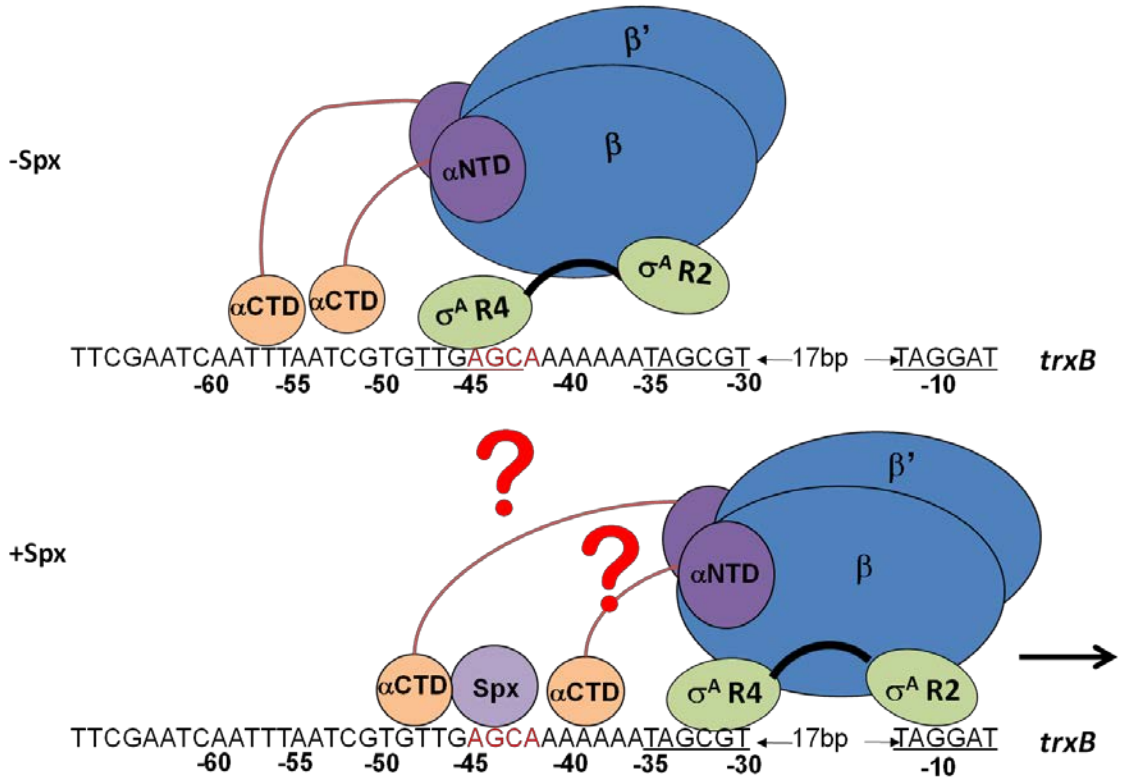

Figure 5.15. Proposed model of Spx-activated *trxB* transcription. By interacting with RNAP and the -44 element, Spx, in its oxidized form, remodels RNAP and repositions σ^A to -35 and -10 core promoter elements. Proper σ^A interaction with the core promoter, induced by Spx contact with the -44 element is required for trxB transcription. However, how Spx interaction with α dimer brings about these changes in promoter DNA contact with RNA polymerase is still unknown.

5.4 MATERIALS AND METHODS

5.4.1 Bacterial strains and culture conditions

All Bacterial strains and plasmids are listed in Table 5.1. To construct *nfrA-lacZ* fusion, the *nfrA* promoter fragment (-176 to +59) was generated by PCR with oligonucleotides oAL9 and oAL10. The resultant PCR fragment was gel-purified and digested with *Eco*RI and *Hin*dIII and cloned in to pDG793, which had been digested with the same enzymes, to yield pAL22 carrying *nfrA-lacZ* fusion. The vector pDG793 is a *thrC* integration plasmid and double-crossover recombination is selected by Thr^- phenotype (Guerout-Fleury *et al.*, 1996). For construction of mutant *trxB* or *nfrA* promoter, pDYR9 and pAL22 were used as PCR templates, respectively, and two-step PCR mutagenesis with pairs of complementary mutagenic oligonucleotides (listed in Table 3.3) was performed as described previously (Nakano *et al.*, 2010b). The pDYR9 carries the *trxB* promoter (-115 to +47) fused to *lacZ* (Reyes & Zuber, 2008). DNA fragments resulting from the second PCR were digested with EcoRI and *Hin*dIII and cloned into pDG793. The pDG793 derivatives were used to transform JH642 to yield strains bearing *trxB-lacZ* and *nfrA-lacZ* fusions. For β-galactosidase assay, the ectopic, IPTG-inducible ClpXP protease-resistant spx^{DD} was introduced into the *amyE* locus of the JH642 derivatives bearing either *trxB-lacZ* or *nfrA-lacZ* fusions by transforming strains with the pSN56 plasmid, a pDR111 derivative carrying spx^{DD} allele.

The *B. subtilis* strains used in this study are derivatives of JH642 and were grown at 37°C in 2× yeast extract-tryptone (2×YT) or Difco sporulation medium (DSM) (Nakano *et al.*, 2001). *E. coli* DH5α was used for plasmid construction. Strain ER2566 (New

England Biolabs) was used for protein production by intein-chitin system. Plasmid-bearing *E. coli* strains were grown at 37°C in 2×YT liquid or on lysogeny broth (LB) solid medium containing 1.2% agar (Difco). For over-production and purification of Spx proteins in *E. coli*, strain ER2566, cells were grown at 37°C in LB liquid medium. Antibiotic concentrations used were as previously reported (Choi *et al.*, 2006, Nakano *et al.*, 2001). For *trpC2 pheA1* phenotype auxotroph check, JH642 derivatives were streak on TSS minimal medium agar plate with or without tryptophan and phenylalanine supplements.

Table 5.1. *B. subtilis* strains and plasmids (Chapter 5)

Strain or plasmid	Relevant genotype or characteristics	Source or reference
***B. subtilis* strains**		
JH642	*trpC2 pheA1* (parental strain)	James Hoch
LAB545	*trpC2 pheA1* SPβ *c2del2*::Tn917:: pMMN92(*srfA-lacZ*)	Zhang *et al.*, 2006
ORB5853	*trpC2 pheA1 sigA*(L366A) *neo rpoC*-His_{10} *cat*	Lin & Zuber, 2012
ORB6129	*trpC2 pheA1* SPβ*c2del2*::Tn917:: pMMN92(*srfA-lacZ*) *amyE*::pSN56(P*spankhy-spx*^{DD})	
ORB7262	*trpC2 pheA1* Δ*spx*::*neo thrC*::pDYR9(*trxB-lacZ*)	Nakano, Lin *et al.*, 2010
ORB7276	*trpC2 pheA1* Δ*spx*::*neo thrC*::pDYR9(*trxB-lacZ*) *amyE*::pSN56(P*spankhy-spx*^{DD})	Nakano, Lin, *et al.*, 2010
ORB7282	*trpC2 pheA1* Δ*spx*::*neo thrC*::pDYR9(*trxB-lacZ*) *amyE*::pMMN683(P*spankhy-spxR60E*^{DD})	Nakano, Lin, *et al.*, 2010
ORB7316	*trpC2 pheA1* Δ*spx*::*neo thrC*::pDYR9(*trxB-lacZ*) *amyE*::pYZ14 (P*spankhy-spxC10A*^{DD})	Nakano, Lin, *et al.*, 2010
ORB7432	*trpC2 pheA1 amyE::*pSN56 *thrC::*pAL22	This study
ORB7457	*trpC2 pheA1 amyE::*pSN56 *thrC::*pAL25	This study
ORB7474	*trpC2 pheA1 amyE::*pSN56 *thrC::*pAL24	This study
ORB7821	*trpC2 pheA1* Δ*spx*::*neo thrC*::pDYR9(*trxB-lacZ*) *amyE*::pAL37(P*spankhy-spxR92A*^{DD})	This study
ORB7822	*trpC2 pheA1* Δ*spx*::*neo thrC*::pDYR9(*trxB-lacZ*) *amyE*::pAL38(P*spankhy-spxR92Q*^{DD})	This study
ORB7904	*trpC2 pheA1* Δ*spx*::*neo thrC*::pDYR9(*trxB-lacZ*) *amyE*::pAL56(P*spankhy-spxC10A,R92A*^{DD})	This study
ORB7906	*trpC2 pheA1* Δ*spx*::*neo thrC*::pDYR9(*trxB-lacZ*) *amyE*::pAL58(P*spankhy-spxR60E,R92A*^{DD})	This study
ORB7945	*trpC2 pheA1* Δ*spx*::*neo thrC*::pDYR9(*trxB-lacZ*) *amyE*::pAL64(P*spankhy-spxK62E,R92A*^{DD}]	This study
ORB7946	*trpC2 pheA1* Δ*spx*::*neo thrC*::pDYR9(*trxB-lacZ*) *amyE*::pMMN684(P*spankhy-spxK62E*^{DD})	This study
ORB7979	*trpC2 pheA1* Δ*spx*::*neo thrC*::pDYR9(*trxB-lacZ*) *amyE*::pAL65(P*spankhy-spxC10A,R60E*^{DD})	This study
ORB7981	*trpC2 pheA1* Δ*spx*::*neo thrC*::pDYR9(*trxB-lacZ*) *amyE*::pAL67(P*spankhy-spxC10A,K62E*^{DD})	This study

ORB8268	*trpC2 pheA1* Δ*spx*::*neo thrC*::pDYR9(*trxB-lacZ*) *amyE*::pAL88(P*spankhy-spxR91A*^{DD})	This study
ORB8269	*trpC2 pheA1* Δ*spx*::*neo thrC*::pDYR9(*trxB-lacZ*) *amyE*::pAL93(P*spankhy-spxF64A*^{DD})	This study
ORB8270	*trpC2 pheA1* Δ*spx*::*neo thrC*::pDYR9(*trxB-lacZ*) *amyE*::pAL94(P*spankhy-spxF64Y*^{DD})	This study
ORB8271	*trpC2 pheA1* Δ*spx*::*neo thrC*::pDYR9(*trxB-lacZ*) *amyE*::pAL95(P*spankhy-spxQ65A*^{DD})	This study
ORB8272	*trpC2 pheA1* Δ*spx*::*neo thrC*::pDYR9(*trxB-lacZ*) *amyE*::pAL96(P*spankhy-spxN68A*^{DD})	This study
ORB8273	*trpC2 pheA1* Δ*spx*::*neo thrC*::pDYR9(*trxB-lacZ*) *amyE*::pAL97(P*spankhy-spxN70A*^{DD})	This study
ORB8274	*trpC2 pheA1* Δ*spx*::*neo thrC*::pDYR9(*trxB-lacZ*) *amyE*::pAL98 (P*spankhy-spxY5A*^{DD})	This study
ORB8275	*trpC2 pheA1* Δ*spx*::*neo thrC*::pDYR9(*trxB-lacZ*) *amyE*::pAL99 (P*spankhy-spxY5F*^{DD})	This study
ORB8309	*trpC2 pheA1* SPβ*c2del2*::Tn917:: pMMN92(*srfA-lacZ*) *amyE*::pAL88(P*spankhy-spxR91A*^{DD})	This study
ORB8310	*trpC2 pheA1* SPβ*c2del2*::Tn917:: pMMN92(*srfA-lacZ*) *amyE*::pAL37(P*spankhy-spxR92A*^{DD})	This study
ORB8323	*trpC2 pheA1* Δ*spx*::*neo thrC*::pDYR9(*trxB-lacZ*) *amyE*::pAL106(P*spankhy-spxR91A,R92A*^{DD})	This study
ORB8565	*trpC2 pheA1* Δ*spx*::*neo thrC*::pDYR9(*trxB-lacZ*) *amyE*::pAL127(P*spankhy-spxR92K*^{DD}]	This study
ORB8566	*trpC2 pheA1* Δ*spx*::*neo thrC*::pDYR9(*trxB-lacZ*) *amyE*::pAL128(P*spankhy-spxG52R,R91A*^{DD}]	This study
Plasmids		
pAL22	pDG793 with *nfrA(-176~+59)-lacZ*	This study
pAL24	pDG793 with *nfrA(G-44T)(-176~+59)-lacZ*	This study
pAL25	pDG793 with *nfrA(C-43A)(-176~+59)-lacZ*	This study
pAL37	pDR111 with *spxR92A*^{DD}	This study
pAL38	pDR111 with *spxR92Q*^{DD}	This study
pAL45	pDR111 with *spx*ΔC*HA*	Lin & Zuber, 2012
pAL46	pTYB4 with *spx*ΔC*HA*	Lin & Zuber, 2012
pAL54	pTYB4 with *spx*^{R92A}	This study
pAL56	pDR111 with *spxC10A,R92A*^{DD}	This study
pAL58	pDR111 with *spxR60E,R92A*^{DD}	This study
pAL64	pDR111 with *spxK62E,R92A*^{DD}	This study
pAL65	pDR111 with *spxC10A,R60E*^{DD}	This study
pAL67	pDR111 with *spxC10A,K62E*^{DD}	This study
pAL73	pTYB4 with *spx*^{C10A}ΔC*HA*	Lin & Zuber, 2012
pAL74	pTYB4 with *spx*^{G52R}ΔC*HA*	Lin & Zuber, 2012
pAL75	pTYB4 with *spx*^{R60E}ΔC*HA*	Lin & Zuber, 2012
pAL82	pTYB4 with *spx*^{R92A}ΔC*HA*	This study
pAL88	pDR111 with *spxR91A*^{DD}	This study
pAL93	pDR111 with *spxF64A*^{DD}	This study
pAL94	pDR111 with *spxF64Y*^{DD}	This study
pAL95	pDR111 with *spxQ65A*^{DD}	This study
pAL96	pDR111 with *spxN68A*^{DD}	This study
pAL97	pDR111 with *spxN70A*^{DD}	This study
pAL98	pDR111 with *spxY5A*^{DD}	This study
pAL99	pDR111 with *spxY5F*^{DD}	This study
pAL106	pDR111 with *spxR91A,R92A*^{DD}	This study
pAL121	pTYB4 with *spx*^{R91A}	This study
pAL122	pTYB4 with *spx*^{R91A}ΔC*HA*	This study
pAL127	pDR111 with *spxR92K*^{DD}	This study
pAL128	pDR111 with *spxG52R,R91A*^{DD}	This study
pAL129	pTYB4 with *spx*^{G52R,R91A}ΔC*HA*	This study
pDG793	*thrC* integration vector with promoter-less *lacZ* reporter	Guérout-Fleury *et al.*, 1996
pDR111	*amyE* integration vector with P*spankhy* promoter	Britton *et al.*, 2002

pDW4	TOPO vector with *trxB* promoter	This study
pDW10	pRLG770 with *trxB* promoter	This study
pDYR26	pDG793 with *trxB(C-43A)(-115~+47)-lacZ*	Reyes and Zuber, 2008
pDYR27	pDG793 with *trxB(C-43A)(-115~+47)-lacZ*	Reyes and Zuber, 2008
pDYR9	pDG793 with *trxB*(-115~+47)-*lacZ*	Reyes and Zuber, 2008
pMMN470	pTYB4 with *spx*	Nakano *et al.*, 2007
pMMN683	pDR111 with $spxR60E^{DD}$	Michiko, Lin *et al.*, 2010
pMMN684	pDR111 with $spxK62E^{DD}$	Michiko, Lin *et al.*, 2010
pMMN747	pDG793 with *trxB(G-33A)(-115~+47)-lacZ*	Michiko, Lin *et al.*, 2010
pRLG770	transcription vector	Ross *et al.*, 1990
pSN56	pDR111 with spx^{DD}	Nakano, Kuster-Schock, *et al.*, 2003
pSN64	pTYB4 with *sigA*	Nakano, *et al.*, 2006
pTYB4	*E. coli* expression vector for IMPACT^{TM} system	New England BioRads
pUC18	cloning vector	
pUC19	cloning vector	
pYZ14	pDR111 with $spxC10A^{DD}$	Zhang & Zuber, 2007

5.4.2 Construction of Spx amino acid substitution mutants

The effect of Spx amino acid substitution was examined using *spx* constructs bearing amino acid codon substitutions (AN to DD) at the carboxyl-terminal coding end, which gives rise to the spx^{DD} allele. The product of spx^{DD} is resistant to ClpXP proteolysis (Nakano *et al.*, 2003b). The previously constructed plasmid pSN56 (Nakano *et al.*, 2003a) is a pDR111 derivative that was used to express spx^{DD} and mutant versions. pDR111 is an *amyE* integration vector, and the cloned *spx* alleles were expressed from the IPTG-inducible $P_{spankhy}$ promoter of the plasmid (Britton *et al.*, 2002).The codon substitutions were generated by two-step PCR mutagenesis with pairs of complementary mutagenic oligonucleotides (listed in Table 5.2) as described previously (Nakano *et al.*, 2010b). Plasmids were used to transform ORB4566 (*spx*::*neo thrC*::*trxB-lacZ*) for assays of *trxB*-directed β-galactosidase activity.

To construct the expression plasmids containing Spx mutant proteins used for in vitro transcription, and in vitro affinity interaction assay, two-step PCR-based mutagenesis was performed using plasmids pMMN470 (Nakano *et al.*, 2002b) and pAL46 (Lin & Zuber, 2012) as templates to generate the desired amino acid substitution. The pMMN470 and pAL46 are pTYB4 derivatives carrying wild-type *spx*, and *spx*ΔC*HA*, respectively. DNA fragments were digested with *Nco*I and *Sma*I and then inserted into pTYB4, which is an *E. coli* expression vector used in the IMPACT™ Kit (New England BioLabs). The recombinant plasmids were introduced by transformation into *E. coli* strain ER2566 for protein expression.

Table 5.2. Oligonucleotides used in the study (Chapter 5)

oligonucleotide	sequence	purpose
oAL9	GGGAATTCGACACTTTCCACGTTAATCG	*nfrA* (-176~-155) w/ *Eco*RI site forward
oAL10	CCGAAGCTTGACCGATGATTCAAAATGG	*nfrA* (+39~+59) w/ *Hin*dIII site reverse
oAL13	GTGCAGATCATTTCACTTTTG	*nfrA*(-51~-41) G-44T forward
oAL14	CAAAAGTGAAATGATCTGCAC	*nfrA*(-51~-41) G-44T reverse
oAL15	GTGCAGAGAATTTCACTTTTG	*nfrA*(-51~-41) C-43A forward
oAL16	CAAAAGTGAAATTCTCTGCAC	*nfrA*(-51~-41) C-43A reverse
oAL25	GATGATCGGAGCGCGAAGC	*spx* R92A reverse
oAL24	GCTTCGCGCTCCGATCATC	*spx* R92A forward
oAL27	GATGATCGGTTGGCGAAGC	*spx* R92Q reverse
oAL26	GCTTCGCCAACCGATCATC	*spx* R92Q forward
oAL62	ATCGGACGGGCAAGCAAACC	*spx* R91A reverse
oAL61	GGTTTGCTTGCCCGTCCGAT	*spx* R91A forward
oAL65	GTTCAAAAGTAGCTCAAAAACTGA	*spx* F64A forward
oAL66	TCAGTTTTTGAGCTACTTTTGAAC	*spx* F64A reverse
oAL68	TCAGTTTTTGATATACTTTTGAAC	*spx* F64Y reverse
oAL67	GTTCAAAAGTATATCAAAAACTGA	*spx* F64Y forward
oAL70	ACATTCAGTTTAGCGAATACTTTTG	*spx* Q65A reverse
oAL69	CAAAAGTATTCGCTAAACTGAATGT	*spx* Q65A forward
oAL72	ACGTTCACAGCCAGTTTTTG	*spx* N68A reverse
oAL71	CAAAAACTGGCTGTGAACGT	*spx* N68A forward
oAL74	GATTCAACAGCCACATTCAG	*spx* N70A reverse
oAL73	CTGAATGTGGCTGTTGAATC	*spx* N70A forward
oAL76	GCTTGGTGATGTTGCTAGTGTA	*spx* Y5A reverse
oAL75	TACACTAGCAACATCACCAAGC	*spx* Y5A forward
oAL78	GCTTGGTGATGTAAATAGTGTA	*spx* Y5F reverse
oAL77	TACACTATTTACATCACCAAGC	*spx* Y5F forward
oAL88	GATCGGAGCGGCAAGCAAACC	*spx* R91A,R92A reverse
oAL87	GGTTTGCTTGCCGCTCCGATC	*spx* R91A,R92A forward
oLA106	ATGATGATCGGTTTGCGAAGCA	*spx* R92K reverse

oAL105	TGCTTCGCAAACCGATCATCAT	*spx* R92K forward
oDW7	GGAATTCATCTGTTGACTCTATGAGCAATC	*trxB* (-200~+20) forward
oDW8	CAAGCTTCCCCATCAAACGTATTCCTTAC	*trxB* (-200~+20) reverse
oAL35	TCCCCCGGGAGCATAATCAGGAACATC	*HA* reverse (pTYB4)
oAL38	CTGAGGACCGAACAGATG	*spx* G52R forward
oAL39	CATCTGTTCGGTCCTCAG	*spx* G52R reverse
oDYR06-032	TAAACCATCTTTAAGCTTTTGGGCTCTTTC	*trxB* (-115~+47) reverse
oDYR07-052	GCGAATTCGGCCTTCTATAAACAGAAGGC	*trxB* (-115~+47) forward
oMMN01-135	AGAGGAGTGAAGATCCATGGTTACACTATAC	*spx* forward (pTYB4)
oMMN01-137	TAACTCCCGGGGTTTGCCAAACGCTGTGCTT	*spx* reverse (pTYB4)
oMMN01-173	CGAGGAAGCTTAGATGTTCATCCTACTA	*spx* forward (pDR111)
oMMN01-174	TACCAGCAGGTCGACAAATAAAAGAAGG	*spx* reverse (pdR111)
oSN03-66	CACATCACCAAGCGCGACTTCATGCAGAA	*spx* C10A forward
oSN03-67	TTCTGCATGAAGTCGCGCTTGGTGATGTG	*spx* C10A reverse
oDYR06-02	[Biotin]-CTGAACTAGAGGCCAAGGCTCTTTCTTTATTAACATATAC	*trxB* template (forward) for crosslinking
oDYR06-03	ATCCCCATCAAACGTATTCCTTAC	*trxB* template (reverse) for crosslinking
oDYR06-05	ATCCCCATCAAACGTATTCCTTACCCATATCC*T	*trxB* -11 crosslinking probe
oDYR07-35	ATCCCCATCAAACGTATTCCTTACCCATATCCTATAAAATCT*C	*trxB* -21 crosslinking probe
oAL47	ATCCCCTCAAACGTATTCCTTACCCATATCCTATAAAATCTCATGGTGATACGCTA*T	*trxB* -36 crosslinking probe
oAL49	ATCCCCTCAAACGTATTCCTTACCCATATCCTATAAAATCTCATGGTGATACGCTATTTT*T	*trxB* -40 crosslinking probe
oAL51	ATCCCCTCAAACGTATTCCTTACCCATATCCTATAAAATCTCATGGTGATACGCTATTTTTTTG*C	*trxB* -44 crosslinking probe
oAL52	ATCCCCTCAAACGTATTCCTTACCCATATCCTATAAAATCTCATGGTGATACGCTATTTTTTTGCTCAA*C	*trxB* -49 crosslinking probe
oDYR06-08	ATCCCCTCAAACGTATTCCTTACCCATATCCTATAAAATCTCATGGTGATACGCTATTTTTTTGCT*C	*trxB* -46 crosslinking probe
oDYR06-09	ATCCCCTCAAACGTATTCCTTACCCATATCCTATAAAATCTCATGGTGATACGCTATTTTTTTGCTCAACAC*G	*trxB* -52 crosslinking probe

5.4.3 β-galactosidase assays

Strains were grown in liquid DS medium. Strains bearing a *trxB-lacZ* fusion (Table 5.1) were grown at 37°C overnight on DS medium agar plates supplemented with appropriate antibiotics. The overnight cultures were used to inoculate the same liquid medium at a starting OD_{600} nm of 0.02. When the OD_{600} of the cultures reached 0.4, the cultures were divided into two flasks and 1 mM IPTG was added to one of the flasks. Samples were collected every 30 min, and β-galactosidase activity was assayed as

previously described (Nakano *et al.*, 1998) and data is presented as Miller units (Miller, 1972).

5.4.4 Western Blot Analysis

Samples were collected at the same time when growing the strains for β-galactosidase assays, and the cells were lysed in lysis buffer (30mM Tris-HCl pH 8.0, 1mM EDTA) by bead-beating method. Cell pellet was suspended with lysis buffer, mixed with 0.1 mm disruption glass beads (RPI Corp.) by vortexing for 5 min, and transferred onto ice for 5 min. Two more vortexing cycles were repeated and followed by centrifugation. The supernatant of each sample was collected and protein concentration was measured with Coomassie Protein Assay Reagent (PIERCE). Ten μg of the total protein for each sample was loaded to SDS-PAG. The western blot was undertaken as previously described using an anti-Spx antibody (Nakano *et al.*, 2001).

5.4.5 Protein purification

His-tagged σ^A-depleted RNAP (SAd-RNAP) was purified from σ^A mutant *B. subtilis* strain ORB5853 (*rpoC-His*$_{10}$, *sigA*L366A), in which the Leu366 substitution in σ^A weakens the interaction to RNAP core enzyme (Zuber *et al.*, 2011). As described previously (Lin & Zuber, 2012), *B. subtilis* cells were grown in 2×YT liquid containing chloramphenicol and neomycin at 37°C until the OD_{600} of the culture reached 0.8-0.9, and then harvested and lysed by passage through a French press. The protein was purified

stepwise with three columns, HisPur^{TM} Ni-NTA (Thermo Scientific) affinity column, heparin column, and BioRad High Q column as previously described (Nakano *et al.*, 2010b, Reyes & Zuber, 2008), and then stored at –20°C in buffer containing 10 mM Tris-HCl pH7.8, 100 mM KCl, 5 mM $MgCl_2$, 0.1 mM EDTA and 50% glycerol.

The genes specifying σ^A and Spx variants were cloned in plasmid pTYB4 (terminus IMPACT^{TM} CN system, New England Biolabs). The products of the recombinant plasmids bear a self-cleavable intein and chitin-binding domains positioned at the C-termini. σ^A was overproduced from plasmid pSN64 (Nakano *et al.*, 2002a) in *E. coli* ER2566 and purified by using chitin resins (New England Biolabs) followed by BioRad High Q column. Purified σ^A was dialyzed and stored at –80°C in buffer containing 25 mM Tris-HCl pH8.0, 100mM KCl, 0.1 mM EDTA, 1 mM $MgCl_2$ and 10% glycerol. Spx variants were expressed from pTYB4 derivatives listed in Table 1. As previously described, Spx proteins were purified by using chitin column followed by BioRad High S column (Nakano *et al.*, 2001). Spx proteins were stored at –80°C in buffer containing 10 mM Tris-HCl pH 8.0, 100 mM KCl, 5% glycerol.

5.4.6 In vitro transcription

The linear *trxB* or *nfrA* promoter fragment was generated by PCR with oligonucleotides pair oDYR07-52/oDYR06-32 and oAL9/oAL10, repectively. The mutant promoter fragments were generated by PCR amplification from pDG793 derivatives carrying *trxB* or *nfrA* mutant promoters.

For in vitro transcription with supercoiled DNA, the *trxB* promoter DNA (-200 to +30) fragment was first generated by PCR amplification with oligonucleotides oDW7 and oDY8, and inserted into TOPO vector with Zero Blunt® TOPO® PCR Cloning Kit (Invitrogen, Life technologies) to generate pDW4 plasmid. The *trxB* promter DNA fragment was further cleaved out of the pDW4 with restriction endonucleases *Eco*RI and *Hin*dIII and inserted into plasmid pRLG770 (Ross *et al.*, 1990) to generate plasmid pDW10. The pRLG770 is designed as a super-coiled DNA template for in vitro transcription, and contains a cloning site for inserting promoter DNA fragments of interest, two terminators and an internal control RNA-1 transcription unit (Ross *et al.*, 1990).

For the transcription reaction, three-fold molar excess of σ^A subunit was pre-incubated with SAd-RNAP at 37°C in buffer containing 10 mM Tris-HCl pH 8.0, 10 mM $MgCl_2$, 30 mM KCl and 50% glycerol for 1 hr to assemble the holo-RNAP. In each reaction, 100 ng of pDW10 template was incubated with 10 nM Spx, 10 nM holo-RNAP and 5 μCi of α-^{32}P-UTP (3000 Ci/mmol) in 50 μl of 10 mM Tris-HCl pH8.0, 30 mM KCl, 0.5 mM $MgCl_2$, and 1 mg/ml BSA at 37°C. After 10 min, the nucleotide mixture (0.2 mM rATP/ rGTP/ rCTP and 10nM UTP for final concentration) was then added to initiate the reaction. Ten μl of sample was taken and mixed with equal volume of sequencing stop solution (95% formamide, 25 mM EDTA, 0.05% bromophenol blue) to stop reaction after 2, 5, 10, and 20 min of incubation. The samples were heated at 90°C for 2 min and were applied to a 6% polyacrylamide-urea gel. The gel was dried and gels were scanned on a Typhoon Trio+ variable imager (GE Healthcare).

5.4.7 In vitro affinity interaction assay

To examine RNAP affinity to HA-tagged Spx variants in vitro, the anti-HA affinity matrix was used for affinity binding assay as described previously (Lin & Zuber, 2012). Briefly, 0.25 μM His-tagged SAd-RNAP and 2.5 μM SpxΔCHA were incubated with or without 0.25 μM σ^A in 150 μl of Reaction Buffer (RB, 10 mM Tris-HCl, pH8.0, 50 mM NaCl, 5 mM $MgCl_2$) at room temperature for 20 min, and protein mixture was then applied to the anti-HA affinity column followed by washing with Washing Buffer (0.05% Tween 20 in RB). The protein complex was eluted from the column with 100 mM triethylamine, pH 11.5, and neutralized with 1/10 volume of 1 M Tris-HCl, pH6.8. The composition of protein complex was analyzed on the SDS-polyacrylamide gel followed by Commassie Blue G250 staining.

For individual RNAP subunit binding assay, equal concentration of α, αCTD, or/and σ^A protein was incubated with 2.5 μM Spx in RB for 20 min. The same affinity pull-down procedure as detailed above was then conducted.

Quantification of band intensities was performed by using ImageJ software on multiple gel images, and the ratio of each RNAP subunits binding to the mutant Spx over that of wild-type Spx was calculated and presented in histograms.

5.4.8 Promoter DNA-protein cross-linking

Cross-linking probes were synthesized as described previously (Reyes & Zuber, 2008) with some modifications. Briefly, biotinylated *trxB* promoter DNA fragment was generated by PCR using forward 5'- biotinyl-oligonucleotide oDYR06-02, and reverse

oligonucleotide oDYR06-03 specifically amplifying *trxB* promoter DNA from -98 to +22. This DNA fragment was purified using low melting agarose gel extraction and then incubated with streptavidin-conjugated magnetic beads (Dynabeads® M280 streptavidin, Invitrogen). Biotinylated *trxB* DNA bound to the beads was denatured with 0.1M NaOH and 1M NaCl, and streptavidin bound single-strand *trxB* promoter was collected by centrifugation and washed with 10 mM Tris-HCl, 1mM EDTA (TE, pH 7.5) buffer containing 0.1% BSA. Oligonucleotides containing a single 3' phosphorothioate substitution at desired nucleotide positions on the *trxB* promoter (Table 2) were then annealed to the strepavidin-bound ssDNA template and radiolabelled with 120 mCi α-^{32}P-dATP (MP Biomedicals) using Klenow Fragment (3'→ 5' exo-) enzyme (New England BioLabs) at an adjacent position. After washing off excess free α-^{32}P-dATP, the full-length extension was performed by adding Klenow Fragment (3'→ 5' exo-) and dNTP mix. The extension reaction was stopped by washing off Klenow enzyme and free dNTP by centrifugation and resuspension in NEBuffer 2 (New England BioLabs). The radiolabelled DNA was released from the streptavidin beads by cleavage with *Hae*III (New England BioLabs). The released, radiolabeled DNA was and subsequently extracted with phenol-chloroform-isoamyl alcohol (PCI) solution and precipitated with ethanol. The promoter DNA, was derivatized with 100 mM *p*-azidophenacylbromide (APB) in 100 mM triethylammonium bicarbonate buffer (pH 8.0) in the dark at room temperature for overnight. The derivatized products were then PCI-extracted, ethanol-precipitated, and dissolved in distilled water.

For the cross-linking experiments, 0.25 μM RNAP with 2.5 μM Spx or Spx variants were incubated with radiolabelled probes (20,000 c.p.m.) at 37°C for 30min in dark in

buffer containing 20 mM Tris-HCl (pH 8.0), 50 mM KCl, 5 mM MgCl2, 0.1 mg/ml BSA and 5% glycerol. Cross-linking was carried out by UV irradiation (UV Stratalinker 1800, Stratagene) for 10 seconds, and then samples were immediately transferred to ice. Samples were treated with 80U DNase I at 37°C for 1 hr, and the crosslinked products was resolved on an 18% SDS-PAG. The dried gels were scanned on a Typhoon Trio+ variable imager (GE Healthcare).

CHAPTER 6

SUMMARY, CONCLUSIONS AND FUTURE DIRECTIONS

6.1 SUMMARY AND CONCLUSIONS

6.1.1 A single Spx monomer interacts with RNAP to generate an active transcriptional complex

Spx activates transcription initiation in *B. subtilis* by directly interacting with C-terminal domain of RNA polymerase (RNAP) α subunit (αCTD), which forms a complex that recognizes the promoter regions of Spx-dependent genes. There are two αCTDs in RNAP and two cis-acting elements found in the upstream of *trxA* and *trxB* promoter regions. Hence, to investigate whether Spx proteins interact with both of the αCTDs to activate transcription, the composition of Spx/RNAP complex was examined in vitro and in vivo by two Spx variants, SpxΔCHA and Spxc-Myc, and a series of affinity chromatography. The result showed that only one Spx monomer interacts with RNAP in vitro and the eluted Spx/RNAP is functional and capable to activate the *trxB* transcription. In vivo production of SpxΔC and SpxΔCHA followed by anti-HA affinity column chromatography of a cleared lysate resulted in retrieval of Spx/RNAP complex with only the SpxΔCHA derivative. Binding reactions that combined active Spxc-Myc, inactive Spx(R60E)ΔCHA, and RNAP, when applied to the anti-HA affinity column, yielded only inactive Spx(R60E)ΔCHA/RNAP complexes. Even in the presence of *trxB*

promoter DNA, only one Spx was detected in the transcriptional active Spx/RNAP/DNA complex in vitro. All the evidence supports a conclusion that only one Spx monomer interacts with RNAP.

6.1.2 Spx and RNAP interaction

From the results of RNAP-binding assay, no direct evidence shows that Spx can interact with any other subunits of RNAP. However, the result of anti-HA affinity chromatography showed that the σ^A subunit is required for optimal Spx-RNAP interaction; although no interaction between Spx and σ^A subunit itself has been demonstrated. The result of the affinity interaction assay and far-western blotting assay showed that only intact α but not αCTD interacts stably with Spx. It suggests that the intact α subunit/dimer is required for optimal α/Spx interaction.

The G52 residue in Spx and Y263 residue in αCTD are known to be involved in the contact of Spx and αCTD. Further mutational analyses in Spx and αCTD of RNAP showed other residues in Spx and αCTD involves Spx interaction with RNAP. The R91 residue in Spx was newly identified to be involved in both Spx-dependent transcriptional activation and repession. The result of anti-HA chromatography showed that R91residue in Spx is required for α binding. The G52R, R91A double mutant abolished the transcriptional activity of Spx in vivo and RNAP binding ability in vitro. It suggests that Spx might establish multiple contacts with the α dimer.

Previous report showed the αCTD(E254A) mutant affects Spx-dependent *srfA* repression (Nakano *et al.*, 2000). The result of alanine-mutant scanning in αCTD showed

E254 residue in αCTD also affects Spx-activated *trxB* transcription. It suggests that the role of E254 residue in αCTD may constitute part of the interface of Spx/αCTD interaction.

6.1.3 The -44 cis-acting element AGCA is conserved and responsible for direct Spx contact in the presence of RNAP

The Spx response cis-acting element was found in the promoter region of another Spx-activated gene, *nfrA*. An AGCA motif is located at position -44 in the *nfrA* promoter, at the same position that the *trxB* -44 cis-acting element resides. In vivo and in vitro transcriptional analysis showed this AGCA motif in *nfrA* promoter is required for Spx-dependent transcriptional activation. The mutations in G-44 and C-43 substantially reduced *nfrA* transcription in the presence of Spx, which is comparable to the result of analysis of the *trxB* -44 cis-acting element. Recent genome-wide study also indicates that the -44 cis-acting element is conserved in genes in Spx regulon (Rochat *et al.*, 2012), and we have proposed that this AGCA element is the site with which the complex of αCTD with oxidized Spx interacts. Here, the result of the *trxB* DNA/RNAP crosslinking experiment showed that Spx, in complex with RNAP, interacts with *trxB* promoter at position -44. Besides, the R60 residue in Spx was thought to be involved in DNA binding, and the RNAP binding ability of Spx(R60E) mutant was not affected. In the crosslinking assay, the Spx(R60E) mutant showed less contact with the *trxB* promoter at position -44. It suggests that the R60 residue in Spx may contribute the contact between Spx and the -44 cis-element.

6.1.4 The R92 residue in Spx may function in redox control

The disulfide bond formation in Spx is required for its function in transcriptional activation. It is known that the C10A mutant affects both in vivo and in vitro activity of Spx. Comparing the structures of the reduced and oxidized structures of Spx, the side chain of R92 residue is turned away from redox center in the reduced form of Spx. The epistasis analysis was performed for C10A and R92A. When introducing R92A to C10A mutant, the level of mutant Spx activity was not changed in vivo. This indicates that the mutant phenotype of R92A is only observed when a disulfide can be generated and suggests that R92 may participate in thiol/disulfide redox control.

6.1.5 Proposed mechanism by which Spx activates *trxB* transcription

The result of DNA/RNAP crosslinking experiment revealed not only where Spx interacts on *trxB* promoter, but also uncoverd the changes in DNA binding patterns of each subunit of RNAP in the absence and presence of Spx. The notable change is the position of σ^A subunit binding. In the *trxB* promoter, there is a -35-like element overlapping with the -44 AGCA element found in Spx activated promoters, and could be cross-linked with σ^A in the assay. In the presence of Spx, the occupancy of cross-linked σ^A was reduced at position -44 but was observed at position -36. It seems that Spx repositions σ^A when it is bound to RNAP. The contact between Spx and -44 cis-element may not be required because the SpxR60E mutant, which poorly cross-linked at position -44 still prevents contact between σ^A and the upstream -35-like element. The result suggests a remodeling of RNAP by Spx interaction, and σ^A repositioning occurs prior to

promoter interaction. Subsequent interaction of σ^A with core promoter elements requires Spx contact with the -44 cis-acting element.

6.2 FUTURE DIRECTIONS

In these studies, the possible mechanism for how Spx activates transcription of target genes in response to oxidative stress is proposed. The evidence provided here suggests one Spx monomer interacts with RNAP and Spx has multiple RNAP-contact surfaces, which results in remodeling of RNAP to promote σ^A interaction with -35 and -10 core promoter elements. These contacts require the RNAP-bound Spx to contact the -44 cis-acting element. How this contact facilitates transcription initiation of target promoter and which steps in initiation Spx accelerates, are still unclear and need to be investigated. Besides SpxG52/αCTDY263 contact, Spx may establish other contacts with the α subunit. Since α is a dimer, it offers more possible binding surfaces for Spx to engage. From mutagenesis analysis it is known that E254 and Y263 residues in αCTD function in both positive and negative Spx-dependent regulation and reside at an interface of Spx-αCTD interaction. The affinity interaction assay of the E254A mutant α subunit/RNAP with Spx will be performed to examine whether E254 residue affects Spx interaction. I have tried to construct and express the N-terminal domain of α subunit (αNTD) a modified α subunit with a TEV protease cleavage site in the linker region separating the N-and C-terminal domains, but these α mutant proteins are either unstable or insoluble. However, the quality and yield of purified wild-type α subunit is much better than the

mutant proteins, so that to solve the crystal structureof α/Spx is another option and necessary to help answer the question.

Under oxidative stress, the disulfide formation in Spx leads to several conformational changes. The obvious change by oxidation is in the α4 helix. This region forms a well-structured helix and may serve as a DNA contact surface for transcription activation. How other conformational changes, perhaps in the linker region of Spx separating the redox and central domains, facilitate transcriptional activation has yet to be fully explained. The mutagenesis of other residues in Spx may be required to further clarify the activation mechanism. Here again, structural information from X-ray crystallography of a tertiary complex consisting of α/Spx bound to target DNA bearing the -44 cis-acting element is necessary to identify potential mutagenic targets. However, this may not provide information to fully explain how Spx interaction with RNAP promotes the contact between the σ subunit and the core promoter elements.

Since binding of Spx to RNAP repositions the σ^A subunit on target promoter, whether Spx can interact with RNAP containing other σ subunits, such as σ^B, to direct transcription from another set of genes, and whether Spx repositions other σ subunits in the same way are interesting questions to be answered. Since we are able to produce purified SAd-RNAP, we can apply to an in vitro transcription reaction an alternative σ factor to test Spx activity using different forms of RNAP holoenzyme and their cognate promoter DNA templates. This approach along with affinity binding assay, can be pursued to examine the interaction between Spx and RNAP containing alternative σ factors and further to understand the regulation of the target genes.

Many of low-GC-content Gram-positive bacteria were identified to have multiple paralogs of Spx protein. Since only a single Spx monomer engages RNAP, a competition among Spx paralogs for RNAP interaction could ensue. Through differential expression of individual Spx paralogs under different environmental or metabolic conditions, different set of genes could be regulated in response to stresses. It raises many questions, such as what kind of signal triggers the expression of Spx paralogs? Do they have distinct DNA target recognition properties? Which are the target genes that Spx paralogs regluate, whether paralogous forms exert the same mechanism of control on transcription and how those paralogs compete for the RNAP binding? All of these questions will need to be addressed. To answer these questions, the constructs for Spx paralogous protein expression, and the identification of the target promoters are required. The RNAP-binding ability of Spx paralogs could be then examined by in vitro RNAP binding assay. From the alignment of target gene promoters, one may identify some conserved sequences in these promoters regulated by Spx paralogs. If there are genes under both Spx and paralogous Spx control, the study of these will be the useful for understanding the regulation or/and competition between two Spx proteins.

REFERENCES

Antelmann, H., M. Hecker & P. Zuber, (2008) Proteomic signatures uncover thiol-specific electrophile resistance mechanisms in *Bacillus subtilis*. *Expert. Rev. Proteomics* 5: 77-90.

Antelmann, H., C. Scharf & M. Hecker, (2000) Phosphate starvation-inducible proteins of *Bacillus subtilis*: proteomics and transcriptional analysis. *J. Bacteriol.* 182: 4478-4490.

Barker, M.M., T. Gaal & R.L. Gourse, (2001) Mechanism of regulation of transcription initiation by ppGpp. II. Models for positive control based on properties of RNAP mutants and competition for RNAP. *J Mol Biol* 305: 689-702.

Barne, K.A., J.A. Bown, S.J. Busby & S.D. Minchin, (1997) Region 2.5 of the Escherichia coli RNA polymerase sigma70 subunit is responsible for the recognition of the 'extended-10' motif at promoters. *EMBO J* 16: 4034-4040.

Barrick, J.E., N. Sudarsan, Z. Weinberg, W.L. Ruzzo & R.R. Breaker, (2005) 6S RNA is a widespread regulator of eubacterial RNA polymerase that resembles an open promoter. *RNA* 11: 774-784.

Barrios, H., B. Valderrama & E. Morett, (1999) Compilation and analysis of sigma(54)-dependent promoter sequences. *Nucleic Acids Res.* 27: 4305-4313.

Bartlett, M.S., M. Thomm & E.P. Geiduschek, (2000) The orientation of DNA in an archaeal transcription initiation complex. *Nat. Struct. Biol.* 7: 782-785.

Beck, L.L., T.G. Smith & T.R. Hoover, (2007) Look, no hands! Unconventional transcriptional activators in bacteria. *Trends Microbiol.* 15: 530-537.

Belyaeva, T.A., J.A. Bown, N. Fujita, A. Ishihama & S.J. Busby, (1996) Location of the C-terminal domain of the RNA polymerase alpha subunit in different open complexes at the Escherichia coli galactose operon regulatory region. *Nucleic Acids Res* 24: 2242-2251.

Benoff, B., H. Yang, C.L. Lawson, G. Parkinson, J. Liu, E. Blatter, Y.W. Ebright, H.M. Berman & R.H. Ebright, (2002) Structural basis of transcription activation: the CAP-alpha CTD-DNA complex. *Science* 297: 1562-1566.

Berka, R.M., J. Hahn, M. Albano, I. Draskovic, M. Persuh, X. Cui, A. Sloma, W. Widner & D. Dubnau, (2002) Microarray analysis of the *Bacillus subtilis* K-state: genome-wide expression changes dependent on ComK. *Mol Microbiol* 43: 1331-1345.

Borezee, E., T. Msadek, L. Durant & P. Berche, (2000) Identification in *Listeria monocytogenes* of MecA, a homologue of the *Bacillus subtilis* competence regulatory protein. *J. Bacteriol.* 182: 5931-5934.

Bougdour, A., C. Lelong & J. Geiselmann, (2004) Crl, a low temperature-induced protein in *Escherichia coli* that binds directly to the stationary phase sigma subunit of RNA polymerase. *J. Biol. Chem.* 279: 19540-19550.

Britton, R.A., P. Eichenberger, J.E. Gonzalez-Pastor, P. Fawcett, R. Monson, R. Losick & A.D. Grossman, (2002) Genome-wide analysis of the stationary-phase sigma factor (sigma-H) regulon of *Bacillus subtilis*. *J. Bacteriol.* 184: 4881-4890.

Brown, N.L., J.V. Stoyanov, S.P. Kidd & J.L. Hobman, (2003) The MerR family of transcriptional regulators. *FEMS Microbiol Rev* 27: 145-163.

Burbulys, D., K.A. Trach & J.A. Hoch, (1991) Initiation of sporulation in *B. subtilis* is controlled by a multicomponent phosphorelay. *Cell* 64: 545-552.

Burgess, R.R., (1971) RNA polymerase. *Annu. Rev. Biochem.* 40: 711-740.

Busby, S. & R.H. Ebright, (1999) Transcription activation by catabolite activator protein (CAP). *J. Mol. Biol.* 293: 199-213.

Cabiscol, E., J. Tamarit & J. Ros, (2000) Oxidative stress in bacteria and protein damage by reactive oxygen species. *Int Microbiol* 3: 3-8.

Campbell, E.A., O. Muzzin, M. Chlenov, J.L. Sun, C.A. Olson, O. Weinman, M.L. Trester-Zedlitz & S.A. Darst, (2002) Structure of the bacterial RNA polymerase promoter specificity sigma subunit. *Mol. Cell* 9: 527-539.

Campbell, E.A., L.F. Westblade & S.A. Darst, (2008) Regulation of bacterial RNA polymerase sigma factor activity: a structural perspective. *Curr. Opin. Microbiol.* 11: 121-127.

Chen, H., H. Tang & R.H. Ebright, (2003) Functional interaction between RNA polymerase alpha subunit C-terminal domain and sigma70 in UP-element- and activator-dependent transcription. *Mol Cell* 11: 1621-1633.

Chen, L., X. Ge, X. Wang, J.R. Patel & P. Xu, (2012) SpxA1 involved in hydrogen peroxide production, stress tolerance and endocarditis virulence in *Streptococcus sanguinis*. *PLoS ONE* 7: e40034.

Chi, B.K., K. Gronau, U. Maeder, B. Hessling, D. Becher & H. Antelmann, (2011) S-bacillithiolation protects against hypochlorite stress in *Bacillus subtilis* as revealed by transcriptomics and redox proteomics. *Mol. Cell. Proteomics*.

Cho, N.Y., M. Choi & L.B. Rothman-Denes, (1995) The bacteriophage N4-coded single-stranded DNA-binding protein (N4SSB) is the transcriptional activator of Escherichia coli RNA polymerase at N4 late promoters. *J Mol Biol* 246: 461-471.

Choi, M., A. Miller, N.Y. Cho & L.B. Rothman-Denes, (1995) Identification, cloning, and characterization of the bacteriophage N4 gene encoding the single-stranded DNA-binding protein. A protein required for phage replication, recombination, and late transcription. *J Biol Chem* 270: 22541-22547.

Choi, S.Y., D. Reyes, M. Leelakriangsak & P. Zuber, (2006) The global regulator Spx functions in the control of organosulfur metabolism in *Bacillus subtilis*. *J. Bacteriol.* 188: 5741-5751.

Claverys, J.P., M. Prudhomme & B. Martin, (2006) Induction of competence regulons as a general response to stress in gram-positive bacteria. *Annu Rev Microbiol* 60: 451-475.

Colland, F., G. Orsini, E.N. Brody, H. Buc & A. Kolb, (1998) The bacteriophage T4 AsiA protein: a molecular switch for sigma 70-dependent promoters. *Mol Microbiol* 27: 819-829.

Dalebroux, Z.D., S.L. Svensson, E.C. Gaynor & M.S. Swanson, (2010) ppGpp conjures bacterial virulence. *Microbiol Mol Biol Rev* 74: 171-199.

Delumeau, O., F. Lecointe, J. Muntel, A. Guillot, E. Guedon, V. Monnet, M. Hecker, D. Becher, P. Polard & P. Noirot, (2011) The dynamic protein partnership of RNA polymerase in *Bacillus subtilis*. *Proteomics* 11: 2992-3001.

Dombroski, A.J., W.A. Walter, M.T. Record, Jr., D.A. Siegele & C.A. Gross, (1992) Polypeptides containing highly conserved regions of transcription initiation factor sigma 70 exhibit specificity of binding to promoter DNA. *Cell* 70: 501-512.

Dorman, C.J., (2006) DNA supercoiling and bacterial gene expression. *Sci .Prog.* 89: 151-166.

Duarte, V. & J.M. Latour, (2010) PerR vs OhrR: selective peroxide sensing in Bacillus subtilis. *Molecular bioSystems* 6: 316-323.

Dubnau, D., (1991a) Genetic competence in Bacillus subtilis. *Microbiological reviews* 55: 395-424.

Dubnau, D., (1991b) The regulation of genetic competence in Bacillus subtilis. *Mol Microbiol* 5: 11-18.

Duwat, P., S.D. Ehrlich & A. Gruss, (1999) Effects of metabolic flux on stress response pathways in *Lactococcus lactis*. *Mol. Microbiol.* 31: 845-858.

Ebright, R.H. & S. Busby, (1995) The Escherichia coli RNA polymerase alpha subunit: structure and function. *Current opinion in genetics & development* 5: 197-203.

Eiamphungporn, W. & J.D. Helmann, (2008) The *Bacillus subtilis* sigma(M) regulon and its contribution to cell envelope stress responses. *Mol. Microbiol.* 67: 830-848.

Engman, J., A. Rogstam, D. Frees, H. Ingmer & C. von Wachenfeldt, (2012) The YjbH adaptor protein enhances proteolysis of the transcriptional regulator Spx in Staphylococcus aureus. *J Bacteriol*.

Frees, D., P. Varmanen & H. Ingmer, (2001) Inactivation of a gene that is highly conserved in Gram-positive bacteria stimulates degradation of non-native proteins and concomitantly increases stress tolerance in *Lactococcus lactis*. *Mol. Microbiol.* 41: 93-103.

Fuangthong, M., S. Atichartpongkul, S. Mongkolsuk & J.D. Helmann, (2001) OhrR is a repressor of *ohrA*, a key organic hydroperoxide resistance determinant in *Bacillus subtilis*. *J. Bacteriol.* 183: 4134-4141.

Gaballa, A., G.L. Newton, H. Antelmann, D. Parsonage, H. Upton, M. Rawat, A. Claiborne, R.C. Fahey & J.D. Helmann, (2010) Biosynthesis and functions of bacillithiol, a major low-molecular-weight thiol in Bacilli. *Proc. Natl. Acad. Sci. U S A* 107: 6482-6486.

Garg, S.K., S. Kommineni, L. Henslee, Y. Zhang & P. Zuber, (2009) The YjbH protein of *Bacillus subtilis* enhances ClpXP-catalyzed proteolysis of Spx. *J. Bacteriol.* 191: 1268-1277.

Ghosh, P., A. Ishihama & D. Chatterji, (2001) Escherichia coli RNA polymerase subunit omega and its N-terminal domain bind full-length beta' to facilitate incorporation into the alpha2beta subassembly. *Eur J Biochem* 268: 4621-4627.

Grainger, D.C., T.A. Belyaeva, D.J. Lee, E.I. Hyde & S.J. Busby, (2004) Transcription activation at the Escherichia coli melAB promoter: interactions of MelR with the C-terminal domain of the RNA polymerase alpha subunit. *Mol Microbiol* 51: 1311-1320.

Griffith, K.L., I.M. Shah, T.E. Myers, M.C. O'Neill & R.E. Wolf, Jr., (2002) Evidence for "pre-recruitment" as a new mechanism of transcription activation in Escherichia coli: the large excess of SoxS binding sites per cell relative to the number of SoxS molecules per cell. *Biochem Biophys Res Commun* 291: 979-986.

Griffith, K.L. & R.E. Wolf, Jr., (2004) Genetic evidence for pre-recruitment as the mechanism of transcription activation by SoxS of *Escherichia coli*: the dominance of DNA binding mutations of SoxS. *J. Mol. Biol.* 344: 1-10.

Gruber, T.M. & C.A. Gross, (2003) Multiple sigma subunits and the partitioning of bacterial transcription space. *Annu. Rev. Microbiol.* 57: 441-466.

Guerout-Fleury, A.M., N. Frandsen & P. Stragier, (1996) Plasmids for ectopic integration in *Bacillus subtilis*. *Gene* 180: 57-61.

Haldenwang, W.G. & R. Losick, (1979) A modified RNA polymerase transcribes a cloned gene under sporulation control in Bacillus subtilis. *Nature* 282: 256-260.

Hamoen, L.W., G. Venema & O.P. Kuipers, (2003) Controlling competence in Bacillus subtilis: shared use of regulators. *Microbiol.* 149: 9-17.

Harwood, C.R. & S.M. Cutting, (1990) *Molecular Biological Methods for Bacillus*. John Wiley & Sons, Chichester, U. K.

Haugen, S.P., M.B. Berkmen, W. Ross, T. Gaal, C. Ward & R.L. Gourse, (2006) rRNA promoter regulation by nonoptimal binding of sigma region 1.2: an additional recognition element for RNA polymerase. *Cell* 125: 1069-1082.

Haugen, S.P., W. Ross & R.L. Gourse, (2008) Advances in bacterial promoter recognition and its control by factors that do not bind DNA. *Nat Rev Microbiol* 6: 507-519.

Hecker, M., J. Pane-Farre & U. Volker, (2007) SigB-dependent general stress response in *Bacillus subtilis* and related gram-positive bacteria. *Annu. Rev. Microbiol.* 61: 215-236.

Hecker, M. & U. Volker, (2001) General stress response of Bacillus subtilis and other bacteria. *Adv Microb Physiol* 44: 35-91.

Heldwein, E.E. & R.G. Brennan, (2001) Crystal structure of the transcription activator BmrR bound to DNA and a drug. *Nature* 409: 378-382.

Helmann, J.D. & M.J. Chamberlin, (1988) Structure and function of bacterial sigma factors. *Annu Rev Biochem* 57: 839-872.

Helmann, J.D. & C.P. Moran Jr, (2002) RNA polymerase and sigma factors. In: *Bacillus subtilis* and its closest relatives: from genes to cells. A.L. Sonenshein, R. Losick & J.A. Hoch (eds). Washington, D. C.: American Society for Microbiology, pp. 289-312.

Helmann, J.D., Y. Wang, I. Mahler & C.T. Walsh, (1989) Homologous metalloregulatory proteins from both gram-positive and gram-negative bacteria control transcription of mercury resistance operons. *J Bacteriol* 171: 222-229.

Helmann, J.D., M.F. Wu, A. Gaballa, P.A. Kobel, M.M. Morshedi, P. Fawcett & C. Paddon, (2003) The global transcriptional response of *Bacillus subtilis* to peroxide stress is coordinated by three transcription factors. *J. Bacteriol.* 185: 243-253.

Herbig, A.F. & J.D. Helmann, (2001) Roles of metal ions and hydrogen peroxide in modulating the interaction of the *Bacillus subtilis* PerR peroxide regulon repressor with operator DNA. *Mol. Microbiol.* 41: 849-859.

Hinton, D.M., S. Pande, N. Wais, X.B. Johnson, M. Vuthoori, A. Makela & I. Hook-Barnard, (2005) Transcriptional takeover by sigma appropriation: remodelling of the sigma70 subunit of *Escherichia coli* RNA polymerase by the bacteriophage T4 activator MotA and co-activator AsiA. *Microbiology* 151: 1729-1740.

Hong, M., M. Fuangthong, J.D. Helmann & R.G. Brennan, (2005) Structure of an OhrR-ohrA operator complex reveals the DNA binding mechanism of the MarR family. *Mol. Cell* 20: 131-141.

Hudson, B.P., J. Quispe, S. Lara-Gonzalez, Y. Kim, H.M. Berman, E. Arnold, R.H. Ebright & C.L. Lawson, (2009) Three-dimensional EM structure of an intact activator-dependent transcription initiation complex. *Proc. Natl. Acad. Sci. U S A* 106: 19830-19835.

Imlay, J.A., (2003) Pathways of oxidative damage. *Annu. Rev. Microbiol.* 57: 395-418.

Imlay, J.A., (2008) Cellular defenses against superoxide and hydrogen peroxide. *Annu Rev Biochem* 77: 755-776.

Ishihama, A., (1992) Role of the RNA polymerase alpha subunit in transcription activation. *Mol. Microbiol.* 6: 3283-3288.

Ishihama, A., (2000) Functional modulation of *Escherichia coli* RNA polymerase. *Annu. Rev. Microbiol.* 54: 499-518.

Jarvis, B., (1967) Resistance to nisin and production of nisin-inactivating enzymes by several Bacillus species. *J. Gen. Microbiol.* 47: 33-48.

Kajfasz, J.K., A.R. Martinez, I. Rivera-Ramos, J. Abranches, H. Koo, R.G. Quivey, Jr. & J.A. Lemos, (2009) Role of Clp proteins in expression of virulence properties of *Streptococcus mutans*. *J. Bacteriol.* 191: 2060-2068.

Kajfasz, J.K., J.E. Mendoza, A.O. Gaca, J.H. Miller, K.A. Koselny, M. Giambiagi-Demarval, M. Wellington, J. Abranches & J.A. Lemos, (2012) The Spx regulator modulates stress responses and virulence in *Enterococcus faecalis*. *Infect. Immun.*

Kajfasz, J.K., I. Rivera-Ramos, J. Abranches, A.R. Martinez, P.L. Rosalen, A.M. Derr, R.G. Quivey & J.A. Lemos, (2010) Two Spx proteins modulate stress tolerance, survival, and virulence in *Streptococcus mutan*s. *J. Bacteriol.*

Kroos, L., B. Zhang, H. Ichikawa & Y.T. Yu, (1999) Control of sigma factor activity during *Bacillus subtilis* sporulation. *Mol. Microbiol.* 31: 1285-1294.

Kunst, F., N. Ogasawara, I. Moszer, A.M. Albertini, G. Alloni, V. Azevedo, M.G. Bertero, P. Bessieres, A. Bolotin, S. Borchert, R. Borriss, L. Boursier, A. Brans, M. Braun, S.C. Brignell, S. Bron, S. Brouillet, C.V. Bruschi, B. Caldwell, V. Capuano, N.M. Carter, S.K. Choi, J.J. Codani, I.F. Connerton, N.J. Cummings, R.A. Daniel, F. Denizot, K.M. Devine, A. Düsterhoft, S.D. Ehrlich, P.T. Emmerson, K.D. Entian, J.C. Errington, E. Fabret, E. Ferrari, D. Foulger, C. Fritz, M. Fujita, Y. Fujita, S. Fuma, A. Galizzi, N. Galleron, S.-Y. Ghim, P. Glaser, A. Goffeau, E.J. Golightly, G. Grandi, G. Guiseppi, B.J. Guy, K. Haga, J. Haiech, C.R. Harwood, A. Hénaut, H. Hilbert, S. Holsappel, S. Hosono, M.-F. Hullo, M. Itaya, L. Jones, B. Joris, D. Karamata, Y. Kasahara, M. Klaerr-Blanchard, C. Klein, Y. Kobayashi, P. Koetter, G. Koningstein, S. Krogh, M. Kumano, K. Kurita, A. Lapidus, S. Lardinois, J. Lauber, V. Lazarevic, S.-M. Lee, A. Levine, H. Liu, S. Masuda, C. Mauél, C. Médrigue, N. Medina, R.P. Mellado, M. Mizuno, D. Moestl, S. Nakai, M. Noback, D. Noone, M. O'Reilly, K. Ogawa, A. Ogiwara, B. Oudega, S.-H. Park, V. Parro, T.M. Pohl, D. Portetelle, S. Porwollik, A.M. Prescott, E. Presecan, P. Pujic, B. Purnelle, *et al.*, (1997) The complete genome sequence of the gram-positive bacterium *Bacillus subtilis*. *Nature* 390: 249-256.

Laemmli, U.K., (1970) Cleavage of structural proteins during the assembly of the head of bacteriophage T4. *Nature* 227: 680-685.

Lambert, L.J., Y. Wei, V. Schirf, B. Demeler & M.H. Werner, (2004) T4 AsiA blocks DNA recognition by remodeling sigma70 region 4. *EMBO J* 23: 2952-2962.

Lamour, V., S.T. Rutherford, K. Kuznedelov, U.A. Ramagopal, R.L. Gourse, K. Severinov & S.A. Darst, (2008) Crystal structure of Escherichia coli Rnk, a new RNA polymerase-interacting protein. *J Mol Biol* 383: 367-379.

Lamour, V., L.F. Westblade, E.A. Campbell & S.A. Darst, (2009) Crystal structure of the in vivo-assembled *Bacillus subtilis* Spx/RNA polymerase α subunit C-terminal domain complex. *J. Struct. Biol.* 168: 352-356

Larsson, J.T., A. Rogstam & C. von Wachenfeldt, (2007) YjbH is a novel negative effector of the disulphide stress regulator, Spx, in *Bacillus subtilis*. *Mol. Microbiol.* 66: 669-684.

Lawson, C.L., D. Swigon, K.S. Murakami, S.A. Darst, H.M. Berman & R.H. Ebright, (2004) Catabolite activator protein: DNA binding and transcription activation. *Curr. Opin. Struct. Biol.* 14: 10-20.

Lee, D.J., S.D. Minchin & S.J. Busby, (2012) Activating transcription in bacteria. *Annu. Rev. Microbiol.* 66: 125-152.

Lee, J.W. & J.D. Helmann, (2006a) Biochemical characterization of the structural Zn2+ site in the *Bacillus subtilis* peroxide sensor PerR. *J. Biol. Chem.* 281: 23567-23578.

Lee, J.W. & J.D. Helmann, (2006b) The PerR transcription factor senses H2O2 by metal-catalysed histidine oxidation. *Nature* 440: 363-367.

Lee, J.W., S. Soonsanga & J.D. Helmann, (2007) A complex thiolate switch regulates the *Bacillus subtilis* organic peroxide sensor OhrR. *Proc. Natl. Acad. Sci. U S A* 104: 8743-8748.

Leelakriangsak, M., K. Kobayashi & P. Zuber, (2007) Dual negative control of *spx* transcription initiation from the P3 promoter by repressors PerR and YodB in *Bacillus subtilis*. *J. Bacteriol.* 189: 1736-1744.

Leelakriangsak, M. & P. Zuber, (2007) Transcription from the P3 promoter of the *Bacillus subtilis spx* gene is induced in response to disulfide stress. *J. Bacteriol.* 189: 1727-1735.

Leisner, M., K. Stingl, E. Frey & B. Maier, (2008) Stochastic switching to competence. *Curr Opin Microbiol* 11: 553-559.

Lennon, C.W., W. Ross, S. Martin-Tumasz, I. Toulokhonov, C.E. Vrentas, S.T. Rutherford, J.H. Lee, S.E. Butcher & R.L. Gourse, (2012) Direct interactions between the coiled-coil tip of DksA and the trigger loop of RNA polymerase mediate transcriptional regulation. *Genes Dev* 26: 2634-2646.

Lin, A.A., D. Walthers & P. Zuber, (2013) Residue substitutions near the redox center of *Bacillus subtilis* Spx affect RNA polymerase interaction, redox control and Spx-DNA contact at a conserved cis-acting element. *J. Bacteriol.*

Lin, A.A. & P. Zuber, (2012) Evidence that a single monomer of Spx can productively interact with RNA polymerase in *Bacillus subtilis*. *J. Bacteriol.* 194: 1697-1707.

Lonetto, M., M. Gribskov & C.A. Gross, (1992) The sigma 70 family: sequence conservation and evolutionary relationships. *J Bacteriol* 174: 3843-3849.

Magnuson, R., J. Solomon & A.D. Grossman, (1994) Biochemical and genetic characterization of a competence pheromone from *Bacillus subtilis*. *Cell* 77: 207-216.

Martin, P., S. DeMel, J. Shi, T. Gladysheva, D.L. Gatti, B.P. Rosen & B.F. Edwards, (2001) Insights into the structure, solvation, and mechanism of ArsC arsenate reductase, a novel arsenic detoxification enzyme. *Structure (Camb)* 9: 1071-1081.

Martin, R.G., E.S. Bartlett, J.L. Rosner & M.E. Wall, (2008) Activation of the Escherichia coli marA/soxS/rob regulon in response to transcriptional activator concentration. *J Mol Biol* 380: 278-284.

Martin, R.G., W.K. Gillette, N.I. Martin & J.L. Rosner, (2002) Complex formation between activator and RNA polymerase as the basis for transcriptional activation by MarA and SoxS in *Escherichia coli*. *Mol. Microbiol.* 43: 355-370.

Martin, R.G. & J.L. Rosner, (2001) The AraC transcriptional activators. *Curr Opin Microbiol* 4: 132-137.

McClure, W.R., (1985) Mechanism and control of transcription initiation in prokaryotes. *Annu Rev Biochem* 54: 171-204.

Merrick, M.J., (1993) In a class of its own--the RNA polymerase sigma factor sigma 54 (sigma N). *Mol. Microbiol.* 10: 903-909.

Miller, A., D. Wood, R.H. Ebright & L.B. Rothman-Denes, (1997) RNA polymerase beta' subunit: a target of DNA binding-independent activation. *Science* 275: 1655-1657.

Miller, J.H., (1972) *Experiments in molecular genetics*. Cold Spring Harbor Laboratory, Cold Spring Harbor, N.Y.

Minakhin, L., S. Bhagat, A. Brunning, E.A. Campbell, S.A. Darst, R.H. Ebright & K. Severinov, (2001) Bacterial RNA polymerase subunit omega and eukaryotic RNA polymerase subunit RPB6 are sequence, structural, and functional homologs and promote RNA polymerase assembly. *Proc Natl Acad Sci U S A* 98: 892-897.

Minakhin, L. & K. Severinov, (2005) Transcription regulation by bacteriophage T4 AsiA. *Protein Expr Purif* 41: 1-8.

Moch, C., O. Schrogel & R. Allmansberger, (2000) Transcription of the *nfrA-ywcH* operon from *Bacillus subtilis* is specifically induced in response to heat. *J. Bacteriol.* 182: 4384-4393.

Murakami, K.S., (2013) X-ray crystal structure of *Escherichia coli* RNA polymerase sigma70 holoenzyme. *J. Biol. Chem.* 288: 9126-9134.

Murakami, K.S. & S.A. Darst, (2003) Bacterial RNA polymerases: the wholo story. *Curr. Opin. Struct. Biol.* 13: 31-39.

Murakami, K.S., S. Masuda, E.A. Campbell, O. Muzzin & S.A. Darst, (2002) Structural basis of transcription initiation: an RNA polymerase holoenzyme-DNA complex. *Science* 296: 1285-1290.

Murakami, K.S., S. Masuda & S.A. Darst, (2003) Crystallographic analysis of *Thermus aquaticus* RNA polymerase holoenzyme and a holoenzyme/promoter DNA complex. *Methods Enzymol.* 370: 42-53.

Nakano, M.M., H. Geng, S. Nakano & K. Kobayashi, (2006) The nitric oxide-responsive regulator NsrR controls ResDE-dependent gene expression. *J. Bacteriol.* 188: 5878-5887.

Nakano, M.M., F. Hajarizadeh, Y. Zhu & P. Zuber, (2001) Loss-of-function mutations in *yjbD* result in ClpX- and ClpP-independent competence development of *Bacillus subtilis*. *Mol. Microbiol.* 42: 383-394.

Nakano, M.M., T. Hoffmann, Y. Zhu & D. Jahn, (1998) Nitrogen and oxygen regulation of *Bacillus subtilis nasDEF* encoding NADH-dependent nitrite reductase by TnrA and ResDE. *J. Bacteriol.* 180: 5344-5350.

Nakano, M.M., A. Lin, C.S. Zuber, K.J. Newberry, R.G. Brennan & P. Zuber, (2010a) Promoter recognition by a complex of Spx and the C-terminal domain of the RNA polymerase alpha subunit. *PLoS One* 5: e8664.

Nakano, M.M., A. Lin, C.S. Zuber, K.J. Newberry, R.G. Brennan & P. Zuber, (2010b) Promoter Recognition by a Complex of Spx and the C-Terminal Domain of the RNA Polymerase Œ± Subunit. *PLoS ONE* 5: e8664.

Nakano, M.M., S. Nakano & P. Zuber, (2002a) Spx (YjbD), a negative effector of competence in *Bacillus subtilis*, enhances ClpC-MecA-ComK interaction. *Mol. Microbiol.* 44: 1341-1349.

Nakano, M.M., Y. Zhu, J. Liu, D.Y. Reyes, H. Yoshikawa & P. Zuber, (2000) Mutations conferring amino acid residue substitutions in the carboxy-terminal domain of RNA polymerase a can suppress *clpX* and *clpP* with respect to developmentally regulated transcription in *Bacillus subtilis*. *Mol. Microbiol.* 37: 869-884.

Nakano, S., K.N. Erwin, M. Ralle & P. Zuber, (2005) Redox-sensitive transcriptional control by a thiol/disulphide switch in the global regulator, Spx. *Mol. Microbiol.* 55: 498-510.

Nakano, S., E. Kuster-Schock, A.D. Grossman & P. Zuber, (2003a) Spx-dependent global transcriptional control is induced by thiol-specific oxidative stress in Bacillus subtilis. *Proc Natl Acad Sci U S A* 100: 13603-13608.

Nakano, S., E. Küster-Schöck, A.D. Grossman & P. Zuber, (2003b) Spx-dependent global transcriptional control is induced by thiol-specific oxidative stress in *Bacillus subtilis*. *Proc. Natl. Acad. Sci. USA* 100: 13603-13608.

Nakano, S., M.M. Nakano, Y. Zhang, M. Leelakriangsak & P. Zuber, (2003c) A regulatory protein that interferes with activator-stimulated transcription in bacteria. *Proc. Natl. Acad. Sci. USA* 100: 4233-4238.

Nakano, S., G. Zheng, M.M. Nakano & P. Zuber, (2002b) Multiple pathways of Spx (YjbD) proteolysis in *Bacillus subtilis*. *J. Bacteriol.* 184: 3664-3670.

Newberry, K.J. & R.G. Brennan, (2004) The structural mechanism for transcription activation by MerR family member multidrug transporter activation, N terminus. *J Biol Chem* 279: 20356-20362.

Newberry, K.J., S. Nakano, P. Zuber & R.G. Brennan, (2005) Crystal structure of the *Bacillus subtilis* anti-alpha, global transcriptional regulator, Spx, in complex with the alpha C-terminal domain of RNA polymerase. *Proc. Natl. Acad. Sci. USA* 102: 15839-15844.

Newton, G.L., M. Rawat, J.J. La Clair, V.K. Jothivasan, T. Budiarto, C.J. Hamilton, A. Claiborne, J.D. Helmann & R.C. Fahey, (2009) Bacillithiol is an antioxidant thiol produced in Bacilli. *Nat. Chem. Biol.* 5: 625-627.

Nguyen, T.T., W. Eiamphungporn, U. Mader, M. Liebeke, M. Lalk, M. Hecker, J.D. Helmann & H. Antelmann, (2009) Genome-wide responses to carbonyl electrophiles in *Bacillus subtilis*: control of the thiol-dependent formaldehyde dehydrogenase AdhA and cysteine proteinase YraA by the MerR-family regulator YraB (AdhR). *Mol. Microbiol.* 71: 876-894.

Niu, W., Y. Kim, G. Tau, T. Heyduk & R.H. Ebright, (1996) Transcription activation at class II CAP-dependent promoters: two interactions between CAP and RNA polymerase. *Cell* 87: 1123-1134.

Nunoshiba, T., E. Hidalgo, C.F. Amabile Cuevas & B. Demple, (1992) Two-stage control of an oxidative stress regulon: the Escherichia coli SoxR protein triggers redox-inducible expression of the soxS regulatory gene. *J Bacteriol* 174: 6054-6060.

Ogura, M., H. Yamaguchi, K. Kobayashi, N. Ogasawara, Y. Fujita & T. Tanaka, (2002) Whole-genome analysis of genes regulated by the Bacillus subtilis competence transcription factor ComK. *J Bacteriol* 184: 2344-2351.

Paget, M.S. & J.D. Helmann, (2003) The sigma70 family of sigma factors. *Genome Biol* 4: 203.

Pamp, S.J., D. Frees, S. Engelmann, M. Hecker & H. Ingmer, (2006) Spx is a global effector impacting stress tolerance and biofilm formation in *Staphylococcus aureus*. *J. Bacteriol.* 188: 4861-4870.

Paul, B.J., M.M. Barker, W. Ross, D.A. Schneider, C. Webb, J.W. Foster & R.L. Gourse, (2004) DksA: a critical component of the transcription initiation machinery that potentiates the regulation of rRNA promoters by ppGpp and the initiating NTP. *Cell* 118: 311-322.

Paul, B.J., M.B. Berkmen & R.L. Gourse, (2005) DksA potentiates direct activation of amino acid promoters by ppGpp. *Proc. Natl. Acad. Sci. U S A* 102: 7823-7828.

Piggot, P.J. & D.W. Hilbert, (2004) Sporulation of *Bacillus subtilis*. *Curr. Opin. Microbiol.* 7: 579-586.

Pineda, M., B.D. Gregory, B. Szczypinski, K.R. Baxter, A. Hochschild, E.S. Miller & D.M. Hinton, (2004) A family of anti-sigma70 proteins in T4-type phages and bacteria that are similar to AsiA, a Transcription inhibitor and co-activator of bacteriophage T4. *J Mol Biol* 344: 1183-1197.

Popham, D.L., D. Szeto, J. Keener & S. Kustu, (1989) Function of a bacterial activator protein that binds to transcriptional enhancers. *Science* 243: 629-635.

Price, C.W., P. Fawcett, H. Ceremonie, N. Su, C.K. Murphy & P. Youngman, (2001) Genome-wide analysis of the general stress response in Bacillus subtilis. *Mol Microbiol* 41: 757-774.

Qi, Y. & F.M. Hulett, (1998) PhoP-P and RNA polymerase sigmaA holoenzyme are sufficient for transcription of Pho regulon promoters in *Bacillus subtilis*: PhoP-P activator sites within the coding region stimulate transcription in vitro. *Mol. Microbiol.* 28: 1187-1197.

Qiu, J. & J.D. Helmann, (2001) The -10 region is a key promoter specificity determinant for the *Bacillus subtilis* extracytoplasmic-function sigma factors sigma(X) and sigma(W). *J. Bacteriol.* 183: 1921-1927.

Read, T.D., S.N. Peterson, N. Tourasse, L.W. Baillie, I.T. Paulsen, K.E. Nelson, H. Tettelin, D.E. Fouts, J.A. Eisen, S.R. Gill, E.K. Holtzapple, O.A. Okstad, E. Helgason, J. Rilstone, M. Wu, J.F. Kolonay, M.J. Beanan, R.J. Dodson, L.M. Brinkac, M. Gwinn, R.T. DeBoy, R. Madpu, S.C. Daugherty, A.S. Durkin, D.H. Haft, W.C. Nelson, J.D. Peterson, M. Pop, H.M. Khouri, D. Radune, J.L. Benton, Y. Mahamoud, L. Jiang, I.R. Hance, J.F. Weidman, K.J. Berry, R.D. Plaut, A.M. Wolf, K.L. Watkins, W.C. Nierman, A. Hazen, R. Cline, C. Redmond, J.E. Thwaite, O. White, S.L. Salzberg, B. Thomason, A.M. Friedlander, T.M. Koehler, P.C. Hanna, A.B. Kolsto & C.M. Fraser, (2003) The genome sequence of *Bacillus anthracis* Ames and comparison to closely related bacteria. *Nature* 423: 81-86.

Reder, A., D. Hoper, C. Weinberg, U. Gerth, M. Fraunholz & M. Hecker, (2008) The Spx paralogue MgsR (YqgZ) controls a subregulon within the general stress response of *Bacillus subtilis*. *Mol Microbiol* 69: 1104-1120.

Reder, A., D.C. Pother, U. Gerth & M. Hecker, (2012) The modulator of the general stress response, MgsR, of *Bacillus subtilis* is subject to multiple and complex control mechanisms. *Environ. Microbiol.*

Reyes, D.Y. & P. Zuber, (2008) Activation of transcription initiation by Spx: formation of transcription complex and identification of a Cis-acting element required for transcriptional activation. *Mol. Microbiol.* 69: 765-779.

Rhodius, V.A. & S.J. Busby, (1998) Positive activation of gene expression. *Curr. Opin. Microbiol.* 1: 152-159.

Rhodius, V.A., D.M. West, C.L. Webster, S.J. Busby & N.J. Savery, (1997) Transcription activation at class II CRP-dependent promoters: the role of different activating regions. *Nucleic Acids Res* 25: 326-332.

Rochat, T., P. Nicolas, O. Delumeau, A. Rabatinova, J. Korelusova, A. Leduc, P. Bessieres, E. Dervyn, L. Krasny & P. Noirot, (2012) Genome-wide identification of genes directly regulated by the pleiotropic transcription factor Spx in *Bacillus subtilis*. *Nucleic Acids Res.*

Rollenhagen, C., H. Antelmann, J. Kirstein, O. Delumeau, M. Hecker & M.D. Yudkin, (2003) Binding of sigma(A) and sigma(B) to core RNA polymerase after environmental stress in Bacillus subtilis. *J Bacteriol* 185: 35-40.

Ross, W., K.K. Gosink, J. Salomon, K. Igarashi, C. Zou, A. Ishihama, K. Severinov & R.L. Gourse, (1993) A third recognition element in bacterial promoters: DNA binding by the alpha subunit of RNA polymerase. *Science* 262: 1407-1413.

Ross, W., J.F. Thompson, J.T. Newlands & R.L. Gourse, (1990) *E.coli* Fis protein activates ribosomal RNA transcription in vitro and in vivo. *EMBO J.* 9: 3733-3742.

Ross, W., C.E. Vrentas, P. Sanchez-Vazquez, T. Gaal & R.L. Gourse, (2013) The magic spot: A ppGpp binding site on *E. coli* RNA polymerase responsible for regulation of transcription initiation. *Mol. Cell* 50: 420-429.

Roy, S., S. Garges & S. Adhya, (1998) Activation and repression of transcription by differential contact: two sides of a coin. *J Biol Chem* 273: 14059-14062.

Rutherford, S.T., C.L. Villers, J.H. Lee, W. Ross & R.L. Gourse, (2009) Allosteric control of Escherichia coli rRNA promoter complexes by DksA. *Genes Dev* 23: 236-248.

Sanderson, A., J.E. Mitchell, S.D. Minchin & S.J. Busby, (2003) Substitutions in the Escherichia coli RNA polymerase sigma70 factor that affect recognition of extended -10 elements at promoters. *FEBS Lett* 544: 199-205.

Savery, N., V. Rhodius & S. Busby, (1996) Protein-protein interactions during transcription activation: the case of the Escherichia coli cyclic AMP receptor protein. *Philos Trans R Soc Lond B Biol Sci* 351: 543-550.

Savery, N.J., G.S. Lloyd, S.J. Busby, M.S. Thomas, R.H. Ebright & R.L. Gourse, (2002) Determinants of the C-terminal domain of the *Escherichia coli* RNA polymerase alpha subunit important for transcription at class I cyclic AMP receptor protein-dependent promoters. *J. Bacteriol.* 184: 2273-2280.

Schleif, R., (2010) AraC protein, regulation of the l-arabinose operon in Escherichia coli, and the light switch mechanism of AraC action. *FEMS Microbiol Rev* 34: 779-796.

Setlow, P., (2003) Spore germination. *Curr, Opin, Microbiol,* 6: 550-556.

Shah, I.M. & R.E. Wolf, Jr., (2004) Novel protein-protein interaction between *Escherichia coli* SoxS and the DNA binding determinant of the RNA polymerase alpha subunit: SoxS functions as a co-sigma factor and redeploys RNA polymerase from UP-element-containing promoters to SoxS-dependent promoters during oxidative stress. *J. Mol. Biol.* 343: 513-532.

Shi, J., R. Mukhopadhyay & B.P. Rosen, (2003) Identification of a triad of arginine residues in the active site of the ArsC arsenate reductase of plasmid R773. *FEMS Microbiol. Lett.* 227: 295-301.

Storz, G. & J.A. Imlay, (1999) Oxidative stress. *Curr. Opin. Microbiol.* 2: 188-194.

Thackray, P.D. & A. Moir, (2003) SigM, an extracytoplasmic function sigma factor of *Bacillus subtilis*, is activated in response to cell wall antibiotics, ethanol, heat, acid, and superoxide stress. *J. Bacteriol.* 185: 3491-3498.

Touati, D., (2000) Iron and oxidative stress in bacteria. *Arch Biochem Biophys* 373: 1-6.

Trach, K., D. Burbulys, M. Strauch, J.J. Wu, N. Dhillon, R. Jonas, C. Hanstein, P. Kallio, M. Perego, T. Bird & *et al.*, (1991) Control of the initiation of sporulation in Bacillus subtilis by a phosphorelay. *Res Microbiol* 142: 815-823.

Turlan, C., M. Prudhomme, G. Fichant, B. Martin & C. Gutierrez, (2009) SpxA1, a novel transcriptional regulator involved in X-state (competence) development in *Streptococcus pneumoniae*. *Mol. Microbiol.* 73: 492-506.

Vassylyev, D.G., S. Sekine, O. Laptenko, J. Lee, M.N. Vassylyeva, S. Borukhov & S. Yokoyama, (2002) Crystal structure of a bacterial RNA polymerase holoenzyme at 2.6 A resolution. *Nature* 417: 712-719.

Veiga, P., C. Bulbarela-Sampieri, S. Furlan, A. Maisons, M.P. Chapot-Chartier, M. Erkelenz, P. Mervelet, P. Noirot, D. Frees, O.P. Kuipers, J. Kok, A. Gruss, G. Buist & S. Kulakauskas, (2007) SpxB regulates O-acetylation-dependent resistance of *Lactococcus lactis* peptidoglycan to hydrolysis. *J. Biol. Chem.* 282: 19342-19354.

Vlamakis, H., Y. Chai, P. Beauregard, R. Losick & R. Kolter, (2013) Sticking together: building a biofilm the Bacillus subtilis way. *Nature reviews. Microbiology* 11: 157-168.

Westers, L., H. Westers & W.J. Quax, (2004) Bacillus subtilis as cell factory for pharmaceutical proteins: a biotechnological approach to optimize the host organism. *Biochim Biophys Acta* 1694: 299-310.

Wise, A., R. Brems, V. Ramakrishnan & M. Villarejo, (1996) Sequences in the -35 region of Escherichia coli rpoS-dependent genes promote transcription by E sigma S. *J Bacteriol* 178: 2785-2793.

You, C., A. Sekowska, O. Francetic, I. Martin-Verstraete, Y. Wang & A. Danchin, (2008) Spx mediates oxidative stress regulation of the methionine sulfoxide reductases operon in *Bacillus subtilis*. *BMC Microbiol.* 8: 128.

Zafar, M.A., N. Sanchez-Alberola & R.E. Wolf, Jr., (2011) Genetic evidence for a novel interaction between transcriptional activator SoxS and region 4 of the sigma(70) subunit of RNA polymerase at class II SoxS-dependent promoters in *Escherichia coli*. *J Mol Biol* 407: 333-353.

Zafar, M.A., I.M. Shah & R.E. Wolf, Jr., (2010) Protein-protein interactions between sigma(70) region 4 of RNA polymerase and *Escherichia coli* SoxS, a transcription activator that functions by the prerecruitment mechanism: evidence for "off-DNA" and "on-DNA" interactions. *J. Mol. Biol.* 401: 13-32.

Zhang, G., E.A. Campbell, L. Minakhin, C. Richter, K. Severinov & S.A. Darst, (1999) Crystal structure of Thermus aquaticus core RNA polymerase at 3.3 A resolution. *Cell* 98: 811-824.

Zhang, X., T. Reeder & R. Schleif, (1996) Transcription activation parameters at ara pBAD. *J Mol Biol* 258: 14-24.

Zhang, Y., Y. Feng, S. Chatterjee, S. Tuske, M.X. Ho, E. Arnold & R.H. Ebright, (2012) Structural basis of transcription initiation. *Science* 338: 1076-1080.

Zhang, Y., S. Nakano, S.Y. Choi & P. Zuber, (2006) Mutational analysis of the *Bacillus subtilis* RNA polymerase alpha C-terminal domain supports the interference model of Spx-dependent repression. *J. Bacteriol.* 188: 4300-4311.

Zhou, Y., T.J. Merkel & R.H. Ebright, (1994) Characterization of the activating region of Escherichia coli catabolite gene activator protein (CAP). II. Role at Class I and class II CAP-dependent promoters. *J Mol Biol* 243: 603-610.

Zuber, P., (2004) Spx-RNA polymerase interaction and global transcriptional control during oxidative stress. *J. Bacteriol.* 186: 1911-1918.

Zuber, P., (2009) Management of oxidative stress in *Bacillus*. *Annu. Rev. Microbiol.* 63: 575-597.

Zuber, P., S. Chauhan, P. Pilaka, M.M. Nakano, S. Gurumoorthy, A.A. Lin, S.M. Barendt, B.K. Chi, H. Antelmann & U. Mader, (2011) Phenotype enhancement screen of a regulatory *spx* mutant unveils a role for the *ytpQ* gene in the control of iron homeostasis. *PLoS ONE* 6: e25066.

Zuo, Y., Y. Wang & T.A. Steitz, (2013) The mechanism of *E. coli* RNA polymerase regulation by ppGpp is suggested by the structure of their complex. *Mol. Cell* 50: 430-436.